Center for Air Environment Studies
The Pennsylvania State University

N71-32046
NASA CR-119669



# CYCLED OPERATION OF WATER VAPOR ELECTROLYSIS CELL

Annual Report for the period

January 1, 1970 - December 31, 1970

for

National Aeronautics and Space Administration

Grant # NGR-39-009-123

prepared by

A. M. Bloom

Project Director

Alfred J. Engel

March 1971

CAES Publication No. 200-71

CAES

# THE CENTER FOR AIR ENVIRONMENT STUDIES

The Center for Air Environment Studies at The Pennsylvania State University was established in 1963 to coordinate research and instruction concerning the interaction of man and his air environment. A unit of the interdisciplinary Institute for Science and Engineering, the Center has a staff with backgrounds in many of the physical, biological, social, and allied sciences.

A broad, flexible research program, dependent on faculty and student interest, is maintained by the Center. Some of the current research topics are:

The operation of an air pollution information service utilizing computers and other mechanized systems for the collection, retrieval, and dissemination of air environment literature. "Air Pollution Titles" and "Index to Air Pollution Research," information retrieval periodicals, are produced using computers. (See inside back cover).

Effects of air pollutants on trees, food, and fiber crops, predisposition to attack by other pathogens, and economic loss through damage to plants.

Studies of small particle behavior.

Development of high accuracy, low cost mobile analysis equipment for routine sampling of ambient air.

Biological effects of air pollutants on animals and natural ecologies.

Studies of basic combustion processes leading to lower contaminant emissions.

A statewide survey of vegetation damage due to air pollution.

Development of rapid response, specialized instrumentation for the quantitative measurement of contaminant concentration.

Controlled atmosphere air quality studies for a life-support system.

Fundamental research on the chemistry of airborne contaminants.

Basis facilities and services are maintained and provided by the Center. In addition, through the direct participation of all University Departments, departmental laboratories and facilities are utilized whenever possible. Collectively, these provide an extensive resource for research at The Pennsylvania State University.

The Center has also developed a unique set of educational programs supported by grants from the National Air Pollution Control Administration. In the Graduate Study Program, students conduct thesis work on an air pollution problem in their major field and take a minor course sequence in air pollution topics. In cooperation with the Graduate School and the academic departments, the Center manages the program and organizes the course sequence.

Potential air pollution administrators are prepared in the Introduction to Air Pollution and Control Administration Program, which involves one term of fulltime work on campus. This program is offered in the Summer for graduate students and advanced undergraduates of many disciplines and representatives of air pollution control agencies at the local, state, and federal level.

The Air Pollution Specialist Training Program is an intensive course designed to provide specialized knowledge and skills necessary for work in air pollution control instrumentation for field monitoring and sampling. The program involves one term of full time work on campus for students who have

continued on inside back cover

# TABLE OF CONTENTS

Page

LIST OF FIGURES----------iii

LIST OF TABLES----------v

INTRODUCTION----------1

SUMMARY----------1

PART I. MATHEMATICAL MODEL OF WATER VAPOR ELECTROLYSIS CELL-------3

CHAPTER 1. THEORY OF OPERATION----------5

1. Reversible emf----------6
2. Concentration Polarization----------9
3. Electrolytic Ohmic Potential Difference----------15
4. Electrode Overvoltage----------16
5. Activity of Water in the Electrolyte----------17
6. Cell Temperature----------19
7. Flux of Water and Cell Current----------21
8. Independent Variables----------22

CHAPTER 2. PHYSICAL-CHEMICAL DATA FOR ELECTROLYTE----------26
AND ELECTRODE OF WVE CELL

1. Electrode Overvoltage----------26
2. Electrolyte Resistivity----------29
3. Aqueous Sulfuric Acid Water Activity----------31
4. Water Activity of Electrolyte Mixture----------32
   4A. Experimental Procedure----------34
   4B. Experimental Results----------34
   4C. Evaluation of Hypothesis and Conclusions-----36

CHAPTER 3. COMPUTER SIMULATION OF THE WATER VAPOR----------39
ELECTROLYSIS CELL

1. Electrolysis Cell Equations----------39
2. Solution of Electrochemical Equations----------43
3. Computer Simulation----------47
4. Evaluation of Simulation----------53
5. Recommendations for Future Work----------67

TABLE OF CONTENTS (CONTINUED)

Page

PART II. CYCLIC OPERATION OF WVE CELL----------71

CHAPTER 4. EXPERIMENTAL EQUIPMENT----------74

1. Experimental WVE Cell----------74
2. WVE Cell Controlled Air Supply----------76
3. WVE Cell Power Supply----------77
4. Measurement of WVE Cell Power Consumption-------81

CHAPTER 5. EXPERIMENTAL PROCEDURE----------84

CHAPTER 6. EXPERIMENTAL RESULTS----------91

1. Cyclic Power Consumption in Pt-Ta Cells---------91
   1A. Experimental Results----------93
   1B. Discussion of Results----------96
2. Cyclic Power Consumption in BRITE Cells--------104
   2A. Experimental Results----------106
   2B. Discussion of Results----------111
3. Conclusions and Recommendations----------115

LIST OF REFERENCES----------117

APPENDICES

APPENDIX A. PROGRAM LISTING, COMPUTER SIMULATIONS

APPENDIX B. USER'S GUIDE, SUBROUTINE AMBWVE

# LIST OF FIGURES


| Figure | | Page |
|---|---|---|
| 1. | Test of Dilution Hypothesis, Expected Value Versus Measured Sample Means | 38 |
| 2. | Electrolysis Cell Equations | 40 |
| 3. | Water Vapor Electrolysis Cell Air Flow Channel Showing Increments in the Space Dimensions for Algebraic Analysis of the Transport Equations | 42 |
| 4. | Information Flow Diagram for Electrochemical Cell Model Segment | 48 |
| 5. | Information Flow Diagram for the Computer Simulation of the WVE Cell | 50 |
| 6. | Computer Simulation Output, Run #1 | 57 |
| 7. | Computer Simulation Output, Run #2 | 58 |
| 8. | Computer Simulation Output, Run #3 | 59 |
| 9. | Computer Simulation Output, Run #4 | 60 |
| 10. | Computer Simulation Output, Run #5 | 61 |
| 11. | Preliminary Data of Engel for Cell Power Consumption Under Cyclic Operation | 72 |
| 12. | Expanded-View Rendering of "ARC Lucite" Experimental WVE Cell | 75 |
| 13. | Constant Flow/Humidity Air Supply | 78 |

LIST OF FIGURES (CONTINUED)


| Figure | | Page |
|---|---|---|
| 14. | Schematic Diagram of the Circuit for the Cyclic Operation of the Water Vapor Electrolysis Cell | 80 |
| 15. | Schematic Diagram of the Special Purpose Analog Computer Used As An Indicating/Integrating Wattmeter | 82 |
| 16. | Rendering of Typical Applied Current Versus Time Under Constant Voltage "ON/OFF" Cyclic Operation of the WVE Cell | 86 |
| 17. | Cyclic Operation Specific Power Consumption as a Function of "ON" and "OFF" Cycles Times, Cells No. 1 and 2 | 95 |
| 18. | Constant Applied Current Charge/Discharge Curve for Cell No. 1 with Pt-Ta Electrodes | 100 |
| 19. | Proposed Current-Time Relationship During "ON" Cycle Time | 103 |
| 20. | BRITE Anode Cell Power Consumption as a Function of Cycle Parameters | 110 |
| 21. | Constant Current Charge/Discharge Curve for a Cell with a BRITE Anode | 113 |

# LIST OF TABLES


| Table | | Page |
|---|---|---|
| I. | Electrode Overvoltage for Water Electrolysis in $H_2SO_4$ at 23°C | 28 |
| II. | Specific Conductivity of Sulfuric Acid Solutions | 30 |
| III. | Equilibrium Activity of Water in Solutions of Sulfuric Acid at 25° | 31 |
| IV. | Partial Molal Heat Capacities and Enthalpy of Water in Sulfuric Acid at 25°C | 33 |
| V. | Cyclic Operation Power Consumption Data Cells No. 1 and 2, Pt-Ta Electrodes, $E_T$ = 2.20 V | 94 |
| VI. | Cyclic Operation Power Consumption Data Cells No. 3 through 8, BRITE Anodes, $E_T$ = 2.60 V | 107 |
| VII. | Cyclic Power Consumption Variation With Cell Voltage, Air Temperature, and Air Flow Rate, Cell No. 8, 5.0/5.0 Cycle | 109 |

## INTRODUCTION

This report deals with further research on "Cycled Operation of Water Vapor Electrolysis Cell," carried out under Grant Number NGR-39-009-123 between the National Aeronautics and Space Administration and The Pennsylvania State University, and administered through the Center for Air Environment Studies.

The purpose of the study was the investigation of the effect of cyclic operation on the power consumption efficiency of a water vapor electrolysis (WVE) cell and the development of a rigorous mathematical model of the WVE cell for predicting operating characteristics under critical conditions.

This is the second annual progress report under this grant and maximum understanding of the work dealt with here requires the prior reading of the previous progress report, CAES Publication Number 159-70, dated March 1, 1970. Only certain abstracted information from the previous reporting period of January 1, 1969 through December 31, 1969 is included.

## SUMMARY

A rigorous mathematical model of the processes occurring in the electrochemical reactor part of the WVE cell was developed. That model was then mated with the previously developed model representing heat, mass, and momentum transfer within the feed/product air channel. The result was a rigorous model of the whole WVE cell, which can generate rapid and accurate steady state response to any set of operating conditions. The model is useful not only for predicting cell operation

under critical conditions but also for rigor and optimum design of an operating WVE cell.

Experimental studies of WVE cell performance under ON/OFF cyclic operation were carried out using test cells with two types of electrodes, black platinized tantalum and solid platinum. Power consumption efficiency of the cells was measured to increase by as much as 13 percent due to cyclic operation, relative to steady state operation. Studies with the platinized tantalum electrode cells were incomplete due to repeated cell failure because of loss of platinum at the anode. With the solid platinum anode, measurements were made such that a minimum cell power consumption was located as a function of both ON and OFF cycle times.

# PART I

## Mathematical Model of Water Vapor Electrolysis Cell

In the previous annual progress report (12) the development and and evaluation of a heat and mass transfer WVE cell model was presented. That model concentrated on the transport processes occurring in the feed/product air stream, flowing over the anode of the water vapor electrolysis cell. Like those WVE cell models previously developed (3, 4, 10, 11), it was electrochemistry - independent. Cell current from an experimental cell, operating at the conditions of interest, was input to the model and current density taken as constant for the mass transfer boundary conditions. Heat generation at the anode was also assumed constant with position in the cell, and calculated from an incorrect equation as a function of cell current density and voltage.

Alone, the heat and mass transfer model had only the advantage of rigor over the WVE cell models of previous workers. It described the air channel processes accurately as entrance region laminar flow of a compressible Newtonian fluid through a rectangular duct, with concurrent heat and mass transfer. The previous models, in order to apply analytical solutions found in the literature, assumed air to be incompressible and imposed arbitrary velocity profiles on the air stream. Considering only the air channel, the large computation time for the present heat and mass transfer model outweighed its advantage in rigor over previous WVE cell models. All yielded essentially similar results.

The major advantage of the present heat and mass transfer model was its adaptability. It was indifferent to whether the boundary conditions

of current density and heat generation flux were constant with position in the cell. The other models required constant boundary conditions. They could not be used in conjunction with an electrochemical cell model, representing variable heat and mass transfer boundary conditions to the air channel model.

In this part of the report, development and evaluation of the complete water vapor electrolysis cell computer simulation is presented. Emphasis is on the electrochemical cell and the total model. The heat and mass transfer model, referred to hereafter as the air channel model segment, has been previously detailed. Therefore it will be treated here as a "black box", with unspecified operations performed on input variables to yield output state variables.

The theory of operation of the WVE cell, presented first, leads to a system of equations representing an operating cell. The resulting computer simulation was a true analog of a WVE cell, with all the independent variables available to the users and no arbitrary assumptions imposed. The following sections will deal with development of that computer simulation. FORTRAN IV coding of the simulation is presented in the Appendix, along with a user's guide. The guide allows utilization of the simulation as a "black box," requiring no knowledge of the operations performed in the program.

# Chapter 1

## THEORY OF OPERATION

To construct a mathematical analog of a process, the process must be intimately understood. The processes occurring in a WVE cell under steady operating conditions may be described completely. Thus, a mathematical analog can be constructed. It is the purpose of this section to provide the theoretical base for development of a computer simulation that is a mathematical analog of an operating WVE cell. This section presents the theoretical analysis of the processes occurring in the water vapor electrolysis cell. The focus is on the electrochemical cell itself, with reference to air flow channel as required. The hydrogen and oxygen generated by the electrolysis reaction are not mentioned explicitly, since such generation is a direct function of the consumption of water vapor. In this analysis, the cell processes are described as individual analytic expressions wherever possible. Where experimental data are required, functional dependencies are written.

The major descriptive relationship is concerned with the electrochemical kinetics - the relationship between current density and voltage - of the cell. The total cell voltage is the sum of constituent voltages

$$E_T = E_{rev} + E_{cp} + E_{IR} + E_{ov} \qquad (1)$$

where $E_T$ is the total applied cell voltage, $E_{rev}$ is the voltage which must be applied to overcome the reversible electromotive force (emf) of the electrode reactions, $E_{cp}$ is the voltage applied to overcome concentration polarization, $E_{IR}$ is the voltage applied to overcome the electrolytic resistivity of the matrix, and $E_{ov}$ is the overvoltage of

the electrode reactions. The last three terms in Eq. 1, concentration polarization, ohmic potential difference and overvoltage, are functions of current - thus the use of the term "current-voltage equation."

In general, the total measured cell voltage includes an ohmic potential difference due to the passage of current through the metallic conductors - electrodes and leads - between the points of measurement. Since those resistances are vanishingly small with respect to the other resistances in series, they are ignored. In the WVE cell, there is also an internal ohmic resistance due to the microporous PVC membrane in the electrolyte. Its resistance has never been measured, but may be assumed negligibly small for two reasons. First, its thickness is insignificant with respect to the thickness of the matrix, and second, its immersion in concentrated sulfuric acid for a week prior to cell assembly ensures that it is sufficiently permeated with charge-carrying species to negate its natural dielectric properties.

For the WVE cell, then, analyses of reversible emf, concentration polarization, ohmic potential difference, and overvoltage are required to describe its electrochemical kinetics. Each will be dicussed in turn.

1. Reversible emf

For an electrochemical reaction of form

$$aA + bB = cC + dD,$$

where i is the stoichiometric number of moles of component I in the reaction, the Gibbs free energy change for the reaction is

$$\Delta G = \Delta G^\circ + RT \ln(a_C^c a_D^d / a_A^a a_B^b) .$$

In the above equation

$\Delta G$ = change in Gibbs free energy due to reaction, cal/mol

$\Delta G^{\circ}$ = change in Gibbs free energy due to reaction with all constituents in their standard states, cal/mol

R = gas law constant, 1.98 cal/mol-°K

T = absolute temperature, °K

$a_I^i$ = activity of component I raised to the ith power

Since the reaction takes place at an electrode, the activities of the reaction constituents are those at the electrode surface.

Electrical work is equal to the product of the potential and the charge carried through the circuit. If the electrode reaction is reversible, in the thermodynamic sense, the Gibbs free energy change and the electrode reversible electromotive force (emf) are related as follows:

$$\Delta G = -n F E$$

where

E = reversible emf for electrode reaction, volt

n = number of equivalents of reactants converted in the reaction as written

F = Faraday constant, 23062 cal/volt-equivalent

nF = charge flow accompanying reaction as written, coulomb (converted to cal/volt).

The reversible emf of the electrode reaction is, then

$$E = E^{\circ} - (RT/nF) \ln(a_C^c a_D^d / a_A^a a_B^b)$$

where $E^{\circ}$ refers to the standard reversible electrode potential, with all reaction constituents at unit activity. This relationship is commonly called the Nernst equation.

For the anodic decomposition of water in an acid medium, the electrode reaction is

$$H_2O = 2H(+) + \frac{1}{2} O_2 + 2e(-)$$

where H(+) signifies ionic hydrogen in the electrolyte, $O_2$ signifies gaseous oxygen evolved at the electrode, and e(-) represents one equivalent of electrons. The reversible emf for the cell reaction is

$$E = -1.229 - (RT/2F)\ln(a^2_{H(+)} a_{O_2}^{\frac{1}{2}} / a_{H_2O}).$$

The activity of the evolved oxygen is its partial pressure, in atmospheres, at its point of evolution. Upon evolution, the oxygen is a bubble expanding against the total pressure impinging upon the electrode. The activity of the evolved oxygen may then be expressed as $P_{tot}$, the total pressure over the electrode.

For the cathodic evolution of hydrogen in an acid medium, the electrode reaction is

$$2H(+) + 2e(-) = H_2,$$

and the reversible emf is

$$E = - (RT/nF) \ln(a_{H_2} / a^2_{H(+)}).$$

Again, the activity of the hydrogen immediately at the electrode surface is $P_{tot}$. Whether the two pressures are the same is dependent upon the design of the WVE cell under consideration. In the laboratory model used in the present work, both the anode and cathode were under ambient pressure.

Only with no concentration polarization and no temperature difference between the electrodes of the WVE cell may the two electrode

emf's be added to obtain the true reversible emf of the cell reaction

$$H_2O = H_2 + \frac{1}{2} O_2,$$

and that reversible cell emf is

$$E = -1.229 - (RT/2F) \ln (P_{tot}^{1.5}/a_w).$$

The activity of water in the electrolyte is written as $a_w$ in the equation, and for convenience the convention will be maintained.

For electrolysis, the applied voltage necessary to overcome the cell reversible emf is, therefore,

$$E_{rev} = 1.229 - (RT/2F) \ln(a_w/P_{tot}^{1.5}). \quad (2)$$

2. Concentration Polarization

The term $E_{cp}$, the concentration polarization voltage, is a correction term for $E_{rev}$, accounting for the presence of electrolyte concentration gradients between electrodes of a cell. It is common to use the average, or bulk, electrolyte composition to supply activities for calculation of $E_{rev}$ by the Nernst equation, and the $E_{cp}$ correction is required if the composition of the electrolyte at the electrodes is different from the bulk composition. Implicit in the $E_{cp}$ correction for concentration gradients is a correction for temperature gradients between electrodes, since both temperature and temperature-dependent activities appear in the Nernst equation. No concentration polarization voltage would ever be observed, were individual electrode reversible potentials calculated using electrolyte component activities and temperatures immediately adjacent to the electrodes.

Concentration and temperature gradients within the electrolyte between electrodes are not mainly electrochemical phenomena, but rather the result of transport processes. Ionic mass transfer is partly

a diffusion process, and a concentration gradient is implicit in mass transfer by diffusion. Heat is generated at electrodes due to chemical reaction and uniformly within the electrolyte due to passage of current through a resistance. Heat is carried away in the air stream by convection on the anode side of the WVE cell, and by the enthalpy of the hydrogen leaving the cathode. Heat transfer occurs by temperature driving force, directly implying temperature gradients in the system. Whether those temperature and concentration gradients are significant in the WVE cell is the subject of the following paragraphs.

The temperature distribution between the anode and the cathode of a WVE cell can be analyzed by a heat balance about an element perpendicular to the direction of current flux. Given that essentially all the heat of electrochemical reaction is liberated at the cell anode, the thermal energy flux toward the cathode at steady state is equal to the enthalpy of the evolved hydrogen leaving the cell. The mass flux of that evolved hydrogen is related to the local current density ( i ) as $1.04 \times 10^{-5} i$ g/cm$^2$-sec. This low flow rate, 0.005 standard cc/sec at a normal average cell current density of 0.05 A/cm$^2$, would yield negligible convective cooling at the cathode. With perfect insulation, the temperature of the cathode ($T_c$) and the temperature of the evolved hydrogen would be equal. With the heat capacity of hydrogen 2.35 cal/g-°C (20-100 °C), the flux of heat within the electrolyte toward the cathode is equal to $2.44 \times 10^{-5} i\, T_c$. Considering only unidimensional heat transport between electrodes, by conduction through the stagnant electrolyte, the following equation relates anode temperature ($T_a$) and cathode temperature:

$$T_a/T_c = 1.0 + 2.44 \times 10^{-5}\ i\ 1/k$$

where l is the distance between electrodes (0.15 cm for the laboratory model cell used in the present work) and k is the thermal conductivity of the electrolyte mixture (0.0011 cal/cm-sec-°C for 60 wt pct $H_2SO_4$ at at 50 °C). Considering a current density of 0.1 A/$cm^2$, twice the normal average for a cell, $T_a/T_c$ = 1.0003. The current would have to be about one hundred times normal for there to be a significant temperature gradient between electrodes of the WVE cell. Temperature differences between electrodes of the WVE cell may therefore be ignored.

Electrolyte concentration gradients can not be analyzed so simply with rigor. Multicomponent diffusion in a concentrated tertiary electrolyte is not presently amenable to mathematical treatment. A simplified model of the situation is used here to provide a first order analysis. The major simplifications involved are the assumptions that the components of the electrolyte move independent of each other and that ionic activity coefficients are unity, unjustifiable in a highly concentrated electrolyte. One further simplification, that concentrated sulfuric acid behaves as a binary electrolyte, is justifiable (24). With those two simplifications, analysis of ionic mass transfer in the WVE cell may be made. The basis for the present analysis is an excellent review by Tobias, et al (28).

Two types of ionic mass transfer occur in an electrolysis cell with a stagnant electrolyte - migration and diffusion. The total flux of an ionic species may be expressed as follows:

$$N_t = cU(d\phi/dy) - D(dc/dy)$$

where

$N_t$ = ionic flux, ion-equivalents/$cm^2$-sec

c = ionic concentration, ion-equivalents/cc

U = ionic mobility, $cm^2$/sec-V

$\phi$ = potential, V

y = distance in direction of current flux, cm

D = ionic diffusivity, $cm^2$/sec.

The first term in the above equation represents ionic migration flux which at steady state is ti/nF, where t is the transport number of the ion, and n is the ion's valence charge. Since the total ionic flux ($N_t$) is i/nF, the diffusion flux - the second term in the above equation - is equal to (1.0 - t)i/nF. It is common practice in electrochemistry to assume a bulk electrolyte of constant composition ($c_b$) and a thin diffusion layer, of thickness d, over which the electrolyte concentration changes from $c_b$ to the concentration at the electrode/electrolyte interface ($c_i$), the "equivalent film thickness" manner of treating mass transfer problems. The diffusion flux may then be expressed as $D(c_b - c_i)/d$, for ionic flux in the direction of the electrode. Equating the two terms for diffusion flux

$$(1.0-t)i/nF = D(c_b - c_i)/d.$$

Obviously, the maximum possible current density occurs when $c_i$ goes to zero, the largest driving force for diffusive mass transport possible, and is called the limiting current density ($i_L$):

$$i_L = nFDc_b/((1.0-t)d).$$

Assuming that d is constant with current density, a value of 0.005 cm has been shown valid for stagnant electrolytes over a wide range of conditions

(17), the interface concentration and current density may be simply related by the equation

$$c_i/c_b = 1.0 - i/i_L$$

To determine the amount of concentration polarization, consider as an example the cathodic evolution of hydrogen in an acid medium. The true reversible potential for the reaction is $-(RT/2F)\ln(a_{H_2}/c_i^2)$, and that calculated from the bulk electrolyte $-(RT/2F)\ln(a_{H_2}/c_b^2)$. The difference between the two values is the concentration polarization.

$$E_{cp} = -(RT/F)\ln(c_i/c_b).$$

The ratio of $c_i$ to $c_b$ may be eliminated from the equation by substitution, leaving

$$E_{cp} = -(RT/F)\ln(1.0 - i/i_L),$$

a useful simplification, since $i_L$ is a function only of the bulk electrolyte concentration of hydrogen ions.

Continuing with the example of cathodic hydrogen evoluation, the amount of concentration polarization in an operating WVE cell may be approximately calculated. Since the gelled electrolyte is stagnant, a d of 0.005 cm may be used. For 60 wt pct sulfuric acid, the transport number of the hydrogen ions is about 0.8. No literature values for the diffusivity of hydrogen ions in concentrated sulfuric acid were found, so the predictive method of Newman, Bennion and Tobias (23) was utilized. A diffusivity for hydrogen ion in water for 60 wt pct sulfuric acid at 25 °C was calculated as $2.7 \times 10^{-5}$ $cm^2/sec$. No great confidence may be placed in the calculated value, since the concentration of acid is about 30 wt pct too high to fall in the linear range of the

theoretical correlation of Newman, et al. It is, however, of the proper order of magnitude and has the virtue of being the only number available.

Assuming 60 wt pct (9.1 M) $H_2SO_4$ to be a binary electrolyte, the bulk ionic concentration of hydrogen ions is $9.1 \times 10^{-3}$ ion-equivalents/cc. The limiting current density for the cathodic evoluation of hydrogen in the case under consideration is then 24 $A/cm^2$. At twice the normal WVE cell average operating current density, 0.1 $A/cm^2$, the ratio $c_i/c_b$ for hydrogen ions at the cathode of the cell is then (1.0 - 0.1/24) or 0.996, a 0.004 M concentration difference between bulk electrolyte and interface concentration. It may be readily shown, given the same assumptions used here, that the concentration polarization at the anode is of the same magnitude (2, 28). The expected concentration gradient between electrodes of a WVE cell would then be on the order of 0.01 M, with a concentration polarization voltage of

$$- 2(RT/F)\ln(0.996) = 0.0002 \text{ V @ 25 °C.}$$

Both concentration gradients and concentration polarization voltage are seen to be negligible in the WVE cell.

The gross simplifications involved in the treatment of concentration polarization cause only mild confidence in the conclusion that concentration polarization is a negligible quantity in the WVE cell. Fortunately, however, experimental observation concurs with the conclusion.

In overvoltage studies of the water electrolysis reaction, it is common practice to avoid correction for concentration polarization by use of a concentrated acid electrolyte (21). Concentration polarization is observed to decrease with strong acid concentration. Acid of 0.1 N

exhibits no concentration polarization of significance at current densities below 0.1 $A/cm^2$. No concentration polarization is observed in concentrated strong acid solutions except at very high current densities (17). Thus, both the present approximate analysis and experimental observation agree that no concentration polarization of any significance is to be expected in a WVE cell under normal operation.

3. Electrolytic Ohmic Potential Difference

The ohmic potential difference ($E_{IR}$) between the electrodes of the cell depends on the current density (i), the resistivity ($\rho$) of the electrolyte, and the distance between the electrodes (1) according to the equation

$$E_{IR} = i \times \rho \times 1 \tag{3}$$

Since the concentration and temperature of the electrolyte has been shown constant between electrodes, the resistivity of the electrolyte is also. The resistivity of the electrolyte is the resistivity of the sulfuric acid plus the added resistance of the silica in the gel. For such a concentrated electrolyte, no theory will predict the restivity of sulfuric acid - a function of acid concentration (c) and temperature (T). Experimental data are required, of the form

$$\rho = f(c, T, \text{wtfr silica}) \tag{4}$$

where "wtfr silica" reflects the dependence of the added resistivity of the electrolyte as a function of weight fraction silica in the mixture.

4. Electrode Overvoltage

Overvoltage at an electrode is a function of many variables. Among them are current density, electrolyte type and composition, electrode type and composition, electrode surface, amount and type of contaminants, temperature, and time. Due expecially to contamination, surface properties, and time, much data prior to about 1950 lacked consistency to such a degree that no good theory of electrode overvoltage could be developed. (1, 13). Consistent data have since been gathered on several systems, but the vast number of variables almost precludes the finding of a general theory. Moreover, practical electrodes - being contaminated and generally lacking well defined surfaces - would not benefit from such a theoretical treatment, yielding data with the same lack of consistency as early overvoltage data for exactly the same reasons. Generally, a given electrode of interest must be submitted to experimental measurement under conditions similar to normal operation, so that reasonably similar electrode surface and contamination exist.

Electrode overvoltage, then, must be considered as a functional relationship, for which data must be acquired. For a given electrode and electrolyte overvoltage is a function of current density, electrolyte concentration (c), and cell temperature (T) at steady state. The functional dependency is

$$E_{ov} = f(i,c,T). \qquad (5)$$

Equations (1), (2), (3), and (5) describe the electrochemical kinetics of the WVE cell. The concentration of the sulfuric acid electrolyte, the cell temperature and pressure, and the resistivity and water activity of the matrix at those conditions are required for the reduction of the

kinetic equations to four equations in five variables - determined by the choice of one of them. The following portions of this section will be devoted to the quantification of those variables necessary for the solution of the electrochemical kinetic equations.

5. Activity of Water in the Electrolyte

The activity of water (aw) in the electrolyte appears explicitly in Equation (2) for reversible emf. It is implicit in the concentration of the electrolyte, and in the cell current density. The equilibrium partial pressure of water vapor over the electrolyte at the anode is the boundary condition for transfer of water vapor from the air stream. The flux of water vapor at the anode (jw) by diffusion is, by Fick's law

$$jw = -D\ d(h\rho)/dy)\Big|_{y=0}, g\ cm^2\text{-sec} \qquad (6)$$

where

D = diffusion coefficient for air-water, $cm^2/sec$

h = absolute humidity of air, g water/g air

$\rho$ = density of air, g/cc

y = unit of distance perpendicular to the anode, with y=0 at the anode and y increasing across the air stream, cm.

The absolute humidity at y=0 is the humidity in equilibrium with the matrix composition, and may be related to the equilibrium activity of water of the matrix by the equation

$$aw = h\Big|_{y=0}(MA/MW)\ (P_{tot}/P_{sat}) \qquad (7)$$

assuming the mass of water in the air is negligible with respect to the mass of air, and where

MA = molecular weight of air

MW = molecular weight of water

$P_{sat}$ = vapor pressure of water at cell temperature.

The activity of water in sulfuric acid solutions is a strong function of acid concentration and temperature. For such a non-ideal solution, experimental data is required for aw versus concentration at one reference temperature. Using the assumption that the partial molal heat capacity of water in sulfuric acid is constant with temperature, the following thermodynamic relationship (20) applies to the change of activity with temperature at constant composition:

$$4.5758\log_{10}(a) = \bar{L}(T_o)/T - 2.303\bar{J}\log_{10}(T) + C \qquad (8)$$

where

$\bar{L}(T_o)$ = partial molal enthalpy of the constituent at the reference temperature $T_o$ and given composition

$\bar{J}$ = $\bar{C}p - Cp_o$

$\bar{C}p$ = partial molal heat capacity of the constituent at $T_o$ and the given composition

$Cp_o$ = heat capacity of the pure component at $T_o$

C = constant of integration

Given experimental data for $\bar{L}$, and $\bar{C}p$ of water in aqueous sulfuric acid at the reference temperature, the constant C may be evaluated and the activity of water at any other temperature may be calculated.

If the electrolyte were merely aqueous sulfuric acid, Equation (8) could be used to relate the activity of water at the anode, cell temperature, and sulfuric acid concentration. However, the sulfuric acid is in gel form, in mixture with silica. There exists no a priori reason to assume that the presence of silica exerts no effect upon the equilibrium activity

of water in the electrolyte. The effect, if any, would definitely be a function of the weight fraction (wtfr) of silica in the gel and requires experimental measurement. A modification of Equation (8) is required to account for the possible effect of silica, and the functional dependency would be of the form

$$C = f(aw, T, \text{wtfr silica}). \tag{8A}$$

6. Cell Temperature

The cell temperature (T) appears, either explicitly or implicitly, in all seven preceding equations. Cell temperature is a function of the heat liberated by electrochemical reaction and the heat carried away in the air stream flowing over the anode. The assumption that all heat generated is accounted for in the air stream is based on assumptions that the cell is well-insulated and that hydrogen is evolved at such a low rate at the cathode that no convective cooling takes place thereby. In operational configuration, WVE cells are stacked atop one another in a battery module, and the assumption of perfect insulation is justifiable, except for the cells on either end of the stack. Hydrogen evolution is on the order of 0.005 standard cc/sec per square centimeter electrode area, insignificant with respect to air flow rate. Clifford (7) reported experimental verification of the assumption, having measured that 96 percent of the heat generated in a cell was accounted for by the temperature rise of the air stream.

The heat generated by the electrolysis may be calculated from the first and second laws of thermodynamics. The first law for isobaric processes with electrical work is

$$\Delta H = \Delta Q - \Delta W_e,$$

and the second law is

$$\Delta G = \Delta H - T\Delta S,$$

where H, Q, $W_e$, G, and S refer to enthalpy, heat, electrical work, Gibbs free energy, and entropy, respectively. Combining the two laws yields

$$\Delta G = \Delta Q - \Delta W_e - T\Delta S.$$

The electrical work done on the environment ($\Delta W$) per equivalent reacted is $F(-E_{electrode})$, where F is the Faraday constant in units of energy per volt, and $E_{electrode}$ is the potential of the electrode. For the cell reaction, the electrical work done is $F(-E_{IR\text{-}free})$. $E_{IR\text{-}free}$ is the total applied cell voltage, less the ohmic potential difference between the electrodes, which has nothing to do with the electrode reaction. The electrical work done on the environment per equivalent reacted is, then,

$$\Delta W_e = F(E_{rev} + E_{ov}).$$

The change in Gibbs free energy for the cell reaction per equivalent is

$$\Delta G = F(E_{rev}).$$

Combining the expressions for electrical work and free energy change with the first and second laws of thermodynamics, the expression for heat generation by electrochemical reaction is

$$-\Delta Q = F\,E_{ov} - T\Delta S.$$

The heat flux due to chemical reaction is calculated by multiplying the above energy generation per equivalent reacting by the number of equivalents reacting per unit time per unit area. The latter is the cell current density divided by the Faraday constant in units of coulombs per equivalent.

In the cgs system, the appropriate constants and units are the following

$\Delta Q$ = cal/equiv

F = 96,500 coul/equiv
23,060 cal/volt-equiv

E = volt

T = degree K

$\Delta S$ = cal/degree-equiv

i = amp/$cm^2$

Assuming that the entropy change for the cell reaction does not vary appreciably from its value of 19.5 calorie per degree Celsius per equivalent, the heat generation of the WVE cell is

$$q = 0.239\ i\ (E_{ov} - 19.5\ T/23{,}060)\ \text{cal/sec cm}^2 \qquad (9)$$

The cell temperature is also the boundary condition for heat transfer to the air stream. By Fourier's law, the heat flux to the air stream - analogous to mass flux from the air stream - is the following:

$$q = -k\ dT/dy\Big|_{y=0} \qquad (10)$$

where q is the heat flux from Equation (9), k is the thermal conductivity of air, and the co-ordinate system is as defined in Equation (6).

7. Flux of Water and Cell Current

The flux of water at the anode ($jw\Big|_{y=0}$ of Equation (6)) is also related to the cell current density at steady state. Since there is no accumulation of mass, the flux of water into the matrix from the air stream must equal the amount of water removed by electrolysis, a process consuming

$9.334 \times 10^{-5}$ gram water per amp-sec. A second expression for mass flux is, then

$$jw = 9.334 \times 10^{-5} \; i \; g/cm^2 - sec \qquad (11)$$

8. Independent Variables

Eleven equations and functional dependencies have been written describing the processes occurring in an operating water vapor electrolysis cell. However, Equations (2), (6), (7) and (10) require information from the air-stream temperature, pressure, velocity, and humidity profiles. Such information must be obtained from the laws of mass, heat, and momentum transport. For the time being, it is assumed that such information is available. The type of electrode, the physical dimensions of the cell, the characteristics of the electrolyte charged to the cell, all are required information. Given this information, the eleven equations of this section still have twelve unknowns. One further variable must be selected before the system of equations is determinate.

Of the 12 variables only one is known to be a scalar quantity. That is the total cell voltage. With the assumption of negligible metallic resistance, the voltage at the anode is everywhere the voltage measured at the anode power lead. The same is true for the cathode.

The other variables are vectors, functions of distance from the air inlet. The reason for this is the changes in the velocity, temperature, and humidity profiles in the air stream as it passes across the anode from the inlet to the outlet of the cell. If the air flow were so great that its temperature and humidity were essentially unchanged within the flow channel, there would be constant driving forces for heat and mass

transfer from cell inlet to cell exit. Under such circumstances the temperature of the cell would be constant throughout, and the concentration of sulfuric acid would also be constant with position. All the other variables would be scalars also, and any one of the twelve could be chosen as a design variable.

However, the air in the channel is flowing at a finite rate, in laminar flow, and its properties change with distance from the cell inlet. First, its flow pattern is changing. A stack of cells receives air from a single blower, and the velocity profile at the inlet of any one cell is essentially flat, changing to parabolic as it moves down the rectangular flow channel. Second, the air temperature increases along the flow channel, and the cell temperature must increase to provide sufficient driving force for heat transfer. Third, the air loses water vapor by absorption as it passes down the flow channel. With higher air humidity at the inlet, the driving force for mass transfer is greater there than at the outlet, and more water would be absorbed there, causing an increasing acid concentration along the length of the cell, and a decreasing current density. As the acid becomes more concentrated, however, its equilibrium water activity decreases tending to increase the driving force for mass transfer with distance from the air inlet. There is no reason to assume, <u>a priori</u>, that any variable except total cell voltage is constant with respect to position in the electrolysis cell.

Thus five independent variables appear in the eleven descriptive relationships for the electrolysis cell processes. The are the following:

1. Total cell voltage
2. Electrode type
3. Cell dimensions

4. Mass silica in electrolyte

5. Mass anhydrous sulfuric acid in electrolyte

Of the cell dimensions, only the distance between electrodes (l in Equation (3)) appears explicitly. The length and width of the cell are required to convert local fluxes to overall quantities, as in the expression for total cell current (I):

$$I = \int_0^L \int_0^W i \, dz \, dx$$

where

L = cell length

W = cell width

x = dimension in direction of air flow

z = dimension parallel with air flow, perpendicular to x

The mass of neither silica nor anhydrous sulfuric acid ($H_2SO_4$) appears explicitly in the eleven relationships. Their concentrations do appear, relative to the electrolyte mixture. As has been stated, acid concentration differences along the length of the cell are probable. In the water vapor electrolysis cell, losses of $H_2SO_4$ and silica must be negligible for adequate long-term performance. Therefore, the mass of water in the electrolyte is the only variable. Concentration gradients within the electrolyte are determined by the interplay of physical-chemical and electrochemical forces, but the absolute amounts of silica and $H_2SO_4$ are limited only by the amount that can physically fit between the electrodes. They are, therefore, independent variables.

Before the eleven cell relationships became determinate, as has been stated, certain physical-chemical data are required, as well as temperature and humidity profiles within the air stream of the adjacent flow channel.

The following section deals with the acquisition of the required physical-chemical data.

# Chapter 2

## PHYSICAL-CHEMICAL DATA FOR ELECTROLYTE AND ELECTRODE OF WVE CELL

The physical chemical data required for the electrolyte have to do with its equilibrium water activity and with its electrochemical resistivity. With respect to the electrode, overvoltage data are required. Resistivity and activity of water in aqueous sulfuric acid alone are functions of acid concentration and temperature. However, the electrolyte in the WVE cell contains silica as well as aqueous sulfuric acid, and both physical-chemical properties may depend upon silica content as well. The overvoltage of the electrode reactions depends primarily upon electrode type, electrolyte activity, current density, and temperature. The purpose of this section is the quantification of these functional dependencies.

Electrode and aqueous sulfuric acid data are available in the literature, but are listed here for the convenience of the reader. The additional electrolyte resistivity due to the presence of silica in the mixture; was measured in the present study, and was reported upon fully in the first Annual Progress Report (12). Experimental work determining the effect of silica content upon electrolyte water activity was partially reported upon in the previous paper. Final results are presented here.

### 1. Electrode Overvoltage

In a prior study of the WVE cell, Connor, et al (8) measured overvoltage as a function of sulfuric acid concentration and current density for the two electrodes used in the present work (bright platinum and platinized tantalum screen). No other such data is available for

the platinized tantalum electrode and for the high concentrations of sulfuric acid used in the WVE cell. The data is questionable for the primary reason that the time required for a given datum was not reported.

Overvoltage is in general a function of time, increasing in response to a step input in current analogously to a charging capacitor. The earliest reference found on the subject was dated 1904, a study performed by Foerster & Piquet ([14]). Overvoltage versus time data for the water electrolysis reaction were presented, showing bright platinum overvoltage to reach its steady-state value in about an hour under the test conditions and platinized platinum (similar to platinized tantalum) overvoltage to continue to increase at the end of the two-hour test. Measurement of electrode overvoltage after an arbitrary "polarization time" has been commonly reported in the literature (1, 9, 13). Such values, while reproducible, are not the final, steady-state value of the overvoltage.

Should the data of Connor , et al, be of the "polarization time" variety, the bright platinum overvoltage data would be much more accurate than those for the platinized tantalum screen. Arguing by analogy with the data of Foerster and Piquet, overvoltage data after one hour would be about one percent low for bright platinum, twenty percent for platinized tantalum. After two hours, the bright platinum overvoltage would be at its steady state, but that for the platinized tantalum would still be about ten percent low.

The only safe assumption that can be made from Connor's work is that the overvoltage reported for bright platinum electrodes is probably reasonably good, and that for platinized tantalum unreasonably low. Excerpts of both sets of data are listed in Table I, and are used in the present work only because no other data are available. Connor , et al,

TABLE I

Electrode Overvoltage for Water

Electrolysis in $H_2SO_4$ at 23 °C *

| Current Density ($amp/cm^2$) | 0.001 | 0.010 | 0.030 | 0.050 | 0.100 |
|---|---|---|---|---|---|
| Weight pct $H_2SO_4$ (electrode) | Sum of Hydrogen and Oxygen Overvoltage (Volt) | | | | |
| 0.55 (BRITE[1]) | 0.770 | 0.948 | 1.036 | 1.090 | 1.201 |
| 0.55 (PT-TA[2]) | 0.379 | 0.524 | 0.610 | 0.703 | 0.866 |
| 0.60 (BRITE) | 0.792 | 0.967 | 1.075 | 1.146 | 1.269 |
| 0.60 (PT-TA) | 0.389 | 0.542 | 0.631 | 0.735 | 0.914 |
| 0.65 (BRITE) | 0.849 | 1.035 | 1.168 | 1.265 | 1.476 |
| 0.65 (PT-TA) | 0.420 | 0.576 | 0.680 | 0.795 | 1.005 |

[1] Bright platinum solid electrodes

[2] Platinized tantalum screen electrodes, Type AA-1, American Cyanamid

* Data of Connor, W. J., et al, "Design and Development of a Water Vapor Electrolysis Unit," Final Report, NASA Contract NAS 2-2630, March 1966.

reported data over the range 30 to 65 weight percent $H_2SO_4$, but the acid strength in the WVE cell electrolyte is on the order of 60 weight percent. Only data for 55, 60, and 65 weight percent are tabulated here.

The data for electrode overvoltage presented in Table I are at a constant temperature of 23 °C. It is known that, in general, overvoltage decreases with increasing temperature. Little data exists, however, the most recent found being from a comprehensive overvoltage study by Hickling and Hill ( 16 ) for essentially the same conditions as found in the WVE cell. Their data was unfortunately limited to a sulfuric acid strength of 1N. A rough temperture coefficient of overvoltage was reported, -0.0025 volt/°C, over the range 20-70 °C.

2. Electrolyte Resistivity

Some excellent data for the resistivity of sulfuric acid may be found in the literature. The data of Roughton (25) is accurate to within one percent and includes the effect of temperature as well as concentration on the conductivity of aqueous sulfuric acid. Excerpts of the reported data are listed in Table II, encompassing the region in which the WVE cell operates. Data are tabulated over the ranges 30 to 75 weight percent $H_2SO_4$ and 25 to 95 degree Celsius.

In the previous Annual Progress Report (12), the effect of silica content upon the resistivity of sulfuric acid was measured. Over the 55-65 wt pct $H_2SO_4$ region of interest, electrolyte resistivity increase was found to be linear with respect to silica content. The data fit the equation

$$\Delta\rho/\rho_o = 2.40 \text{ (wtfr CAB·O·SIL M5)}$$

where

$\rho_o$ = resistivity of sulfuric acid alone, ohm-cm

TABLE II

Specific Conductivity of Sulfuric Acid Solutions *

| Temp °C | 25 | 60 | 95 |
|---|---|---|---|
| Weight pct $H_2SO_4$ | Specific | Conductivity | ($ohm^{-1}$ $cm^{-1}$) |
| 0.30 | 0.823 | 1.211 | 1.513 |
| 0.35 | 0.810 | 1.224 | 1.562 |
| 0.40 | 0.763 | 1.186 | 1.551 |
| 0.45 | 0.695 | 1.105 | 1.486 |
| 0.50 | 0.615 | 1.000 | 1.366 |
| 0.55 | 0.524 | 0.873 | 1.221 |
| 0.60 | 0.428 | 0.732 | 1.059 |
| 0.65 | 0.336 | 0.600 | 0.901 |
| 0.70 | 0.253 | 0.479 | 0.752 |
| 0.75 | 0.182 | 0.378 | 0.627 |

* Data of Roughton, J. E., J. Appl. Chem., S2, 141 (1951)

$\rho$ = resistivity of silica/sulfuric acid mixture, ohm-cm

$\Delta\rho$ = $\rho - \rho_o$, ohm cm

wtfr = weight fraction CAB·O·SIL M5 in silica/sulfuric acid mixture

3. Aqueous Sulfuric Acid Water Activity

The equilibrium activity of water - the equilibrium relative humidity - of mixtures of sulfuric acid at 25 degree Celsius is readily available in the literature as a function of acid concentration. The following is an excerpt of the tabulation of Robinson and Stokes (27), chosen arbitrarily for reproduction here from among several similar data sets. The data in Table III list equilibrium relative humidity as a function of weight percent $H_2SO_4$ in the acid.

TABLE III

Equilibrium Activity of Water in Solutions of Sulfuric Acid at 25° *

| $a_W$ | wt% $H_2SO_4$ | $a_W$ | wt% $H_2SO_4$ |
|---|---|---|---|
| .90 | 17.91 | .45 | 45.41 |
| .85 | 22.88 | .40 | 47.71 |
| .80 | 26.79 | .35 | 50.04 |
| .75 | 30.14 | .30 | 52.45 |
| .70 | 33.09 | .25 | 55.01 |
| .65 | 35.80 | .20 | 57.76 |
| .60 | 38.35 | .15 | 60.80 |
| .55 | 40.75 | .10 | 64.45 |
| .50 | 43.10 | .05 | 69.44 |

* Data of Robinson and Stokes, IEC, 9, 2013 (1949).

Since the above data are for 25 degree Celsius, further information is required to include the temperature dependence of activity. The relationship for activity as a function of temperature (Eq(8) of Chapter 1) requires experimental data for the partial molal heat capacity and enthalpy of the constituent of interest. Such data for water in sulfuric acid is present in Table IV, excerpted from Giauque et al (15) and from the International Critical Tables (ICT) (22).

4. Water Activity of Electrolyte Mixture

The electrolyte mixture is a gel of nominal composition ten weight percent CAB·O·SIL M5 silica and ninety weight percent 8.1 M (55 weight percent) sulfuric acid. No reason existed, a priori, to assume that the water activity of the mixture is the same as that of the aqueous sulfuric acid alone. The electrolyte water activity controls both the emf of the cell electrolysis reaction and the water vapor absorption from the feed/product air stream. Should the addition of silica to sulfuric acid change the water activity of the acid, both electrochemical and mass transfer aspects of WVE cell operation would be affected. The present work was undertaken to determine any such effects.

The present work was almost complete at the time of the previous Annual Progress Report (12), and only two data sets, and the conclusions drawn therefrom, are missing in the earlier publication. The two data sets further confirmed the hypothesis that dry CAB·O·SIL M5 silica does not affect the activity of water of the electrolyte mixture. A mixture of sulfuric acid and dry silica, in the region of interest of zero to ten weight percent silica, has the same water activity as the sulfuric acid solution alone.

However, should the silica contain adsorbed water prior to mixing, with the sulfuric acid, the sulfuric acid would be diluted by that

TABLE IV

Partial Molal Heat Capacities and Enthalpy of Water in Sulfuric Acid at 25 degree C

| Mol Fr $H_2SO_4$ | $\bar{C}p_w$ [1] cal/°K-mol | $\bar{L}_w$ [2] cal/mol |
|---|---|---|
| 0 | 17.996 | 0 |
| 0.05 | 17.770 | -43.7 |
| 0.10 | 18.609 | -293.3 |
| 0.15 | 17.927 | -580 |
| 0.20 | 16.657 | -1000 |
| 0.25 | 15.329 | -1450 |
| 0.30 | 13.391 | -1910 |
| 0.35 | 11.626 | -2470 |
| 0.40 | 10.20 | -3060 |
| 0.45 | 11.48 | -3880 |
| 0.50 | 15.06 | -4850 |
| 0.55 | 20.39 | -5730 |
| 0.60 | 22.54 | -6300 |
| 0.65 | 21.77 | -6690 |
| 0.70 | 20.61 | -7010 |
| 0.75 | 19.00 | -7280 |
| 0.80 | 17.22 | -7490 |
| 0.85 | 15.21 | -7700 |
| 0.90 | 13.20 | -7870 |
| 0.95 | 10.49 | -8050 |

[1] Data of Giauque et al, J. Am. Chem. Soc. 82, 62, (1960).

[2] Data from ICT, Vol. 7, p. 237.

amount of water, raising the electrolyte water activity accordingly.

The experimental procedures and intermediate results leading to that conclusion may be found in the previous Annual Progress Report and are not reiterated in the present work. The final results, consisting of two trials previously reported and two further trials, are presented below.

4A. Experimental Procedure

Four batches of silica were stored under atmospheres of known relative humidity (RH), ranging from zero to eighty percent. From the previously measured water vapor adsorption isotherm, at 75 °F, the adsorbed water content of the silica in each batch was known. From each batch, several samples of known mass were mixed with known masses of 55 wt pct sulfuric acid. From the equilibrium relative humidity of each mixture, the data of Robinson and Stokes yielded a corresponding concentration of sulfuric acid.

The amount of water apparently added to the sulfuric acid to attain the concentration corresponding to the mixture equilibirum RH was calculated. The mass of water added per unit mass dry silica in the mixture was then compared with the adsorbed water content of the silica prior to mixing. A significant difference between the two values would be cause for rejection of the hypothesis.

4B. Experimental Results

Four sets of trials were performed. Each set was based upon silica stored under a different equilibrium RH prior to mixing with sulfuric acid. The first data set again had silica stored in an open container in the laboratory prior to mixing. Spot data showed the ambient humidity to have varied from 12 to 19 percent, with an average of 15 percent RH.

The silica thus contained an average of 0.0085 g adsorbed water per gram dry silica. Five mixtures, ranging from 3 to 9 weight percent silica, showed the average water gain of the sulfuric acid to be 0.0098 g water per gram dry silica added to the mixture. The standard deviation of the data was 0.0133 g water per g silica, and a t-test comparing the sample mean with the expected value of 0.0085 yield a t of 0.219, indicating a 15% probability that the sample and the expected value are not from the same population. No effect of weight percent silica was observed on the water gain of the sulfuric acid per g silica. The large standard deviation of the data in the first set was indicative of the large scatter in the data. The RH of the air in contact with the silica was thereafter both controlled and monitored, and mixing of silica and acid was accomplished as quickly as possible to prevent interactions with the ambient laboratory RH.

For the second and third data sets, the silica was stored in dessicators containing dilute sulfuric acid solutions. The silica containers were undisturbed for two weeks each prior to mixing the silica and acid, so that the silica samples came to equilibrium with the atmospheres of 68 and 83 percent RH, respectively. The silica in contact with the 68% RH atmosphere contained 0.043 g adsorbed water per g silica prior to mixing with the sulfuric acid. Equilibrium RH measurements for four mixtures, of from 2 to 9 weight percent silica, showed an average water gain of the sulfuric acid of 0.042 g water per g dry silica in the mixture, with a standard deviation of 0.0070. Comparing the sample mean with the expected value, a t of 0.286 was calculated, corresponding to a twenty percent probability that the sample and expected value were not from the same population.

The silica stored under 83% RH contained 0.123 g adsorbed water per g silica. Measurement showed the sulfuric acid to be diluted by an average of 0.121 g water per g dry silica added, with standard deviation 0.0064. A t of 0.311 was calculated, indicating a fifteen percent probability that the sample and expected value are from the same population, but the water vapor adsorption isotherm is rising so quickly with equilibrium RH in the range that the amount of water contained by the silica is itself uncertain.

The final data set was for dry silica, stored in an oven at a temperature of 300 degrees Fahrenheit for two weeks prior to mixing. The stored silica was kept in a stoppered bottle, which was sealed prior to removal for weighing, allowing negligible ambient water vapor contact. A known mass of sulfuric acid was quickly transferred to the bottle and the mixture swirled together with the bottle sealed. This required that the final silica/acid mixture be liquid - silica content of less than five weight percent. The mixture was then transferred to the humidity measuring chamber and its equilibrium RH measured. Over the range 2 to 5 weight percent silica, no change was observed in the equilibrium RH from that of the acid alone. The standard deviation was zero, and essentially no possibility existed that the sample and the expected value were from different populations.

4C. Evaluation of Hypothesis and Conclusions

The previous section showed that in each of the four data sets taken, an average of 12 percent probability existed that the hypothesis was incorrect. T-tests between samples showed the water gain per gram silica added to the sulfuric acid was significantly different between samples. Therefore, the equilibrium RH over the silica in storage had a definite effect upon the dilution of the sulfuric acid prior to mixing.

Evaluation of the hypothesis is shown graphically in Figure 1, with measured sulfuric acid dilution per gram silica added superimposed upon the equilibrium water vapor adsorption isotherm for the silica. The four sample means and the isotherm are almost coincident, showing the hypothesis to have merit.

It appears, to about 90 percent confidence, that silica exerts no effect upon the activity of water in sulfuric acid/silica mixtures. However, should the silica contain adsorbed water prior to mixing, a dilution of the sulfuric acid will occur upon mixing, raising the water activity. Mixtures of sulfuric acid and dry silica have the same water activity as mixtures of sulfuric acid alone.

FIGURE 1

Test of Dilution Hypothesis, Expected Value Versus Measured Sample Means

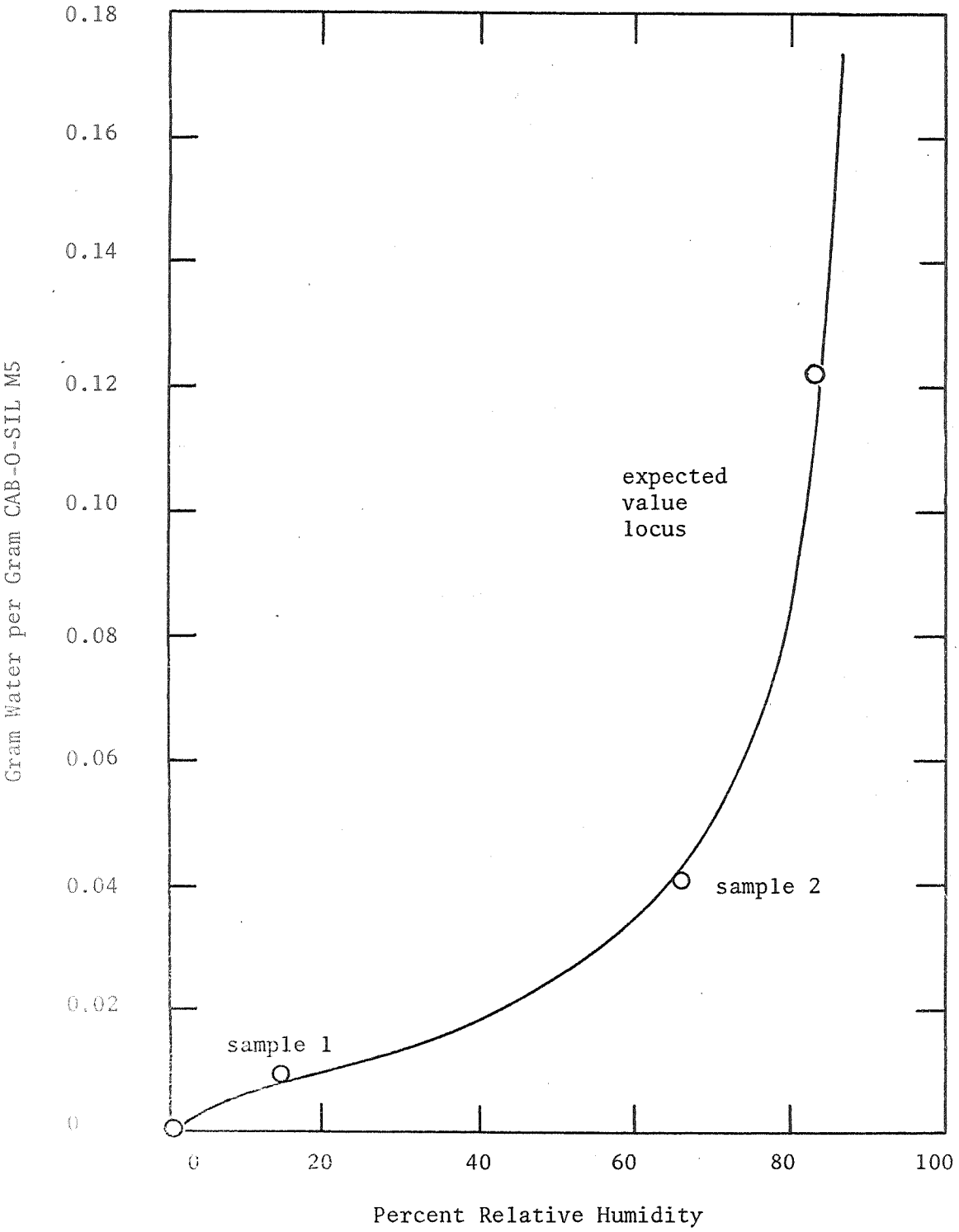

# Chapter 3

# COMPUTER SIMULATION OF THE WATER VAPOR ELECTROLYSIS CELL

With required physical-chemical data (Chapter 2) and heat and mass transfer profiles from the air channel model segment available (12), the eleven descriptive equations and relationships of Chapter 1 may be brought together quantitatively. The simultaneous solution of that set of equations is the primary part of the computer simulation of the WVE cell. Such peripheral parts as input-output formats and controls are not discussed here, but may be found in the Appendix I. In this chapter, the equations descriptive of an operating WVE cell will be reiterated. The algorithm for the simultaneous solution of the set of non-linear equations will be developed. The fully developed computer simulation of the WVE cell will then be evaluated, and simulation output presented and discussed.

## 1. Electrolysis Cell Equations

A reiteration of the eleven discriptive relationships for the electrolysis cell, derived in Chapter 1, is presented in tabular form in Figure 2 for convenience. Relationships 1, 2, 3, 7, and 8 are equations relating only to the electrolysis cell. Relationships 4, 5, and 6 also relate only to the electrolysis cell, but require the experimental physical-chemical data of Chapter 3 to become equations. Relationships 9, 10, and 11 are equations requiring information about the heat and mass transfer profiles in the air flow channel from Chapter 4.

FIGURE 2

ELECTROLYSIS CELL EQUATIONS

---

1. $E_T = E_{REV} + E_{IR} + E_{ov}$

2. $E_{REV} = 1.229 - (RT/2F) \ln (P^{1.5}/a_w)$

3. $E_{IR} = i \rho$

4. $E_{ov} = f$ (electrode, i, c, T, time)

5. $a_w = f$ (c, T)

6. $\rho = f$ (c, T, wtfr silica)

7. $q = 0.239\ i\ (E_{ov} - T\Delta S_{RXN}/F)$

8. $j_w = 9.334 \times 10^{-5}\ i$

9. $q = -k\ (\partial T/\partial y)\big|_{y=o} = f(T(I,0))$

10. $j_w = -D\rho(\partial h/\partial y)\big|_{y=o} = f(h(I,0))$

11. $a_w = h(I,0)\ (M_A/M_W)\ (P/P_{SAT})$

These equations are to be added to, or blended with, the system of equations comprising the model of the feed/product air channel. It may appear strange to cast the central part of the WVE cell model in a secondary role; the electrochemical cell model segment is mathematically nothing more than a variable boundary condition for heat and mass transfer. In effect, the electrochemical cell is viewed as row (I,O) of the air channel model, whose increment network for finite difference analysis is reproduced in Figure 3.

The assumptions required to ignore the physical attributes of the electrochemical cell are not unreasonable. Three have already been made and justified in Chapter 1. The first of these is the constancy of temperature between electrodes, $(\partial T/\partial y)=0$ within the electrolyte. Almost all the heat of reaction is generated at the anode, almost all the heat of reaction has been shown to be accounted for in the exit air stream, and therefore the cathode temperature is approximately that of the anode. Second is the lack of concentration polarization brought about by the high concentration of electrolyte and low-to-moderate current density. The final assumption, based upon experimental observation, is zero electrolyte mobility in the x-direction. Under that assumption, the mass of $H_2SO_4$ and silica in an increment along the cell length is constant and equal to that in every other increment. The assumption is based upon experimental observation of the lack of x-direction mobility of water in the gelled electrolyte (Clifford, Connor , Wydeven, Engel, present work). With no lateral water mobility, the assumption of no $H_2SO_4$ and silica mobility would appear justified. The assumptions result in the elements (I,O) representing the cell interacting only with elements (I,1) in the air channel and not with any other elements in the 0th column. Assuming no lateral heat

FIGURE 3

Water Vapor Electrolysis Cell Air Flow Channel Showing Increments in the Space Dimensions for Algebraic Analysis of the Transport Equations

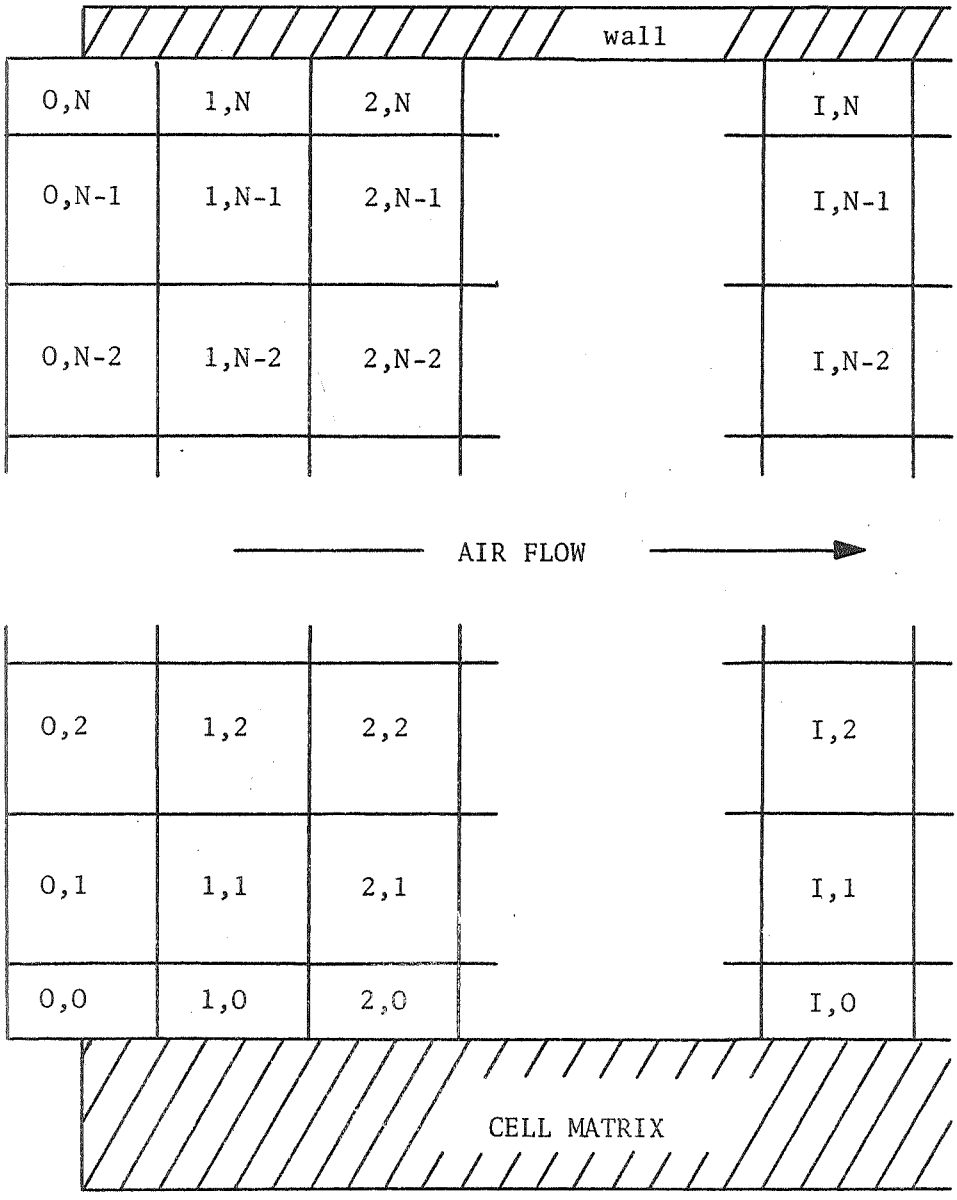

conduction within the electrolyte cannot be justified prior to the determination of the relative amounts of temperature differences between elements of row (I,0) and convective heat transfer. The assumption was made, pending evaluation based upon model results.

2. Solution of Electrochemical Equations

The eleven descriptive relationships tabulated in Figure 2 that comprise the model of the WVE cell may all be made into equations, although several represent tabular data rather than analytic functions. The non-linear and partly non-analytic nature of the equations requires an iterative solution. Form and order of calculation are important in efficient computation in such an instance, and the equations as written in Figure 2 are not necessarily of either the proper form or order for computational purposes. Order is self-explanatory, but by "form" is meant the proper variable being on the left hand side of the equation.

Choice of equation form and order of solution is aided greatly by the "design variable selection" algorithm of Lee, Christensen, and Rudd (19). Operations on a Rudd Array consisting of the eleven cell relationships showed that a minimum of two variables must be guessed at every iteration. Since the air channel model segment required values of heat generation and current density (q and i, respectively) for the system of equations to be determinate, those two variables were selected to be guessed.

Guessing two variables is not as difficult as it may appear. The obvious first guess of current density and heat generation at an increment along the length of the flow channel are the corresponding values from the preceding increment. For the first increment, a guess of current density equal to expected current draw divided by electrode area would

be a reasonable first approximation. For heat generation at the first increment along the flow channel, the following incorrect equation will yield an estimate:

$$q = 0.239\ i\ (E_T - E_{rev})\ cal/cm^2 sec\ .$$

The above is, of course, that used by Engel (10,11) and Clifford (3,4) in the previous models of the WVE cell. In the present work, $E_{rev}$ was replaced arbitrarily by 1.48, the no-heat voltage at 75 °F, for the first guess of electrolysis heat generation.

With the two variables i and q guessed at the beginning of the iteration, the "Rudd Array" yielded a straight-forward order of computation and form of equations. First, the air flow channel model segment was to be solved at an increment along the channel length, yielding a temperature and humidity at the anode side of the channel. From the temperature and humidity at the anode, the activity of water vapor in the air at the anode, equal to the equilibrium activity of water of the electrolyte, may be calculated from relationship 11. Given the temperature and activity of water of the electrolyte, the concentration of $H_2SO_4$ in the aqueous sulfuric acid may be calculated from relationship 5, noting that the effect of silica content on the activity of the electrolyte has been proven (Chapter 2) to be zero.

The silica content of the electrolyte at a given increment in the x-direction is not an independent variable. From the constant mass of $H_2SO_4$ present in the increment, the sulfuric acid concentration yields the amount of water present in the acid in the increment. From there, knowledge of the mass of silica in the increment leads to the mass fraction silica present in the electrolyte within the increment. Note that the assumption of zero electrolyte lateral mobility implies

that the mass of silica and the mass of $H_2SO_4$ are independent variables, subject to a design decision, although the concentrations of each are not.

Given the sulfuric acid concentration, the cell temperature, and the weight fraction silica in the mixture at the increment, relationship 6 gives the resistivity of the electrolyte at that point. Electrolyte resistivity, current density, and the distance between electrodes yield the ohmic potential difference between the cell electrodes. Subtracting the previously calculated ohmic potential difference and reversible emf from the total cell voltage yields the cell overvoltage via relationship 1.

At this point a new guess of current density is calculated from the known overvoltage, sulfuric acid concentration and temperature via relationship 4, and the new guess of heat generation from relationship 7, using overvoltage, current density and temperature. As with any iterative solution, the new guesses and the old guesses must be identical, else further iteration is required.

The method of Lee, Christensen, and Rudd can give no clue as to the proper values of i and q for guesses in succeeding iterations. Proper values of i and q, those leading to algorithm convergence, must be selected by what is in essence a trial and error procedure. To that end, trials with the electrochemical cell model segment alone were initiated. This was accomplished by ignoring heat and mass transfer, leaving a mathematic analog of an isothermal electrolysis cell. Selected independent variables were the following:

| | |
|---|---|
| Cell temperature | 23 °C |
| $H_2SO_4$ concentration | 55 wt pct |

| | |
|---|---|
| Silica in Electrolyte | 10 wt pct |
| Electrodes | bright Pt |
| Electrode Spacing | 1 cm |
| Cell Voltage | 2.45 V |

The cell voltage of 2.45 V was the result of back calculation from a desired cell current density of 0.05 amp/cm$^2$, the overvoltage data of Connor (8), and the electrolyte resistivity data of Roughton (25) and the present work.

Algorithm accuracy was not in question, save for possible errors in transcribing data or "typographical" errors in writing the equations. As an isothermal electrolysis cell at 23 °C, model segment and experimental data are one and the same. Model segment accuracy at other temperature could be questioned but not evaluated, since the only available overvoltage-temperature data was that used to provide the model with its temperature coefficient, leaving no further degrees of freedom. Given the above independent variables, convergence of the algorithm to other than a current density of 0.05 amp/cm$^2$ would mean only that an error in the FORTRAN IV coding of the model segment existed.

The computer trials of the electrochemical cell model segment, then, were strictly for the development of a convergence scheme. Methods were to be tested against their ability to cause the algorithm to converge to a current density of 0.05 amp/cm$^2$ from initial guesses of from zero to one amp/cm$^2$. Convergence of the variables overvoltage and current density would insure convergence of the heat of reaction term q, so no generality was lost by its not being utilized in the isothermal case.

In development of the convergence scheme, the simplest method of obtaining a new guess of current density for a succeeding iteration was tried first. That was using the current desnity calculated in the preceding iteration. This led to undamped oscillation in current density. The next trial involved looping from the new guess of current density to the equation calculating the ohmic potential difference until this "inner loop" yielded a constant current density. The resultant current density became the new guess of i for the succeeding iteration. This led to undamped oscillation in current density, but it was a successful modification as will be seen. Next, the average of old and new guesses of current density from an iteration was used as the guess of current density for the succeeding iteration. Convergence was swift and non-oscillatory. Inadvertently, however, the "inner loop" was not removed for that trial. Upon rectification of the oversight, current density oscillated in an undamped manner with each iteration. The "inner loop" was returned to the algorithm. Only one justification for the method of selecting guesses of i and q for succeeding iterations exists, that it works.

A information flow diagram, showing the above algorithm graphically, is presented in Figure 4. As can be seen, the forms of equations 1, 4, 5, and 10 of Figure 2 were altered, solving for different variables. The heat of reaction, q, is calculated from the most recent overvoltage and temperature and the new guess of current density prior to the succeeding iteration.

3. Computer Simulation

Only a certain amount of control logic is now required to join the air channel and electrolysis cell model segments into the computer

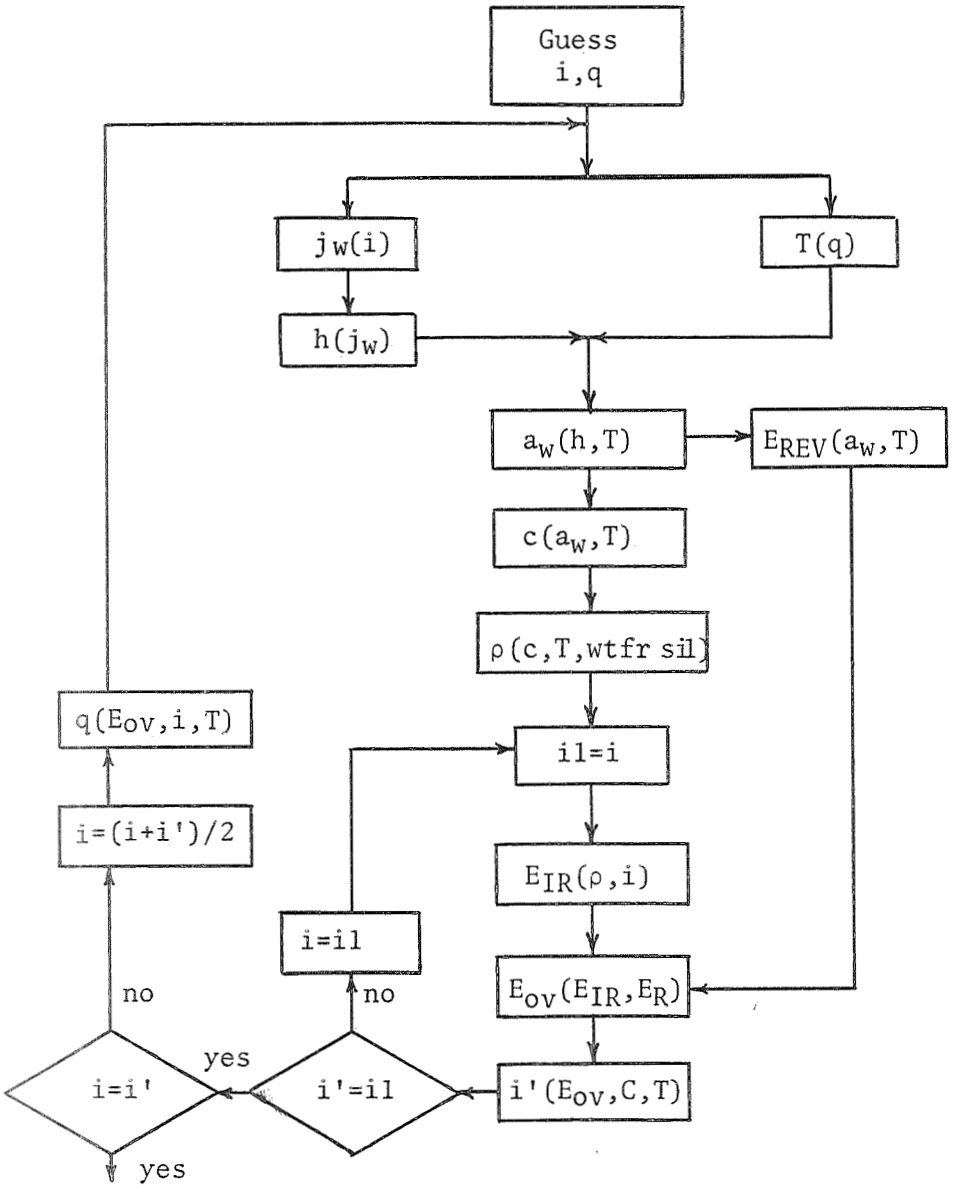


FIGURE 4

Information Flow Diagram for Electrochemical Cell Model Segment

simulation of the water vapor electrolysis cell. An information flow diagram of the simulation, whose FORTRAN IV coding is listed in full in the Appendix, is shown in Figure 5. The simplified flow diagram shows that properties of the inlet air stream provide the starting point of the simulation. From guesses of i and q, air properties are calculated iteratively for the first increment along the anode. The humidity profile at that point is then calculated. The electrochemical model segment then computes new guesses of i and q. If the new guesses are not the same as the original, the transport equations are solved again for the new guesses of i and q, and the process continues until current densities from succeeding iterations match. At that time the succeeding increment along the flow channel is operated upon in the same manner, and the process continued until the end of the channel has been reached.

Information which must be supplied to the computer simulation is of two types, physical constants of the air stream and design variables. The required physical constants are thermal conductivity and heat capacity of the air and the diffusitivity of the binary air-water mixture.

The decision to input the physical constants rather than build them into the model, was made to provide flexibility. The physical constants are average values for given ranges of conditions. Should different ranges of conditions be of interest, the change of an input datum may be made simply. The design variables change with every use of the computer simulation.

Design variables, those free to be independently manipulated, constitute the interface between the model and the user. With the present model, all design variables available in an operating WVE cell are present. No simplifying assumptions have been made that would limit the degrees of freedom of the computer simulation.

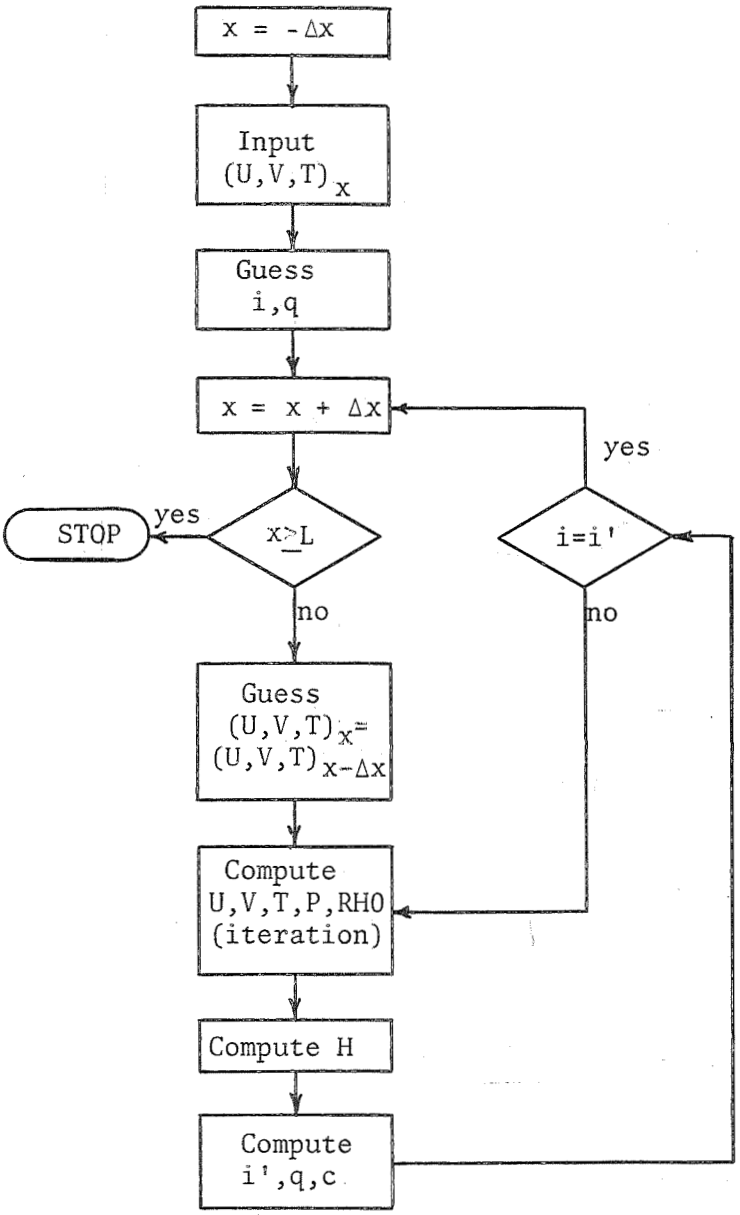


FIGURE 5

Information Flow Diagram for the Computer Simulation of the WVE Cell.

There are ten independent design variables for the steady-state operation of the WVE cell. In the present computer simulation they are the following:

1. Inlet air stream velocity profile
2. Characteristic magnitude of inlet air stream velocity
3. Inlet air stream temperature
4. Inlet air stream pressure
5. Inlet air stream humidity
6. Dimensions of air channel and electrolyte compartments
7. Total cell voltage
8. Mass anhydrous sulfuric acid in electrolyte
9. Mass silica in electrolyte
10. Type electrodes

In the simulation, two of the above are built into the model, and may be changed only by altering blocks of FORTRAN IV coding. The first is the inlet air stream velocity profile, taken to be flat ($V_x(o,y)$ = constant, $V_y(o,y) = 0$) in the model. This is the general approximation for the present WVE cell design - cells stacked in a battery, each taking a small part of the output of a fan ahead of the battery in an air duct. However, any arbitrary initial velocity profile may be loaded into the $V_x$ and $V_y$ arrays in the simulation.

The second is the type of electrode used in the cell. While hydrogen overvoltage is reasonably the same for any type of platinum cathode, anodic oxygen overvoltage is strongly dependent upon electrode type. Interpolation of the overvoltage data of Connor (8) is most accurately done on a log-log basis, but other data could yield other bases. For the sake of accuracy, different types of electrodes should have their overvoltage - current - composition data individually

inserted into the model.

The two "built-in" design variables are fixed for a definite reason. The air source is decided upon early in the design stage and is not likely to change. The type of electrode used has only one design criterion - that it is to be a long-lasting porous solid with the lowest overvoltage available. Cost is, in general, no object. Such a criterion can be evaluated before inclusion in the cell design. Neither is likely to be changed often.

The properties of the feed air to the WVE cell are generally not subject to design decision. The feed is a life support medium (the spacecraft atmosphere), and its temperature, pressure, and humidity are generally determined by consideration of crew comfort. Steady state response of the WVE cell to any deviations in these properties (lower temperature due to conservation of spacecraft power, for example) may be studied via the simulation. Thus the properties are free to be manipulated from trial to trial.

The mass of silica in the electrolyte has been decided upon by early experimental work. By vibration and acceleration tests, Connor, et al (8) showed that a minimum of 9.2 weight percent silica in the electrolyte was required to retain the sulfuric acid in the gel. The only effect of silica in the gel is in increasing the cell resistance propertional to its weight fraction (this work - conductivity and water activity sections). Thus the least possible silica should be present in the electrolyte.

The design parameters that are free to be manipulated are, then, the following:

1. Characteristic magnitude of inlet air stream velocity

2. Dimensions of air channel and matrix compartments

3. Total cell voltage

4. Mass anhydrous sulfuric acid in electrolyte

The simulation yields the steady state response of any dependent variable to changes in as many design parameters as required. The final four freely manipulated parameters are of primary use in an optimization procedure for normal operation. Variation of inlet air properties would be of primary value in predicting WVE cell response to abnormal conditions. Changes in inlet air velocity profile, silica content of the electrolyte, and electrode type would constitute response to major design decisions - availability of an improved electrode, different module design, or new constraints upon the minimum allowable silica content of the electrolyte.

Evaluation of the computer simulation of the WVE cell will end the present study. No attempt was being made to conduct a design study of the cell via the model. Such would be of intellectual interest, but of no practical value. Design constraints and optimization objective functions must take into account much more than the WVE cell alone for a valid optimization.

4. Evaluation of Simulation

One part of the computer simulation of the WVE cell, the feed/product air flow channel model segment, has been independently evaluated. It has been shown to be both accurate and applicable with respect to predicting mass momentum and heat transport within the air channel in the region of normal cell operation. Within limits previously set down, the electrolysis cell model segment has been proven accurate and theoretically rigorous. That which remains is the evaluation of the combination of the two, the computer simulation of the WVE cell.

Since the current-voltage relationship is of primary importance in electrochemical kinetics, the ability of the simulation to predict the current drawn by an operating WVE cell under a variety of conditions would be a sensitive test. Several sets of data for the steady state operation of laboratory models of the WVE cell have been reported by previous workers (8,10,34) for cells with the platinized tantalum (PT-TA) electrodes. All cells were similar, supplied by the Ames Research Center of NASA, known as ARC-Lucite Modules. Common cell parameters were the following:

| | |
|---|---|
| length of air channel | 4.75 cm |
| height of air channel | 0.159 cm |
| width of air channel | 4.75 cm |
| electrode spacing | 0.15 cm |
| electrode surface area | $4.75^2$ $cm^2$ apparent |
| $H_2SO_4$ concentration (initial) | 0.55 wt ft $H_2SO_4$ |
| Silica content of electrolyte (initial) | 0.10 wt fr silica |

Electrode area is taken by convention to mean the length of the electrode multiplied by its width. This apparent area bears no relationship to the active area of the electrodes and yields apparent current densities.

Connor, et al, (8) reported that two cells of the sulfuric acid/silica type were constructed, and that both failed within hours of start-up, generating only some transient data. Wydeven and Smith (31) reported one thousand-hour steady state experiment, under the following conditions:

| | | |
|---|---|---|
| inlet air | temperature | $80 \pm 2$ °F |
| | pressure | 1 atm |
| | humidity | $0.011 \pm 0.002$ lb/lb |
| | flow rate | 25 scc /sec |

cell voltage 2.20 ± .02 volt

cell current 1.0 amp

Engel (10) reported one eighteen-hour steady state experiment under approximately the same conditions, with a cell current of 0.9 amp at 2.2 volt.

Steady state operating data were taken in conjunction with the experimental cyclic operation studies reported upon in Part II of the present work. Results of those studies, described in full in Part II, are utilized here for model evaluation purposes. All data are for cells with platinized tantalum screen cathodes, and with an inlet air relative humidity of 50.0 ± 0.5 % RH and pressure of 735 ± 3 mm Hg. In addition, none of the data is for a cell which had been operating for less than ten days after initial start-up. The data are the following:

| Cell No. | Anode Type | Inlet Air Flow Rate (scc /sec) | Inlet Air Temp (°F) | Cell Voltage (V) | DC Time (hr) | Cell Current (A) |
|---|---|---|---|---|---|---|
| 1 | PT-TA | 24.0 | 84 | 2.20 | 430 | 1.00 |
| 2 | PT-TA | 24.0 | 84 | 2.20 | 50 | 1.00 |
| 3 | BRITE | 24.0 | 84 | 2.60 | 50 | 0.92 |
| | | | | | 50 | 0.92 |
| | | | | | 25 | 0.92 |
| 6 | BRITE | 24.0 | 84 | 2.60 | 50 | 0.92 |
| 8 | BRITE | 24.0 | 84 | 2.60 | 250 | 0.93 |
| | | 24.0 | 84 | 2.60 | 50 | 0.92 |
| | | 24.0 | 84 | 2.40 | 50 | 0.74 |
| | | 24.0 | 74 | 2.60 | 50 | 0.88 |
| | | 51.0 | 74 | 2.60 | 50 | 1.12 |

The constraint of ten days of cell operation prior to taking any measurements reflected observed lack of agreement of data before and after that period of time. Cell current under constant voltage approached its steady state reproducible value asymptotically after about a week of initial operation of a cell.

For comparison of model current predictions, there are five sets of experimental data, one for a cell with platinized tantalum (PT-TA) screen electrodes, and four for cells with bright platinum (BRITE) anodes. Given common cell data and specific run parameters, the computer simulation predicted cell currents at each of the five conditions.

Reproductions of the computer output for the five executions of the simulation are presented in Figures 6 through 10. Shown are cell dimensions and operating parameters, samples of cell current density, temperature, and electrolyte concentration at points along the flow channel, and overall data. The cell current for each execution, listed among the overall data, is arrived at by integration of the local cell current density over the length and breadth of the electrolysis cell. Abstracting cell current from the data for each execution of the simulation, the comparison of model and experiment is shown in the following tabulation:

| Anode Type | Inlet Air Temp (°F) | Inlet Air Flow (scc /sec) | Cell Voltage (V) | Cell Current Exp (A) | Cell Current Model (Error) (A) |
|---|---|---|---|---|---|
| PT-TA | 84 | 24.0 | 2.20 | 1.00 | 1.23 (+ 23%) |
| BRITE | 84 | 24.0 | 2.60 | 0.92 | 0.92 (0) |
| BRITE | 84 | 24.0 | 2.40 | 0.74 | 0.75 (+ 1%) |
| BRITE | 74 | 24.0 | 2.60 | 0.88 | 0.90 (+ 2%) |
| BRITE | 74 | 51.0 | 2.60 | 1.12 | 1.13 (+ 1%) |

FIGURE 6

Computer Simulation Output, Run #1

Cell Dimensions

| | |
|---|---|
| Length of Air Channel | 4.75 cm |
| Height of Air Channel | 0.159 cm |
| Length of 1 Matrix Compartment | 4.750 cm |
| Width of 1 Matrix Compartment | 4.750 cm |
| Depth of 1 Matrix Compartment | 0.075 cm |

Cell Operating Parameters

| | |
|---|---|
| Cell Voltage | 2.200 volt |
| Electrodes | PT-TA |
| Initial Acid Concentration | 0.550 wtfr $H_2SO_4$ |
| Initial CAB-O-SIL Content | 0.100 wtfr silica |
| Inlet Air Temperature | 302.000 degree K |
| Pressure | 1.000 atm |
| Humidity | 50.000 percent RH |
| Flow Rate | 35.200 cm/sec |

Consolidated Data

| X/L Fraction of Cell Length from Entrance | Local Current Density amp/cm**2 | Local Matrix Temp Degree F | Local Matrix Conc wtfr $H_2SO_4$ |
|---|---|---|---|
| 0.00 | 0.1120 | 99.9 | 0.549 |
| 0.05 | 0.0929 | 109.3 | 0.591 |
| 0.10 | 0.0847 | 113.3 | 0.607 |
| 0.15 | 0.0790 | 115.9 | 0.618 |
| 0.20 | 0.0747 | 118.0 | 0.626 |
| 0.25 | 0.0713 | 119.9 | 0.633 |
| 0.30 | 0.0681 | 121.6 | 0.639 |
| 0.35 | 0.0654 | 123.3 | 0.645 |
| 0.40 | 0.0628 | 124.9 | 0.650 |
| 0.45 | 0.0601 | 126.4 | 0.655 |
| 0.50 | 0.0575 | 127.9 | 0.661 |
| 0.55 | 0.0552 | 129.3 | 0.666 |
| 0.60 | 0.0530 | 130.7 | 0.670 |
| 0.65 | 0.0511 | 132.1 | 0.674 |
| 0.70 | 0.0493 | 133.4 | 0.678 |
| 0.75 | 0.0477 | 134.7 | 0.682 |
| 0.80 | 0.0461 | 136.0 | 0.685 |
| 0.85 | 0.0447 | 137.3 | 0.688 |
| 0.90 | 0.0435 | 138.6 | 0.691 |
| 0.95 | 0.0423 | 139.9 | 0.694 |
| 1.00 | 0.0411 | 141.1 | 0.696 |

| | |
|---|---|
| Cell Current | 1.23 amp |
| Air Delta-T | 47.04 degree F |
| Air Delta-H | -0.0037 lb/lb |
| Humidity Change | -30.22 pct |

FIGURE 7

Computer Simulation Output, Run #2

Cell Dimensions

| | |
|---|---|
| Length of Air Channel | 4.75 cm |
| Height of Air Channel | 0.150 cm |
| Length of 1 Matrix Compartment | 4.750 cm |
| Width of 1 Matrix Compartment | 4.750 cm |
| Depth of 1 Matrix Compartment | 0.075 cm |

Cell Operating Parameters

| | |
|---|---|
| Cell Voltage | 2.600 volt |
| Electrodes | BRITE/PT-TA |
| Initial Acid Concentration | 0.550 wtfr $H_2SO_4$ |
| Initial CAB-O-SIL Content | 0.100 wtfr silica |
| Inlet Air Temperature | 302.000 degree K |
| Pressure | 1.000 atm |
| Humidity | 50.000 percent RH |
| Flow Rate | 35.200 cm/sec |

Consolidated Data

| X/L Fraction of Cell Length from Entrance | Local Current Density amp/cm**2 | Local Matrix Temp Degree F | Local Matrix Conc wtfr $H_2SO_4$ |
|---|---|---|---|
| 0.00 | 0.1165 | 110.4 | 0.587 |
| 0.05 | 0.0774 | 119.4 | 0.621 |
| 0.10 | 0.0659 | 122.6 | 0.631 |
| 0.15 | 0.0593 | 124.6 | 0.638 |
| 0.20 | 0.0545 | 126.3 | 0.643 |
| 0.25 | 0.0506 | 127.8 | 0.647 |
| 0.30 | 0.0470 | 129.2 | 0.651 |
| 0.35 | 0.0434 | 130.3 | 0.655 |
| 0.40 | 0.0404 | 131.4 | 0.659 |
| 0.45 | 0.0376 | 132.4 | 0.663 |
| 0.50 | 0.0352 | 133.5 | 0.666 |
| 0.55 | 0.0330 | 134.5 | 0.669 |
| 0.60 | 0.0310 | 135.5 | 0.672 |
| 0.65 | 0.0292 | 136.5 | 0.675 |
| 0.70 | 0.0276 | 137.4 | 0.677 |
| 0.75 | 0.0261 | 138.4 | 0.680 |
| 0.80 | 0.0247 | 139.3 | 0.682 |
| 0.85 | 0.0235 | 140.2 | 0.684 |
| 0.90 | 0.0224 | 141.1 | 0.686 |
| 0.95 | 0.0214 | 142.0 | 0.688 |
| 1.00 | 0.0205 | 142.8 | 0.689 |

| | |
|---|---|
| Cell Current | 0.92 amp |
| Air Delta-T | 50.63 degree F |
| Air Delta-H | -0.0025 lb/lb |
| Humidity Change | -20.91 pct |

FIGURE 8

Computer Simulation Output, Run #3

Cell Dimensions

| | |
|---|---|
| Length of Air Channel | 4.75 cm |
| Height of Air Channel | 0.159 cm |
| Length of 1 Matrix Compartment | 4.750 cm |
| Width of 1 Matrix Compartment | 4.750 cm |
| Depth of 1 Matrix Compartment | 0.075 cm |

Cell Operating Parameters

| | |
|---|---|
| Cell Voltage | 2.400 volt |
| Electrodes | BRITE/PT-TA |
| Initial Acid Concentration | 0.550 wtfr $H_2SO_4$ |
| Initial CAB-O-SIL Content | 0.100 wtfr silica |
| Inlet Air Temperature | 302.000 degree K |
| Pressure | 1.000 atm |
| Humidity | 50.000 percent RH |
| Flow Rate | 35.200 cm/sec |

Consolidated Data

| X/L Fraction of Cell Length from Entrance | Local Current Density amp/cm**2 | Local Matrix Temp Degree F | Local Matrix Conc wtfr $H_2SO_4$ |
|---|---|---|---|
| 0.00 | 0.0598 | 95.2 | 0.519 |
| 0.05 | 0.0530 | 103.0 | 0.561 |
| 0.10 | 0.0477 | 105.9 | 0.574 |
| 0.15 | 0.0441 | 107.7 | 0.581 |
| 0.20 | 0.0413 | 109.1 | 0.586 |
| 0.25 | 0.0390 | 110.3 | 0.591 |
| 0.30 | 0.0369 | 111.5 | 0.595 |
| 0.35 | 0.0350 | 112.5 | 0.599 |
| 0.40 | 0.0330 | 113.5 | 0.603 |
| 0.45 | 0.0311 | 114.3 | 0.607 |
| 0.50 | 0.0294 | 115.2 | 0.611 |
| 0.55 | 0.0278 | 116.0 | 0.614 |
| 0.60 | 0.0264 | 116.8 | 0.617 |
| 0.65 | 0.0250 | 117.5 | 0.620 |
| 0.70 | 0.0238 | 118.2 | 0.623 |
| 0.75 | 0.0227 | 119.0 | 0.626 |
| 0.80 | 0.0216 | 119.6 | 0.628 |
| 0.85 | 0.0206 | 120.3 | 0.631 |
| 0.90 | 0.0197 | 121.0 | 0.633 |
| 0.95 | 0.0189 | 121.6 | 0.635 |
| 1.00 | 0.0181 | 122.2 | 0.637 |

| | |
|---|---|
| Cell Current | 0.75 amp |
| Air Delta-T | 32.31 degree F |
| Air Delta-H | -0.0019 lb/lb |
| Humidity Change | -15.78 pct |

FIGURE 9

Computer Simulation Output, Run #4

Cell Dimensions

| | |
|---|---|
| Length of Air Channel | 4.75 cm |
| Height of Air Channel | 0.159 cm |
| Length of 1 Matrix Compartment | 4.750 cm |
| Width of 1 Matrix Compartment | 4.750 cm |
| Depth of 1 Matrix Compartment | 0.075 cm |

Cell Operating Parameters

| | |
|---|---|
| Electrodes | BRITE/PT-TA |
| Cell Voltage | 2.600 volt |
| Initial Acid Concentration | 0.550 wtfr $H_2SO_4$ |
| Initial CAB-O-SIL Content | 0.100 wtfr silica |
| Inlet Air Temperature | 297.000 degree K |
| Pressure | 1.000 atm |
| Humidity | 50.000 percent RH |
| Flow Rate | 35.200 cm/sec |

Consolidated Data

| X/L Fraction of Cell Length from Entrance | Local Current Density amp/cm**2 | Local Matrix Temp Degree F | Local Matrix Conc wtfr $H_2SO_4$ |
|---|---|---|---|
| 0.00 | 0.1169 | 101.6 | 0.592 |
| 0.05 | 0.0765 | 109.9 | 0.625 |
| 0.10 | 0.0650 | 112.9 | 0.636 |
| 0.15 | 0.0585 | 115.0 | 0.642 |
| 0.20 | 0.0538 | 116.6 | 0.647 |
| 0.25 | 0.0497 | 118.0 | 0.651 |
| 0.30 | 0.0459 | 119.1 | 0.656 |
| 0.35 | 0.0425 | 120.2 | 0.660 |
| 0.40 | 0.0396 | 121.3 | 0.664 |
| 0.45 | 0.0370 | 122.3 | 0.667 |
| 0.50 | 0.0346 | 123.3 | 0.671 |
| 0.55 | 0.0324 | 124.3 | 0.674 |
| 0.60 | 0.0305 | 125.2 | 0.676 |
| 0.65 | 0.0288 | 126.2 | 0.679 |
| 0.70 | 0.0272 | 127.1 | 0.682 |
| 0.75 | 0.0257 | 128.0 | 0.684 |
| 0.80 | 0.0244 | 128.9 | 0.686 |
| 0.85 | 0.0232 | 129.8 | 0.688 |
| 0.90 | 0.0222 | 130.6 | 0.690 |
| 0.95 | 0.0212 | 131.5 | 0.692 |
| 1.00 | 0.0202 | 132.3 | 0.694 |

| | |
|---|---|
| Cell Current | 0.90 amp |
| Air Delta-T | 49.19 degree F |
| Air Delta-H | -0.0025 lb/lb |
| Humidity Change | -27.24 pct |

FIGURE 10

Computer Simulation Output, Run #5

Cell Dimensions

| | |
|---|---|
| Length of Air Channel | 4.75 cm |
| Height of Air Channel | 0.159 cm |
| Length of 1 Matrix Compartment | 4.750 cm |
| Width of 1 Matrix Compartment | 4.750 cm |
| Depth of 1 Matrix Compartment | 0.075 cm |

Cell Operating Parameters

| | |
|---|---|
| Electrodes | BRITE/PT-TA |
| Cell Voltage | 2.600 volt |
| Initial Acid Concentration | 0.550 wtfr $H_2SO_4$ |
| Initial CAB-O-SIL Content | 0.100 wtfr silica |
| Inlet Air Temperature | 297.000 degree K |
| Pressure | 1.000 atm |
| Humidity | 50.000 percent RH |
| Flow Rate | 73.500 cm/sec |

Consolidated Data

| X/L Fraction of Cell Length from Entrance | Local Current Density amp/cm**2 | Local Matrix Temp Degree F | Local Matrix Conc wtfr $H_2SO_4$ |
|---|---|---|---|
| 0.00 | 0.1219 | 100.5 | 0.588 |
| 0.05 | 0.0907 | 106.8 | 0.613 |
| 0.10 | 0.0778 | 109.5 | 0.624 |
| 0.15 | 0.0707 | 111.3 | 0.630 |
| 0.20 | 0.0660 | 112.6 | 0.635 |
| 0.25 | 0.0624 | 113.7 | 0.638 |
| 0.30 | 0.0594 | 114.6 | 0.641 |
| 0.35 | 0.0569 | 115.5 | 0.644 |
| 0.40 | 0.0547 | 116.3 | 0.646 |
| 0.45 | 0.0527 | 117.0 | 0.648 |
| 0.50 | 0.0509 | 117.7 | 0.650 |
| 0.55 | 0.0488 | 118.3 | 0.652 |
| 0.60 | 0.0470 | 118.9 | 0.655 |
| 0.65 | 0.0453 | 119.4 | 0.657 |
| 0.70 | 0.0436 | 119.9 | 0.659 |
| 0.75 | 0.0421 | 120.4 | 0.661 |
| 0.80 | 0.0407 | 120.9 | 0.662 |
| 0.85 | 0.0394 | 121.4 | 0.664 |
| 0.90 | 0.0381 | 121.9 | 0.666 |
| 0.95 | 0.0368 | 122.4 | 0.668 |
| 1.00 | 0.0357 | 122.9 | 0.669 |

| | |
|---|---|
| Cell Current | 1.13 amp |
| Air Delta-T | 32.83 degree F |
| Air Delta-H | -0.0016 lb/lb |
| Humidity Change | -17.86 pct |

It is obvious that the computer simulation of the WVE cell simulated the cell with a platinized tantalum anode poorly, predicting a current measured experimentally. However, the simulation and experiment agreed almost totally for the cell with a bright platinum anode, the model predicting a current generally about one percent high.

The only difference between the simulation of the PT-TA anode cell and that of the BRITE anode cell was in the overvoltage data used. It appears obvious that the data of Connor , et al, for the oxygen overvoltage of the PT-TA electrode was seriously in error. Had those overvoltage data been measured at one-hour "polarization time", they would have been low enough to cause the current-prediction discrepancies, as previously discussed in Chapter 2.

With confidence in the ability of the simulation to predict cell current comes a certain confidence that the electrochemical cell model segment is valid. Still, however, remains the justification of one assumption, that heat conduction within the electrolyte is zero in the x-direction. The lack of physical mobility of the electrolyte has been observed experimentally, probably due to the strong electric field in the y-direction. Such a field also affects molecular transport of heat, but the method used to test the assumption made no use of the effect. The method was based upon the output of calculated variables for one execution of the simulation, Run #2, under the above-mentioned conditions leading to a cell current of 0.92 amp for a BRITE anode cell. From the difference between temperatures at (I,0) and (I,1) at a point, the heat loss from the cell to the air stream was calculated. Similarly, the temperature difference between elements (I-1,0) and I,0), and a thermal conductivity of the electrolyte of 0.0011 cal/cm-sec°K, yielded a value for the lateral heat conduction at that point.

Ratios of convective to conductive heat transfer were calculated along the length of the cell. These started at 5.4 at the air channel inlet, increased to 7.2 at 2.2 cm along the cell length, and dropped to 4.8 at the exit side, 4.75 cm from the inlet. The ratios were sufficiently large to allow the statement that the assumption is valid to a first approximation. Since the electric field was not taken into account, the true ratios would be higher still.

With this final test of the computer simulation of the WVE cell, and all previous tests, the simulation has proven to be a true analog of an operating cell, a useful tool in predicting the steady state response to any given set of operating parameters. However, evaluation implies more than merely testing for validity. The value of the simulation must be established, by comparison with the only other method of obtaining operating data: experimental measurement. This comparison may be made with respect to both time and amount of information obtainable.

In the following discussion, reference to experimental measurement is based primarily on the present work, found in Part II. Specific references to the present computer simulation are based upon the four executions of the model of the BRITE anode cell discussed previously. Operating parameters and consolidated output data appear in Figures 7 through 10.

The value of the computer simulation with respect to time is undeniably the simulation required from 100 to 150 seconds of IBM 360/67 execution time. The steady state response of a WVE cell to the change in any combination of cell dimensions or operating parameters can therefore be predicted within about two minutes. Response of an experimental cell to a change in operating conditions requires one to two days to measure,

assuming that the experiment progressed smoothly. The four experimental data sets, corresponding to the four simulation executions, were typical with respect to difficulties encountered in the present experimental work. The gathering of the four data sets required two weeks. The simulation required less than ten minutes.

To measure the response of the WVE cell to a change in cell dimensions, the simulation is again clearly preferable to experiment. Experimental measurement would require fabrication of WVE cell components of different dimensions. Both time and cost could readily become large. The simulation is indifferent to whether a change represents an increased air flow rate or a special order solid platinum electrode that may arrive in a month. The simulation will yield the WVE cell response to any design variable change in about two minutes.

The computer simulation possesses more than a time advantage over experimental measurement. More information is generated by the simulation than has been measured experimentally in the preceding period of nine years during wich the WVE cell has been under study. Any variable that has been mentioned in connection with the model development is available as simulation output. Much is, of course, of no practical interest. However, the current density, the cell temperature, and the electrolyte concentration distributions are of importance, and have never been experimentally measured.

Variation of current density, cell temperature, and sulfuric acid concentration with position in the electrolysis cell are shown in Figures 7 through 10 for the four executions of the simulation under consideration. The current density distribution is most striking in all four instances. On the basis of the simulation output, it is immediately apparent that

the design of the ARC-Lucite module could be improved upon. The current density is so low at the exit end of the cell that the value of the extra cell length comes into question. Subject to design constraints, such as total cell current (oxygen generation rate) and space limitations, it is conceivable that an optimum cell width to length ratio exists and is greater than the 1.0 in the ARC-Lucite module.

The cell temperature distributions for the four simulation executions are of interest from both heat and mass transfer viewpoints. The maximum cell temperature is important in consideration of proper construction materials for the WVE cell components. For example, as the name implies, the ARC-Lucite module has air and hydrogen manifolds of methyl methacrylate, with upper limit of temperature tolerance in the range of from 160 to 200 °F. (30). Simulation output in Figure 7 for the BRITE anode cell with 0.92 amp current shows a peak cell temperature of 143 °F. At corners of the air channel, neglected in the model, convective cooling of the cell could be less efficient, with localized higher temperatures. In the present experimental work, under corresponding conditions, the anode rim was invariably found imbedded in the air manifold. In some cases, the air exit port was found partially blocked by solidified plastic. Mid-channel electrode supports evidenced no heat deformation. In this instance the present simulation is only a guide.

Local sulfuric acid concentrations are also shown in Figures 7 through 10 for the four executions of the simulation. In each instance, the simulation represented a cell charged initially with sulfuric acid of 0.55 wtfr $H_2SO_4$. Under the operating conditions considered, simulation output shows both that the steady state acid concentration has no relationship to the concentration of acid loaded into the cell and that the acid becomes more concentrated

with distance from the air inlet. Again referring to the simulation execution whose output is displayed in Figure 7, experimental observation of cells under corresponding conditions in the present work tended to verify the model output. During the first week that a cell was on-stream, cell current continually decreased, approaching its reproducible steady state value asymptotically. Overvoltage would build to its steady state value in several hours, so the only possible explanation for the week-long start-up time would be that, under the physical-chemical driving forces at those conditions, the electrolyte initially contained an excess of water.

With a charge of 0.55 wtfr $H_2SO_4$ sulfuric acid and a maximum steady state concentration of 0.69 wtfr, the maximum sulfuric acid specific gravity changed from about 1.45 to 1.60, corresponding to about a ten percent loss of electrolyte volume (18). This change in electrolyte volume given charged acid of considerably different concentration from the mean at steady state, could lead to cell failure.

For example, had the cell been charged with a much higher concentration, the volume increase could force the electrolyte through the electrodes, clogging the manifolds. Conversely, a large volume decrease could cause the electrolyte to pull away from the electrodes, causing cell failure by poor electric contact. The computer simulation does not account for either physically possible situation. It is, however, well suited to predict them, by simply comparing the output steady state acid concentration distribution with the initial acid concentration.

These distributions of current density and sulfuric acid concentration within the cell were first postulated by Engel (11) qualitatively, and the postulation was expanded upon in Chapter 1 of the present work.

Regarding the simulation as a true analog of the WVE cell, the output data constitute the first quantitative proof of their existence.

In conclusion, the present computer simulation of the water vapor electrolysis cell has been shown to be valid by all available theoretical and experimental methods of evaluation. Its value has been discussed in generating far more data far more quickly than is possible by experimental measurement. Information generated by the simulation has been shown to lay the groundwork for future, rational design of the water vapor electrolysis modules that will eventually be a part of manned spacecraft life support systems.

## 5. Recommendations for Future Work

The present work has confined itself to the development and evaluation of a rigorous computer simulation of the water vapor electrolysis cell operating at steady state. Future work with the simulation is conceived to fall under two broad classifications. They are further model development and utilization of the model in the study and design of an operating WVE system. The former can be done as an extension of the present work, but the latter is in the domain of the contract agency.

With respect to the present steady state model, the next steps in model development should involve simplification and verification. In the present work, much information generated by the computer simulation had no experimentally measured counterpart, and the maximum possible rigor was required to impart confidence in the output. Simplifications could be made to increase computational efficiency without seriously affecting accuracy, and experimental data could be gathered to verify the concentration, temperature, and current density distributions predicted by the simulation.

Under simplification, model output under normal operating conditions showed the air density change to be about five percent from channel inlet to exit. Viewing that as negligible, variable density calculations would be eliminated, and both density and temperature vectors would be removed from the air channel iteration loop. Indeed a velocity distribution may be found for the air stream, eliminating all iteration in the air channel model segment, with a projected savings of at least forty seconds of execution time. Such simplifications, of course, must be evaluated with respect to the present rigorous simulation.

Experimental verification of the temperature, concentration, and current density distributions predicted by the simulation would be useful in imparting more confidence in the value of the model as a rigorous analog of an operating WVE cell. There is always some doubt involved in the utilization of theoretical information which has never been experimentally observed. A suggested method of obtaining that data involves the construction of a special large segmented-electrode cell. Several short electrodes with individual power leads along the length of the cell would give an indication of the current density variation along the cell length. If the distance between electrodes were large, protected thermocouples could be imbedded in the electrolyte along the cell length to measure cell temperature variations. The measuring probes must be much smaller than the electrolyte compartment to minimize "observer effects." Concentration gradients could be measured upon attainment of steady state by one or both of the following methods: attaching opposing electrode segments to the "unknown" arm of an impedance bridge and relating conductivity to acid concentration, or scooping out electrolyte samples along the cell length and titrating them.

Further model development is conceived to be in the area of extension of the present simulation into the time domain. Were this to be done, transient response of the cell to changes in operating conditions could be investigated. Of particular interest with respect to the present work would be the response of the cell to ON/OFF cyclic operation of the power supply. Since, however, the presently accepted mode of cell operation is not cyclic, more general interest would involve cell response to accidental perturbations, for example temporary spacecraft depressurization or loss of power. The present simulation cannot deal with cell response to any time-dependent change in the independent variable vector. Approximate response may, however, be predicted to slowly changing conditions by simply executing the simulation with successively altered input variables.

True time response prediction by the simulation would require a great deal of further work, both theoretical and experimental. Addition of the variable time to the transport equations of the air stream presents no theoretical difficulty, but the model would require great simplification to make the addition worthwhile. In the present work, both explicit and implicit algorithms were investigated for digital computer simulation. The best the implicit algorithm could do was 5000 computer execution seconds per problem second, limited by stability criteria on the size of the increment in time that could be used. The simplest implicit algorithm required about sixty seconds of execution time per individual time increment. The large EAI 680 analog computer of the PSU Hybrid Computer Laboratory contained insufficient components and digital-analog channels for any solution method conceived to take advantage of its excellent time integration capability.

With respect to the electrochemical cell model segment, transient electrode processes are little understood. Exhaustive experimental half-cell studies will be required to obtain time-dependent overvoltage characteristics. The result would be a "black box" transfer function for each electrode type and electrode reaction as a function of the variables current density, electrolyte type and concentration, temperature, and time. Certain qualitative theories and observations concerning transient electrode processes are available in the literature to assist in designing the transfer function, but there will be a good deal of empiricism involved, as well as the experimental determination of arbitrary constants. There can be no guarantees that actual experimental determination will not be the more rapid, accurate, and inexpensive means of studying transient response of the WVE cell.

# PART II

## Cyclic Operation of WVE Cell

In a preliminary experimental investigation, Engel (10) observed that cyclic operation of the WVE cell power supply led to increased power consumption efficiency. On the basis of the electrical work required to electrolyze a given mass of water, up to eight percent improvement over DC operation was reported. Power consumption was reported to be a function of cycle parameters and DC operation time prior to cycling. Such an efficiency increase is significant, particularly so in a spacecraft with its limited power generation equipment. The present work, based upon the preliminary study of Engel, was to more fully study the effects upon cell power consumption of cyclic operation.

To summarize the work done in the preliminary study, Engel reported that "ON/OFF" cycling was the only type capable of effecting a performance increase. A cycle consisted of a period of "ON" time during which the cell was connected to an electric power supply, followed by "OFF" time during which power was disconnected and both cell electrodes grounded. Simultaneous grounding of the gas barrier was observed to increase efficiency somewhat. The degree of improvement due to cycling was reported more dependent upon the length of time that the cell was operated at steady state before cycling was begun than upon the cycle parameters. The data of Engel are summarized in Figure 11.

The experimental procedure used in gathering the data was the following. In the first series, the cell was allowed to operate under direct current, supplied by a constant voltage power source, for two hours after start-up. After two hours, cycling was initiated, with

FIGURE 11

Preliminary Data of Engel* for Cell Power Consumption Under Cyclic Operation

Experimental Parameters

| | |
|---|---|
| Cell type: | ARC Lucite module |
| Electrodes: | PT-TA[1] |
| Air flow rate: | 25 cc/sec |
| humidity: | ca 50% RH |
| Steady state voltage: | 2.1 - 2.2 V DC |
| Steady state current: | 1.1 - 0.9 A DC |
| Steady state work: | 400 - 450 watt-sec/25 cc $H_2$ |

Experimental Data

| "ON" time sec | "OFF" time sec | Prior Steady State Time hr | % Improvement[2] |
|---|---|---|---|
| 130 | 0.5 | 2 | 3.5 |
| 130 | 0.5 | 18 | 7.3 |
| 130 | 1.0 | 2 | 5.2 |
| 130 | 1.0 | 18 | 7.9 |
| 130 | 2.5 | 2 | 4.6 |
| 130 | 2.5 | 18 | 7.7 |
| 130 | 5.0 | 2 | 2.7 |
| 130 | 5.0 | 18 | 7.1 |
| 280 | 1.0 | 18 | 4.8 |
| 280 | 5.0 | 2 | 4.4 |
| 280 | 5.0 | 18 | 6.2 |
| 280 | 15.0 | 2 | 3.3 |
| 420 | 15.0 | 2 | 3.8 |

* Engel, A. J., ASEE-NASA Summer Inst. Final Report (1967).

[1] Type AA-1 black platinized tantalum screen electrodes, American Cyanamid.

[2] Improvement in power consumption efficiency relative to DC power consumption.

each set of cycle parameters maintained for about six cycles. The work required to produce 25 cc of hydrogen gas was then measured and the cell then operated under a different set of cycle parameters. The acquisition of the second set of data was essentially the same, except that the cell was run for eighteen hours under DC prior to cyclic operation. The steady state voltage, current, and work were those quantities measured at the end of each period of DC operation. The cell voltage at the end of two hours of DC operation was 2.1 V; 2.2 V after 18 hours.

Part of the purpose of the present experimental work was to be the confirmation that cyclic operation did indeed increase the efficiency of the water vapor electrolysis cell. Given that confirmation, cycle parameters were to be manipulated over broad ranges in order to attempt to isolate a combination that would give a maximum WVE cell power consumption efficiency. Cells with two different electrode types, bright platinum and platinized tantalum screen, were to be investigated to determine whether the phenomenon was electrochemical in nature.

The following description of the experimental work performed in the present investigation begins with details of the special equipment, and procedures for their use, involved. Following that are presented the results of the experimental investigation of power consumption efficiency under cyclic operation for cells with both electrode types. Finally is a discussion of those results and the conclusions drawn therefrom.

# Chapter 4

## EXPERIMENTAL EQUIPMENT

The experimental equipment used in the present study of the NASA water vapor electrolysis cell fell into three categories: the WVE cell itself, independent variable measurement and control equipment, and devices for measurement of cell dependent variables. Beginning with the experimental WVE cell, each category of equipment is discussed, in turn, below.

### 1. Experimental WVE Cell

A bench scale model of a single water vapor electrolysis cell was used in the present experimental investigation. The cell was manufactured and supplied by the Ames Research Center of the National Aeronautics and Space Administration. It is a standard laboratory cell, referred to as the "ARC Lucite Module", after its place of manufacture and material of construction. An exploded-view rendering of the test cell is presented in Figure 12.

The air manifold, shown at the bottom of Figure 12, was a machined block of methyl methacrylate containing the 4.75 cm square by 0.159 cm high feed/product air flow channel, one side of which supported the 4.75 cm square cell anode. Two types of anode were studied in the present work, platinized tantalum screen (PT-TA)[1] and 45 mesh bright platinum wire gauze (BRITE)[2], with spot-welded platinum foil leads connecting the electrode to the external electric circuit. The electrolyte mixture was contained in two compartments, separated by a 0.015 cm thick microporous polyvinylchloride[3] gas barrier membrane.

---

[1] Type AA-1, American
[2] Engelhard Industries, 700 Blair Rd, Carteret, N.J.
[3] Synpor, Electric Storage Battery, Yardley, Pa.

FIGURE 12

Expanded-View Rendering of "ARC Lucite"

Experimental WVE Cell*

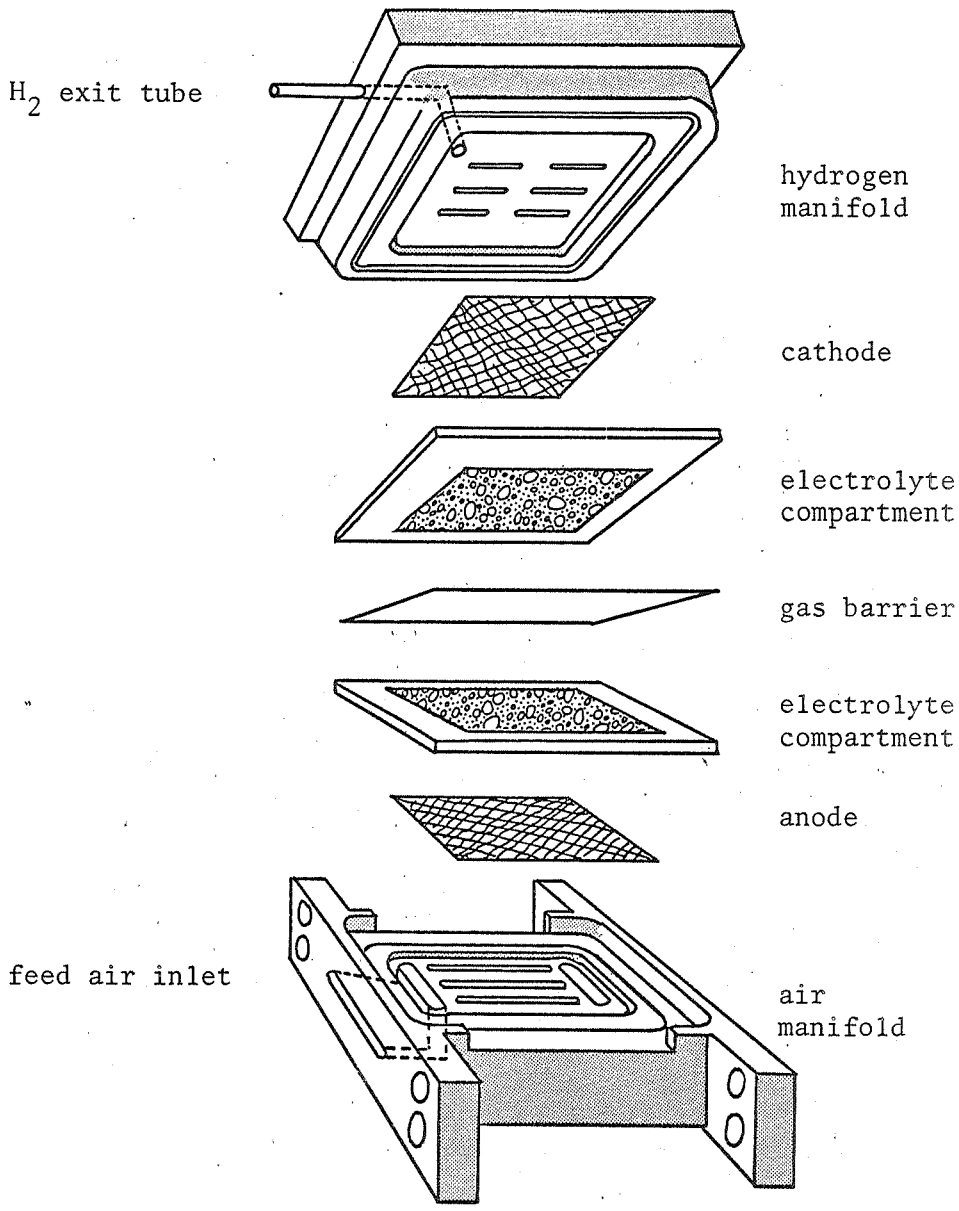


*Courtesy of Graphics Dept., CAI Laboratory, P.S.U.

Each compartment was 4.75 cm square, cut from 0.075 cm Teflon sheet. The electrolyte mixture loaded into the compartments consisted of one part dry CAB·O·SIL M5 silica[1] and nine parts fifty-five weight percent sulfuric acid, by mass. The gas barrier membrane was immersed in the same concentration sulfuric acid for at least a week prior to cell assembly, ensuring that its pores were saturated with charge-carrying species. The cathode, a 4.75 cm square, was of the PT-TA type, and was positioned between the electrolyte and the hydrogen manifold. The hydrogen manifold was again constructed of methyl methacrylate, with a 4.75 cm square by 0.159 cm high closed compartment for the collection of evolved hydrogen gas. A 0.3 cm diameter tube was inserted into the compartment to allow the escape of the evolved hydrogen.

2. WVE Cell Controlled Air Supply

Four independent variables in WVE cell operation refer to the feed air stream: its temperature, pressure, humidity, and flow rate. Inlet air temperature, and the temperature of all other experimental equipment, was controlled at a constant value by control of the laboratory temperature. The heating system of the laboratory, supplemented by a thermostatted electric heater, provided temperature control to within one degree Fahrenheit.

The exit air stream of the WVE cell was vented to the atmosphere, and ambient pressure rarely varied from 735 $\pm$ 3 mm Hg. The pressure drop from cell inlet to exit was too small to be measured at normal flow rates of 25 to 50 standard cc air per second, predicted at about one mm Hg by the present computer simulation of the WVE cell. Inlet air pressure was taken to be ambient, and periodically measured with a

[1] Cabot Corporation, Boston, Mass.

mercury barometer.

With temperature and pressure controlled to the desired degree, the apparatus diagrammed in Figure 13 was assembled to provide the cell with feed air of constant flow rate and humidity. Dried compressed air passed through two-stage pressure reduction and regulation and entered the humidification section. The air stream was then split, part to be passed through a second container filled with calcium chloride particles. The humidified and dry air streams were then rejoined, forming a mixture whose relative humidity depended upon the proportion of the total stream which passed through each container. Control of humidity and flow rate, at constant ambient pressure and temperature, was effected by the pressure regulator and needle valves in each stream of the humidification system. Measurement of air flow rate was by calibrated rotameter, and air temperature and humidity were measured by a precision potentiometric-output hygrometer[1]. Air flow rate was maintained constant to well within one cc per second, usually with no observable deviation. Air humidity was maintained to within 0.3% RH, except during times when slugs of water from the compressed air supply exceeded the ability of the two drying segments to deal with them. Such slugs occurred randomly, and the WVE cell required about two hours to return to normal operation after the perturbation. No damage to the cell was done, the cell current simply increased to account for the excess moisture.

3. WVE Cell Power Supply

Three independent variables are associated with the electric power supply to the WVE cell under cyclic operation: applied voltage, ON

[1] Model 15-3001, Hygrodynamics Inc., Silver Spring, Md.

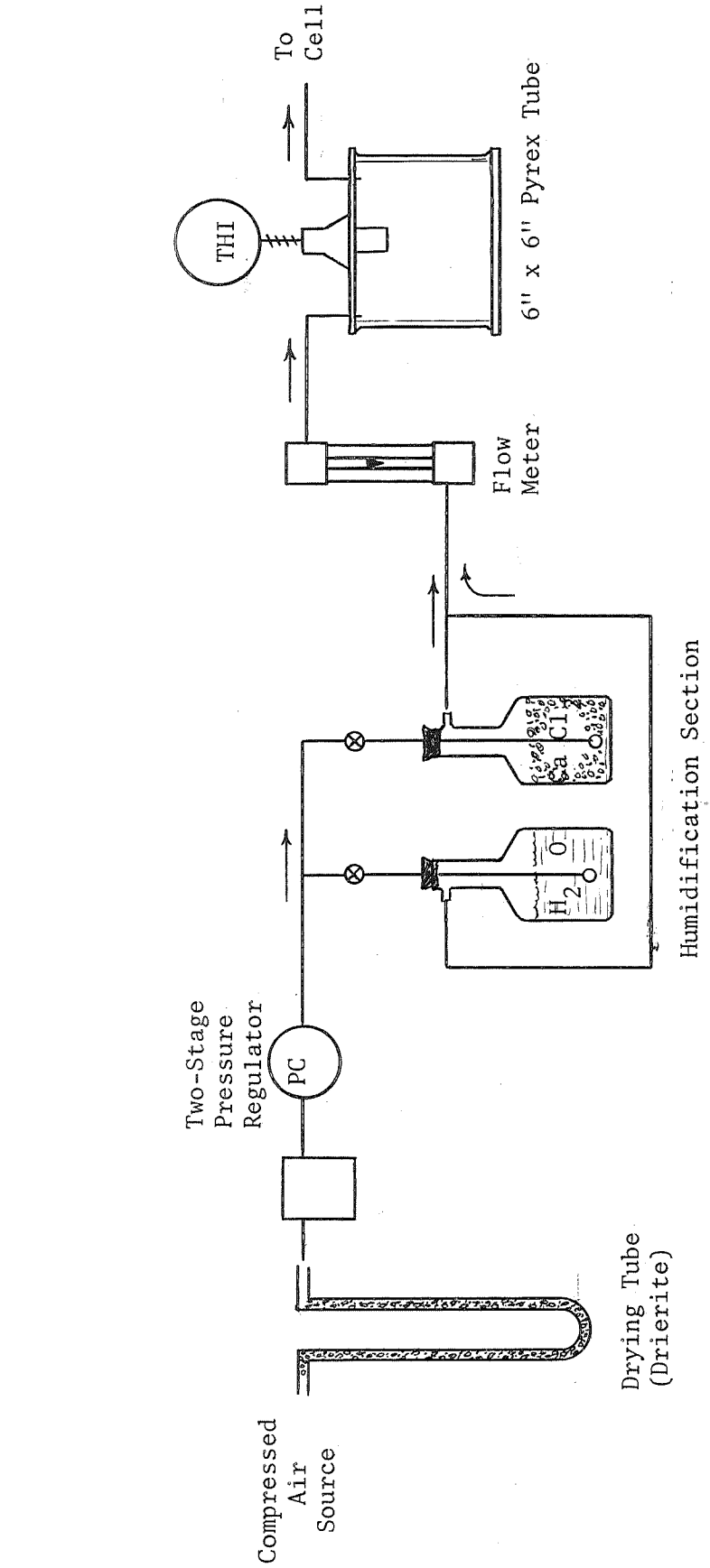


Figure 13

Constant Flow/Humidity Air Supply

cycle time, and OFF cycle time. For direct current operation, the latter two do not apply. Cyclic operation of the water vapor electrolysis cell was effected by the electric circuit diagrammed in Figure 14.

The cyclic operation of this circuit in Figure 11 was controlled by two timers, A and B.[1] They were loaded with the selected "ON" time (Timer A) and the "OFF" time (Timer B), for a cycle. When one timer counted down to zero, it would reset and start the other timer. The circuit diagram shows logical control of the two relays. The state of the timer is either "true/on" or "false/off". If the state of timer A is "true", the flip-flop sets and puts the relays in their "true" positions. When the state of Timer B is true, the flip-flop resets, putting the relays in their "false" positions.

The logic control in the diagram is, for simplification, an abstraction of the electro-mechanical system used.

The other circuit components shown in Figure 14 are the electrolysis cell, a variable dc power source, and a resistance R1. The DC power source[2] was capable of operating in either constant current or constant voltage mode. The resistance R1 was an NBS type 0.1 ohm precision resistor[3] and was used to measure the current drawn by the cell. The ground shown was common to all measuring devices as well. Measurement at all points within the common ground network, showed equality of potential to within one millivolt, with one millivolt 60 Hz noise. The voltage $V_1$, measured at the platinum foil lead to the cell anode, is the total cell voltage. The voltage $V_2$, equal to one tenth the current drawn

---

[1] Series HP5, Eagle Signal, Davenport, Iowa
[2] Model CK5-M, Kepco, Flushing, N.Y.
[3] Model 4015-B, Leeds and Northrup, North Wales, Pa.

FIGURE 14

Schematic Diagram of the Circuit for the Cyclic Operation of the Water Vapor Electrolysis Cell

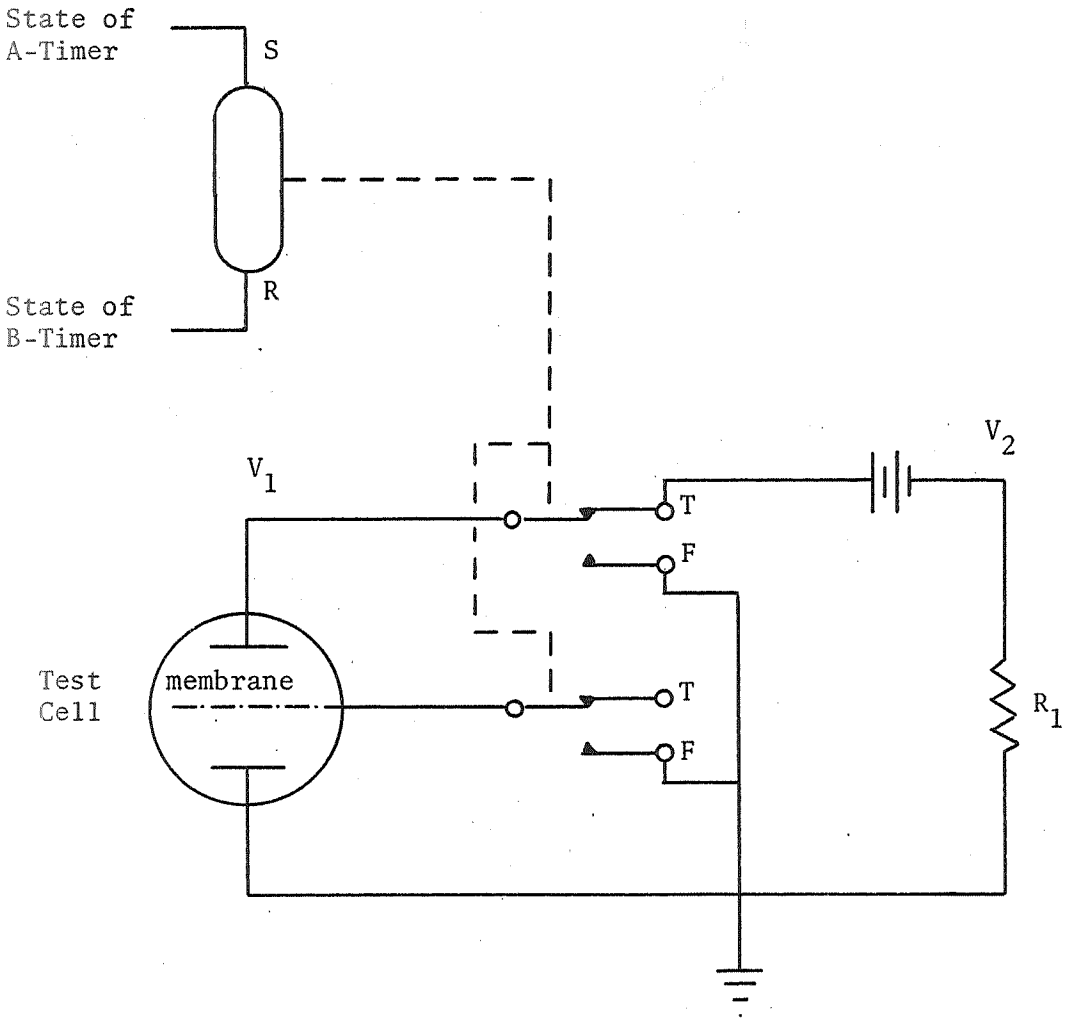

by the cell, was to be multiplied by $V_1$ for measurement of instantaneous cell power consumption, the result being one tenth the power consumed in units of watts. For DC operation the relays were held in the "true" position.

4. Measurement of WVE Cell Power Consumption

Measurement of instantaneous and integral WVE cell power consumption was accomplished by a special purpose electronic analog computer. The two-element computer, shown schematically in Figure 15, consisted of a multiplier and an integrator. The voltages of the current sensing resistor and the WVE cell were multiplied to yield a voltage proportional to the instantaneous cell power consumption, and that voltage was integrated with respect to time to yield a voltage proportional to the electrical work done during the period of integration. Tests performed by Electronics Services, Department of Electrical Engineering, The Pennsylvania State University showed the specific multiplier used[1] to exhibit no output error with output voltage as low as 20 mV. In the integrator, the low dissipation factor feedback capacitor had a measured capacitance of 2.00 μF, and the input resistor was 2.69 M, making the exact integrator "gain" 0.186.

The basis for the power consumption measurements was selected to be the electrolysis of a given mass of water. In transient electrode processes, only part of the total cell current is Faradaic, so that cell current is not related to the rate of electrolysis. Hydrogen production is directly related to the Faradaic current, and also to oxygen generation and water consumption. Volumetric hydrogen production was easily measured

[1]Model 420B, Fairchild Instrumentation, Mtn. View, Calif.

FIGURE 15

Schematic Diagram of the Special Purpose Analog Computer Used As An Indicating/Integrating Wattmeter

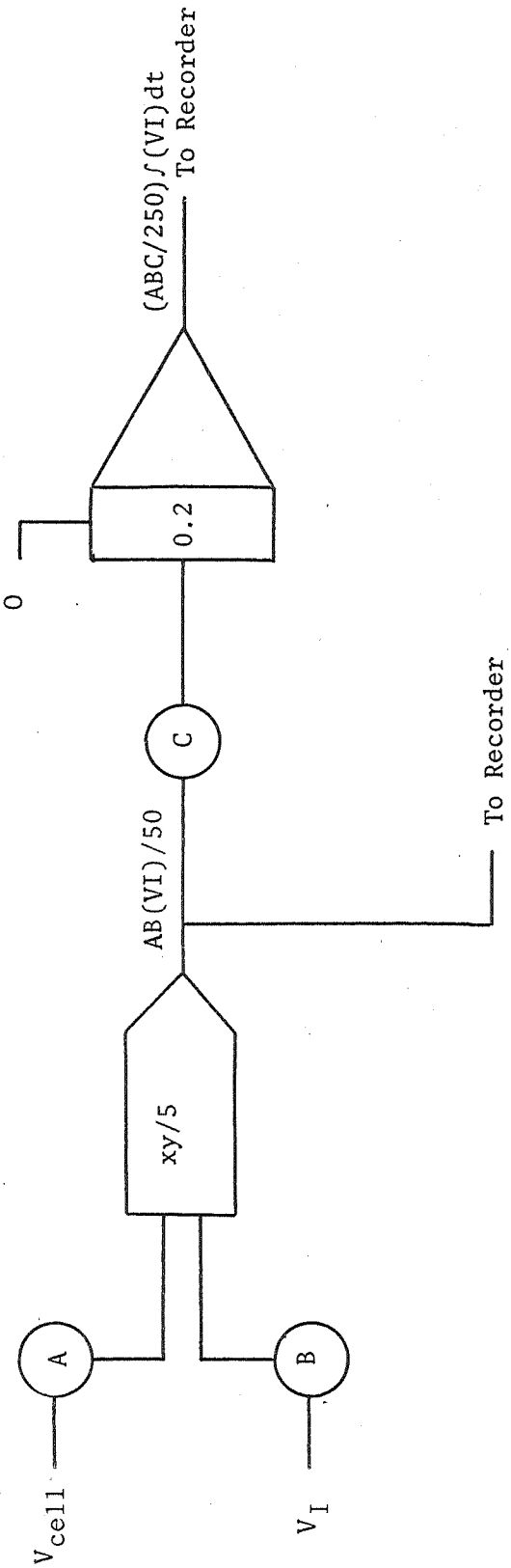

by connecting the WVE cell exit hydrogen line to a soap bubble flow meter. Integral power was therefore measured over the time interval required for a given volume of hydrogen to be produced, generally 50.0 ambient cc.

The hydrogen under the rising soap bubble was saturated with water vapor, and the ambient volumetric production was corrected to account for that and normalized to standard temperature and pressure. Integral power consumption was then calculated in units of watt-sec per 50.0 standard cc hydrogen produced. That value was then multiplied by the hydrogen collection efficiency of the system, which ranged from 0.95 to 1.00 and depended on how well a particular test cell was assembled. Hydrogen collection efficiency was measured under DC operation while the cell was at steady state, all current being Faradaic. Measured hydrogen production, converted to dry $H_2$ at STP, was divided by actual hydrogen production, calculated from cell current, to determine system hydrogen collection efficiency.

# Chapter 5

## EXPERIMENTAL PROCEDURE

The experimental procedure began with the assembly of a test cell, as described earlier. After each assembly procedure the resulting WVE cell was given a new sequence number. Upon attachment of the assembled cell to the power leads and to the feed air and hydrogen collection lines, the power relays were switched to the "ON" position. The cell was then operated in the DC constant voltage mode until the cell current reached a steady value.

The initial period during which cell current decreased lasted at least a week, usually about ten days. Overvoltage rise accounted for only the initial few hours of high current draw, low initial overvoltage allowing large initial current, since the sum of voltages was constant. The decline of cell current over a period of a week, approaching a steady value asymptotically, indicated that the electrolyte charged to the cell was more dilute than the electrolyte at steady state. This was confirmed by the computer simulation, in output presented in Part I.

Upon attainment of steady state operation, the hydrogen collection system efficiency was measured, and the steady state current noted. Since the cyclic power consumption was based upon a given amount of hydrogen generated, the ratio of hydrogen collected to that produced was important. Steady state current, unlike cyclic operation current, had no effect on the integral power required for a given amount of electrolysis. That base state, against which cyclic power consumption was compared, was a function of cell voltage only. Steady state current was used primarily as a diagnostic tool. A change in that current, after the start-up

period, indicated that something was wrong with the cell. After the steady state reference data were acquired, cycling began.

Cyclic operation was initiated by loading the "ON" and "OFF" cycle timers with a selected combination of cycle parameters. The power relays were then switched to the control of the cycle timers. During the first few cycles, each timer setting was independently checked and adjusted as necessary. The current supplied by the constant-voltage DC source was continuously monitored with a strip-chart recorder. The current versus time profile was akin to that of a changing curve for a capacitor and resistor in parallel, a step change high followed by decrease in current draw appearing to be exponential. At the end of the cycle, the current supplied by the power source dropped to zero in a step change. This is shown in Figure 16.

The term "steady state" has no meaning in a cyclic process, but after a period of time, succeeding current-time profiles became identical. The term "pseudo steady state" has been applied to that condition. As in the case of steady state operation, cell current was observed to be characteristic of cell operation.

The current at the end of a cycle was quite easy to measure on the strip chart: the intersection of a slowly changing horizontal line at the end of "ON" time and a straight vertical line at the initiation of "OFF" time. That value of current ($I_c$ in Figure 16) was observed to be characteristic of the cell current-time profile. For a given data set, the equality of succeeding values of $I_c$ indicated the attainment of pseudo steady state.

Power consumption measurements began after the cell was operating at its pseudo steady state. This was usually two or three days after

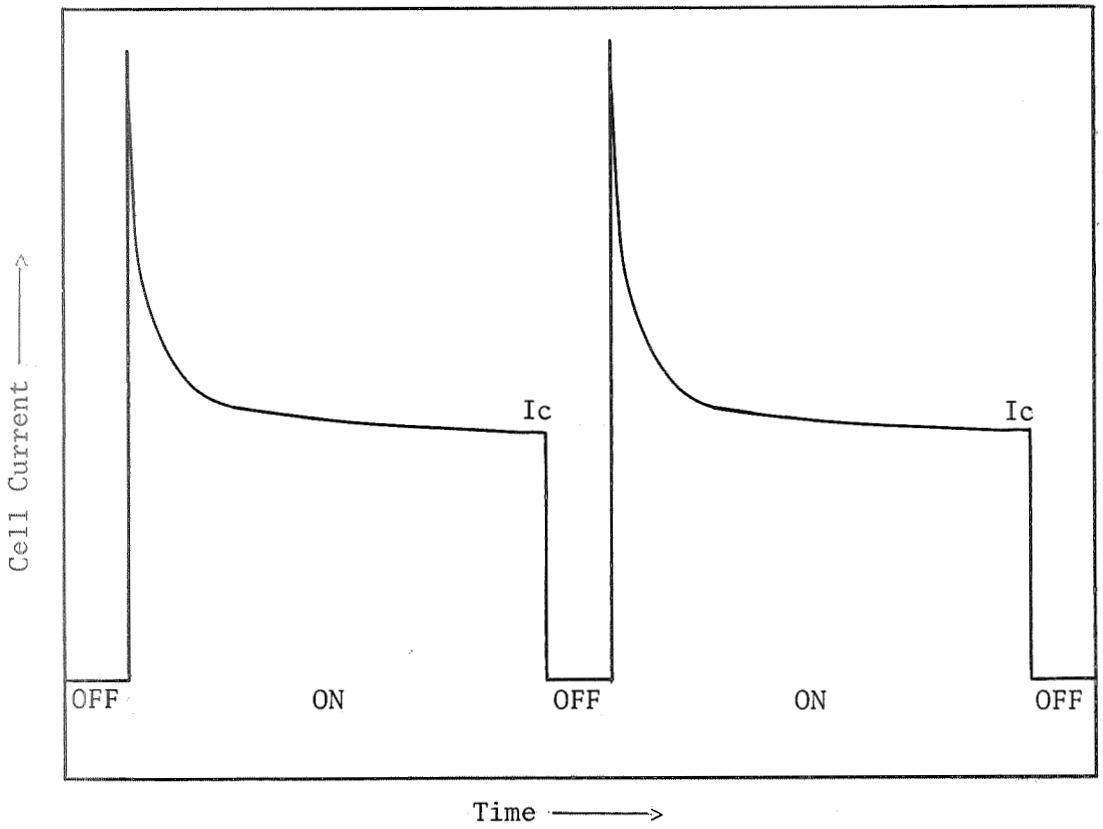


FIGURE 16

Rendering of Typical Applied Current Versus Time Under Constant Voltage "ON/OFF" Cyclic Operation of the WVE Cell.

cycle initiation from steady state operation. Starting from a previous pseudo steady state, the time period ranged from five to twenty hours, depending on the magnitude of the change in cycle parameters. Non-desired perturbations in the WVE cell independent variable vector caused extension of those time periods.

The measurement of cyclic operation power consumption started with a soap bubble beginning its rise in the hydrogen flow meter. When the meniscus reached the zero-volume mark, a DPDT switch was thrown to begin measurement. The closing of one contact started an electric timer, which gave a direct reading of the time interval involved in the measurement. The second pole of the switch was a remote "hold/operate" integrator mode control. Open, the control caused the integrator output to remain constant, and upon closing the contact the integrator was permitted to integrate the output of the multiplier. Before a measurement, the integrator output was held at zero volt.

Monitoring of the voltages proportional to cell instantaneous and integral power consumption was carried out using the two channel strip chart recorder. When the soap bubble meniscus in the hydrogen flow meter reached the end point, usually the 50.0 $cm^3$ mark, the DPDT switch was opened, ending the measurement. The data recorded for measurement were the following:

1. Date and time of measurement
2. Ambient temperature
3. Ambient pressure
4. Feed air flow rate
5. Feed air relative humidity
6. Steady state cell voltage
7. "ON" cycle time

8. "OFF" cycle time
9. Volume ambient hydrogen produced
10. Time required for hydrogen production
11. Integral power required for hydrogen production, in terms of integrator output voltage

Variations in measured integral power consumption were observed which were dependent on when in a cycle the measurement was initiated. This was particularly true for the cases where measurement time and cycle time were approximately equal. For such cases several measurements were made with initation points at different parts of the cycle, and the results were averaged. Those were apart from replicate measurements.

The raw experimental data were then refined, first by the conversion of the measured ambient volume of water-saturated hydrogen production to true dry hydrogen production at standard conditions. The integrator output voltage was then converted to electrical work in watt-seconds. The ratio of work to true hydrogen production was multiplied by the arbitrary base hydrogen production of fifty standard cubic centimeters. The result of the power measurements was then expressed as the amount of electrical work required by the cell to produce 50 standard cc dry hydrogen. This was then compared with the work required to produce the same amount of hydrogen at steady state.

A series of cyclic operation power measurements usually involved changing of the "ON" cycle time while maintaining a constant "OFF" time. No pattern was followed in the choice of successive "ON" times, so that the possibility of a time-dependent bias was minimized. Constant "OFF" time for a series was arbitrarily selected for convenience. For validity, all cyclic operation power consumption measurements required the same base

state reference. That reference was the WVE cell operating at steady state but otherwise controlled by the same independent variable vector. Therefore, cyclic operation of the WVE cell would be interrupted every ten days, and the "cell" would be switched to DC operation. If steady state cell current and hydrogen collection efficiency remained unchanged from the previous measurements, the cyclic operation data were considered valid. If however, either value was different from its predecessor invariably lower - an abnormal condition was indicated.

If the deviation was in cell current, the series was terminated and the cell disassembled. A decrease in hydrogen collection efficiency required leak detection and correction procedures, but not series termination. In either case, the data from the preceeding period of cyclic operation could not be assumed referenced to a constant base state and were discarded.

Decisions related to the values of controlled independent variables, apart from cycle parameters, were either arbitrary or imposed. Feed air flow rate was selected to be 24.0 standard cc/sec. Previous work with the ARC Lucite module (10,31) had a value of 25, and the flow rate in the present work was the closest marked point on the air flow meter. Cell voltage of 2.20 V for cells with PT-TA electrodes was that used by the previous workers. For the BRITE anode cells, 2.60 V gave approximately equal cell current. Feed air humidity used by the previous workers was 50% RH. The closest mark on the hygrometer indicator corresponded to 49.5% RH at the base air temperature of 84 °F. That temperature was chosen as the lowest that would generally be above the uncontrolled temperature of the laboratory, since measurements began in late spring and continued throughout the remainder of the year. The temperature was

unusually high because air conditioning equipment was not available. With no theoretical basis, the preliminary cyclic operation data of Engel (10) and experience were the bases for selection of cyclic parameters.

# Chapter 6

## EXPERIMENTAL RESULTS

In the present investigation of cyclic operation of the water vapor electrolysis cell, power consumption was measured as a function of three real variables. They were electrode type, "ON" cycle time, and "OFF" cycle time. Consolidated data sets are presented for each of the two different electrodes.

The investigation of cyclic operation power consumption in PT-TA electrode cells is discussed first. The experimental data are presented, followed by a discussion of the results. The same is then presented for studies with the BRITE electrode cells.

### 1. Cyclic Power Consumption in PT-TA Cells

Chronologically, the first data set was generated from cells with PT-TA electrodes. The WVE cell sequence numbers were 1 and 2. Cell number one was to be the basis for a preliminary study of WVE cell operation, both DC and cyclic. It was initially operated for an extended period, 430 hr., under direct current prior to cyclic operation. Apart from confirmation of the extended operation capability of the cell, the period of time was used in on-line evaluation of the experimental equipment and familiarization with measurement and operation procedures.

Upon initiation of cyclic operation only a single measurement was made for each set of cycle parameters. Contrary to later practice, "ON" time was held constant while "OFF" time was varied from one to five seconds, the range investigated in the preliminary study of Engel (10). In the earlier work, a range of two through seven minutes "ON" time was covered. In the present work, "ON" time was to be greater than or equal

to 0.5 min. After nine cyclic operation power consumption measurements, the cell was returned to DC mode for a period of twenty hours. It returned to its original steady state of 1.00 amp at 2.20 volt. A replicate power measurement at 2.0 min "ON" and 1.0 sec "OFF" was made after resumption of cyclic operation. Before the DC operation the power consumption at that cycle was measured to be 895 watt-sec/50 scc $H_2$. The replicate, after 20 hr. DC, yielded a value of 897. No difference existed between cell cyclic power consumption after 430 hr. DC operation and that after 20 hr. DC operation. Following another seven cyclic operation power measurements, the 2.0/1.5 cycle was again replicated. The measured integral power consumption of 888 watt-sec/50 scm $H_2$ was not at all significantly different from the preceding two values. Previous history apparently had no effect on cyclic operation power consumption.

Data after that replicate 2.0/1.5 cycle were discarded for Cell No. 1. The next period of DC operation showed a cell current of 0.75 amp. The series was terminated and the cell disassembled, after 23 days total operation, five cyclic. Cell No. 2 was assembled and put on-stream for 100 hr. of initial DC operation. Cell steady state current was 1.05 amp at 2.20 V, and hydrogen collection system efficiency was 0.97. Upon initiation of cyclic operation, more replicate power consumption measurements were taken than earlier. After three days of cyclic operation, a DC run confirmed the constancy of the base state. After three more days of cyclic operation, another period of DC operation showed cell current decreasing again. Cell No. 2 had been operating properly for a period of ten days, three under cyclic operation. Again a data set was discarded.

Upon disassembly of both Cells No. 1 and 2, inspection showed only two obvious abnormalities in each case. First the anode was almost totally

denuded of platinum black, leaving only the tantalum screen support. Second, the electrolyte had become infused with black color. The anode compartment electrolyte had a shiny, brittle black surface at the gas barrier interface. The cathode compartment electrolyte was generally less black and brittle than that on the anode side of the barrier. It was apparent that platinum black particles had migrated from the anode toward the cathode, possibly clogging the pores of the gas barrier to decrease cell current by increasing internal resistance. The change in the anode surface, from an essentially continuous surface of fine platinum black particles to a coarse mesh of tantalum screen, affected the electrode kinetics unfavorably. The result, of effectively changing both anode type and surface area, could not be analyzed quantitatively by visual inspection. Qualitatively, the result would be a decrease in apparent current density with decrease in real electrode surface area, and increased overvoltage, since tantalum is a less effective catalyst than platinum.

1A. Experimental Results

The results of power consumption measurement for Cells No. 1 and 2 under cyclic operation are summarized in Table V, and displayed graphically in Figure 17. The data are not comprehenisve, but are nonetheless quite informative. They show a strong dependence on cyclic operation parameters. As "ON" cycle time approaches zero, power consumption per unit hydrogen production tends to infinity. For increasing "ON" time, the data show decreasing power consumption with a maximum measured efficiency improvement of ten percent at the 5.0/1.0 cycle, relative to steady state operation. Obviously, as "ON" time approaches infinity, the 1.0, 3.0, and 5.0 second "iso-OFF" lines of Figure 17 will approach the steady state value of 948 watt-sec for the production of

TABLE V

Cyclic Operation Power Consumption Data

Cells No. 1 and 2, PT-TA Electrodes, $E_T$ = 2.20 V

| Cell No. | ON[1] (min) | OFF[2] (sec) | N[3] | $Work_M$[4] (watt-sec) | Coll[5] Eff | $Work_C$[6] (watt-sec) | %[7] IMP |
|---|---|---|---|---|---|---|---|
| 1 | 0.5 | 5 | 1 | 1239 | 0.96 | 1189 | -25.4 |
| 1 | 1 | | 1 | 1040 | 0.96 | 998 | - 5.3 |
| 2 | 1 | | 5 | 1036 | 0.97 | 1005 | - 6.0 |
| 1 | 1.5 | | 1 | 992 | 0.96 | 952 | - 0.4 |
| 1 | 2 | | 1 | 948 | 0.96 | 910 | 4.0 |
| 1 | 3 | | 1 | 924 | 0.96 | 887 | 6.4 |
| 1 | 0.5 | 3 | 1 | 1099 | 0.96 | 1055 | -11.3 |
| 1 | 1 | | 1 | 975 | 0.96 | 936 | 1.3 |
| 1 | 1.5 | | 1 | 957 | 0.96 | 919 | 3.1 |
| 1 | 2 | | 1 | 932 | 0.96 | 895 | 5.6 |
| 1 | 3 | | 1 | 908 | 0.96 | 871 | 8.1 |
| 1 | 0.5 | 1 | 1 | 992 | 0.96 | 952 | - 0.4 |
| 1 | 1 | | 1 | 932 | 0.96 | 895 | 5.6 |
| 2 | 1 | | 3 | 943 | 0.97 | 915 | 3.5 |
| 1 | 1.5 | | 2 | 917 | 0.96 | 880 | 7.2 |
| 1 | 2 | | 3 | 930 | 0.96 | 893 | 5.8 |
| 1 | 3 | | 1 | 900 | 0.96 | 864 | 8.9 |
| 2 | 5 | | 1 | 883 | 0.97 | 857 | 9.6 |
| 2 | 1 | 0.5 | 2 | 897 | 0.97 | 870 | 8.2 |
| 2 | | 0.3 | 6 | 894 | 0.97 | 868 | 8.3 |
| 2 | | 0.2 | 6 | 896 | 0.97 | 870 | 8.2 |

[1] "ON" cycle time, min

[2] "OFF" cycle time, sec

[3] Number of measurements

[4] Average measured electrical work to produce 50 standard cc $H_2$

[5] Hydrogen collection system efficiency

[6] Average electrical work corrected for $H_2$ collection efficiency

[7] Percent improvement in power consumption efficiency, related to steady state power consumption of 948 watt-sec for production of 50 standard cc$H_2$ at 2.20 V.

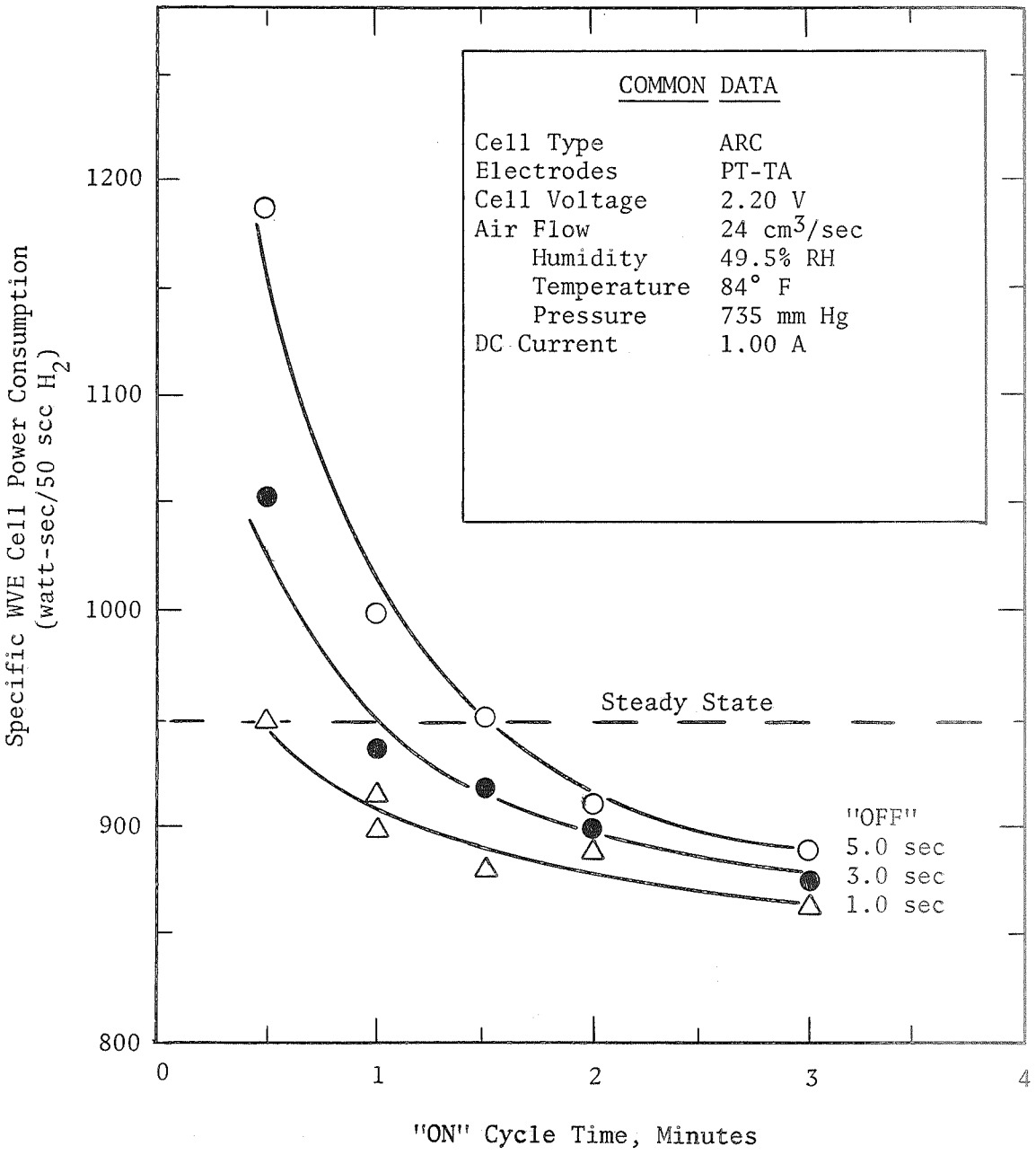


FIGURE 17

Cyclic Operation Specific Power Consumption as a Function of "ON" and "OFF" Cycles Times, Cells No. 1 and 2.

50 standard cc hydrogen. The three iso-OFF specific power consumption curves must, then, go through a minimum. An optimum specific WVE cell power consumption, therefore, exists as a function of "ON" cycle time for the PT-TA electrode cell. That optimum is larger than any "ON" cycle time measured with Cells No. 1 and 2.

The data are inconclusive with respect to the possibility of optimum "OFF" times. The data show monotonic efficiency increase with decreasing "OFF" cycle time. The last valid series of cyclic operation measurements with Cell No. 2 were with the "OFF" cycle timer progressively approaching its minimum setting, 1/6 second, for a constant "ON" time of 1.0 minute. No difference in specific power consumption was measured over the range 0.5 to 0.2 second "OFF" time, indicating approach to a constant value as "OFF" time approaches zero. It is apparent that iso-ON curves, corresponding to the iso-OFF's of Figure 17 would show specific power consumption variation almost linear with "OFF" cycle time. The small range of "OFF" cycle times investigated precludes making that generalization, however.

1B. Discussion of Results

There were observed six general results of the cyclic operation power consumption investigation of Cells No. 1 and 2, with PT-TA electrodes. They are the following:

1. Specific power consumption (integral power required for the electrolysis of a given mass of water) under cyclic operation is not a function of previous operation history at pseudo steady state.
2. Specific power consumption tends toward positive infinity as "ON" cycle time decreases.

3. Specific power consumption decreases as "OFF" cycle time decreases.

4. Specific power consumption approaches a finite value as "OFF" cycle time approaches zero.

5. Specific power consumption may be at least ten percent lower than under non-cyclic operation, and a minimum as a function of "ON" cycle time exists in those cases.

6. The PT-TA type electrode is not suited for extended or severe use in the WVE cell.

The first result apparently contradicts the preliminary results of Engel (10), that specific power consumption efficiency increase depended more strongly on the length of the preceeding period of steady state operation than on the cycle parameters. The difference is, however, only with respect to the reference state. The present work is referenced to an absolute steady state, which cannot be attained within two hours of non-cyclic operation, the base state for the first data set of Engel.

The second result is not as obvious as it would appear intuitively. Indeed, results 2, 3, and 4 are due to the same phenomena - the nature of the platinum electrode in the water electrolysis reaction, and the electrical connections involved in the "OFF" part of the cycle. Simply, the electrochemical reaction depends on a layer of adsorbed atomic oxygen on the anode (atomic hydrogen on the cathode). In the initial application of power to the cell, a certain amount of electrical charge (non-Faradaic current) is required for coverage of the metal surface. In general, the higher the steady state surface coverage, the better the electrochemical reaction. A platinized surface results in higher specific surface area, and lower reaction overvoltage, than for solid platinum. Chemisorption

is a relatively slow physical process, and providing a charge "sink" by grounding both electrodes during the "OFF" cycle does not result in immediate desorption of all the atoms. As long as the anode has any adsorbed oxygen (hydrogen for the cathode) it will continue to have a potential (9).

With the above as a basis, results number 2, 3, and 4 may be readily explained. Upon initiation of the "OFF" part of the cycle, the adsorbed species do not immediately desorb, and the reaction most readily taking place at the still-charged electrodes is production of water from hydrogen and oxygen. This "fuel cell" reaction generates current sufficient to maintain a fraction of atomic hydrogen and oxygen adsorbed onto the platinum. Even with the strong tendency for desorption provided by the grounding of both electrodes, the fuel cell reaction continues, consuming at least a part of the hydrogen and oxygen generated during the "ON" part of the cycle.

Therefore, for finite "OFF" cycle time, a sufficiently short period of "ON" time will generate exactly as much hydrogen and oxygen as consumed in the succeeding "OFF" part of the cycle. Electric power will have been expended for no net again, and the specific cell power consumption would be positive infinity. At constant "ON" time, a shorter period of "OFF" cycle time would mean less product consumed in the fuel cell reaction. Since hydrogen production would then be greater per unit of power expended in the "ON" cycle, the specific cell power consumption would decrease. As "OFF" time approaches zero, no hydrogen is consumed during the infinitesimally small period that the electrodes are grounded. This would not, however, be equivalent to DC operation, as a great deal of discharge is almost instantaneous.

This is shown in the charge/discharge curve of Figure 18. The curve was obtained in the following way. Beginning with both WVE cell electrodes at ground potential a step input of 1.0 amp was fed to the cell. After forty seconds, power was disconnected and the cell electrodes shorted together. Cell voltage rose vertically with time initially due to cell impedance, then rose more slowly as overvoltage increased with time. Cell voltage reached ninety percent of its steady state value of 2.20 V over the forty seconds, but overvoltage had attained only 75 to 80 percent of its steady state value. Upon current cut-off cell voltage dropped, as both electrodes were attached to ground, but it leveled off at about 0.25 V for about ten seconds before falling off to ground potential.

During the discharge phase the WVE cell acted as a fuel cell, consuming hydrogen and oxygen to make water. The length of time that the plateau value of 0.25 V was maintained depended on the amount of pure hydrogen available as fuel in the collection system reservoir. Starting a discharge with more than fifty cc of hydrogen trapped under a soap bubble in the flow meter, the plateau value of cell voltage was maintained until the soap bubble had been sucked into the hydrogen manifold. It is apparent that in cyclic operation of the PT-TA WVE cell, a sufficiently large "OFF" time could consume all the hydrogen and oxygen produced in any given "ON" cycle time, assuming a sufficient hydrogen fuel supply. Hydrogen supply is the controlling factor, since it is likely to be exhausted before the oxygen in the feed air stream.

Result 5, referring to the change of specific cell power consumption with "ON" cycle time, is not wholly understood at present. It probably has to do with the potentiostatic (constant applied voltage) method of cycling, applying and disconnecting a constant voltage power source to the

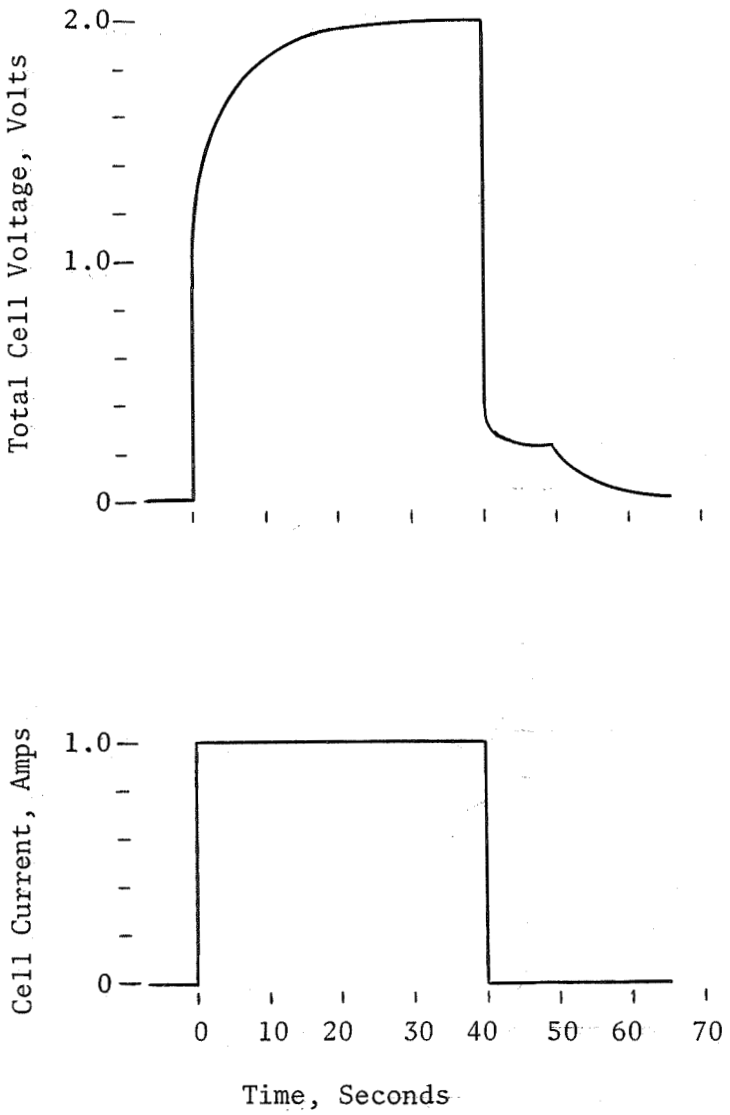


FIGURE 18

Constant Applied Current Charge/Discharge Curve for Cell No. 1 with PT-TA Electrodes.

cell. In potentiostatic cylcing, the cell voltage versus time profile remains much like that portrayed in Figure 18 for galvanostatic charge/discharge. However, the applied current-time relationship is quite different. At initiation of "ON" time, applied current makes a step change from zero to a very high value, immediately thereafter falling off rapidly, then progressively more slowly until the end of the "ON" cycle. It then changes stepwise to zero, as shown in Figure 16.

All that is known at present of the magnitude of the initial current surge is that it is greater than five amps at applied voltage of 2.20 V. The power supply used was protected against higher amp draw, switching electronically from constant voltage to constant current mode automatically at its design limits. While part of the initial high current is non-Faradaic, observation showed a great deal of electrolysis also occurring. Soap bubble rise in the hydrogen flowmeter was always more rapid at the beginning of an "ON" cycle, as was bubble evolution at the electrodes, than near the end.

Initially, all the current drawn in an "ON" cycle is non-Faradaic. Measurement has shown a minimum period of time of 10 to 13 microseconds under power before water electrolysis can proceed (29). Therefore, as "ON" cycle time approaches zero, cell specific power consumption approaches positive infinity. As "ON" time increases from zero, the Faradaic fraction of applied cell current increases toward unity.

As "ON" time increases from zero, cell voltage increases, ever less rapidly, toward its steady state value, as overvoltage builds up. Cell power consumption is the product of cell voltage and cell current drawn, so the lower initial cell voltage would tend to decrease the magnitude of the expression relative to its steady state value.

However, the high initial voltage, and displays of instantaneous power versus time resembled current-time profiles.

Although initially the fraction of Faradaic current was low in the "ON" cycle, the total current was so high that the absolute amount of Faradaic current was higher than would have been at an equal steady state instantaneous current-voltage product. It is thought that the Faradaic current, starting from zero at a few microseconds after initiation of "ON" cycle time, builds up rapidly, overshoots its corresponding steady state value, and approaches steady state asymptotically from above, as shown in Figure 19. The Faradaic current would be initially lower than the steady state current at the same level of power consumption, then higher and eventually the same.

The time integral of specific power consumption would not begin to show improvement until some time after the Faradaic current had exceeded its corresponding steady state value because of the initially relatively low Faradaic current. Then, if Faradaic current were still higher than the corresponding steady state current at the same power consumption, the specific integral power consumption would become lower than that for an equal period of steady state operation. As Faradaic current decreased to its steady state value, specific integral power would still be less than for a like period of steady state operation. As time approached infinity, the specific power consumption difference would approach a constant, but the ratio of cyclic to steady specific integral power consumption would approach unity.

The preceeding analysis of WVE cell power consumption under cyclic operation did not mention the dilution of the cell electrolyte during the "OFF" cycle, by both water generated in the fuel cell reaction and water

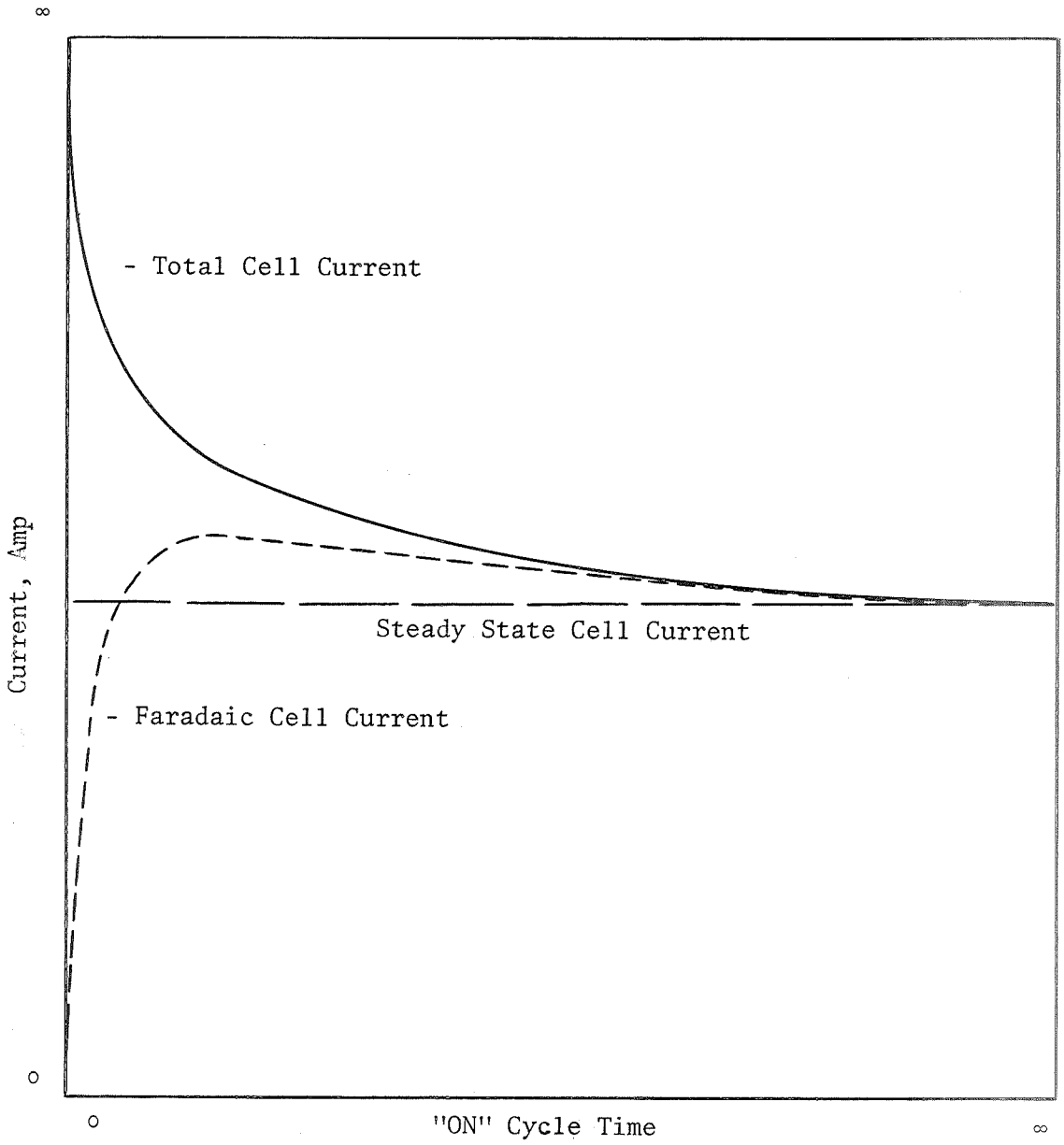


FIGURE 19

Proposed Current-Time Relationship During "ON" Cycle Time

absorbed from the air stream. Such dilution lowers the resistivity of the sulfuric acid, above about forty weight percent, allowing increased Faradaic current to an unknown degree. Neither electrode regeneration, hypothesized by Engel (67), nor other possible unknown effects was mentioned.

Implicit in the above analysis was the assumption that the cell was operating normally, which it did for unsatisfactorily short periods of time with the PT-TA type anode. Loss of platinum black from the cell anode, increasing with operation time and cell temperature, has been reported by all previous investigators (3,6,7,8,31), invariably as a minor observation. That this built-in self-destruct property was not pointed out is unaccountable.

The remainder of the present investigation of cyclic operation of the water vapor electrolysis cell was carried out using a solid bright platinum anode. Study of the variation of cyclic operation performance with electrode type had been planned, but the changeover occurred before completion of the PT-TA electrode cell data set. A cell failure rate of twice per month due exclusively to inherent anode properties was considered excessive.

2. Cyclic Power Consumption in BRITE Cells

Operation of the WVE cells with bright platinum anodes was at a steady state voltage of 2.60 V. Due to the lower specific surface area of platinum wire, the overvoltage for the water electrolysis reaction was higher than that of the PT-TA electrodes. The particular value of 2.60 was selected as the cell voltage most accurate to measure which would yield a current draw comparable to that of the PT-TA cells. The scales on the potentiometric recorder were such that maximum reading accuracy was obtained at intervals of 0.05 V. The steady state cell current of 0.92

amp, eight percent lower than in the PT-TA cells, was as close as was attainable. Apart from the change of anode and of steady state cell voltage, there was no change in the values of the independent variables from the PT-TA cell investigation.

The WVE cells used had sequence numbers 3 through 8. None of the cells exhibited failure due to inherent electrode problems, but four of the six did fail, due to non-desired perturbations. Cells No. 3 and 6 failed due to flooding, after normal operation of 45 and 21 days, respectively. Cell No. 3 was improperly sealed from the atmosphere during a 4-day interruption of experimental work. The electrolyte absorbed ambient water vapor and expanded through the porous electrodes, clogging the air and hydrogen manifolds. Cell No. 6 flooded while on-stream due to a 12-hour university power failure over a weekend.

Cell No. 5 failed due to the electrolyte drying out after 15 days of normal operation. During an unattended overnight on-stream period, the flow rate of the feed air went to zero. An inadvertent movement of the pressure regulator valve stem by the maintenance staff is assumed. Cell No. 7 failed while being attended by a colleague to allow the taking of a short business trip. No good explanation was discovered.

Cell No. 4 did not fail, but was disassembled for visual inspection after 33 days of normal operation at the end of a series of measurements.

Beyond non-desired operating condition perturbations, the BRITE electrode cell data set distinguished itself from that of the PT-TA series in four ways. First, there were many replicate power consumption measurements at each set of "ON" and "OFF" cycle parameters, allowing statistical analysis of the confidence to be placed in the measurements. Second, sufficient data were acquired to isolate an optimum power consumption

efficiency with respect to cycle parameters. Third, the region in the neighborhood of the optimum was investigated, holding cycle parameters constant and varying air temperature and flow rate and cell voltage. Finally, a cell was operated at a given set of cycle parameters for at least two days, much longer than for the PT-TA cells, to assure attainment of pseudo-steady state.

2A. Experimental Results

The results of power consumption measurements for Cells No. 3 through 7 are shown in Table VI. The common operating data were the following:

| | | |
|---|---|---|
| 1. | Cell type | ARC Lucite |
| 2. | Electrodes | BRITE Anode |
| | | PT-TA Cathode |
| 3. | Air Flow Rate | 24.0 cc/sec |
| | Humidity | 49.5% RH |
| | Temperature | 84.0 °F |
| | Pressure | 735 mm Hg |
| 4. | DC Cell Voltage | 2.60 V |
| 5. | DC Cell Current | 0.92 A |

Cell No. 8, operated primarily for the purpose of investigating the region of the optimum, had only one data point at the above conditions. That one is included in the table.

Specific integral power consumption versus "ON" time data were acquired for two constant "OFF" cycle times, 1.5 and 5.0 seconds. The purpose of the two iso-OFF's was the location of their optimum specific integral power consumptions as a function of "ON" cycle time. This was done with Cells No. 3 and 4. Had the minimum for the 1.5 second iso-OFF

TABLE VI

Cyclic Operation Power Consumption Data

Cells No. 3 through 8, BRITE Anodes, $E_T$ = 2.60 V

| Cell No. | ON[1] (min) | OFF[2] (sec) | N[3] | $Work_M$[4] (watt-sec) | Error[5] | Coll[6] Eff | $Work_T$[7] (watt-sec) | %[8] IMP |
|---|---|---|---|---|---|---|---|---|
| 3 | 3 | 1.5 | 10 | 1242 | 14 | 0.95 | 1175 | -4.9 |
| | 4 | | 19 | 1104 | 11 | | 1044 | 6.8 |
| | 5 | | 8 | 1075 | 8 | | 1017 | 9.2 |
| | 6 | | 12 | 1107 | 19 | | 1047 | 6.5 |
| | 7 | | 8 | 1162 | 12 | | 1099 | 1.8 |
| 4 | 2 | 5 | 6 | 1034 | 4 | 0.99 | 1025 | 8.5 |
| | 3 | | 6 | 1023 | 2 | | 1013 | 9.6 |
| | 4 | | 7 | 1005 | 3 | | 996 | 11.1 |
| | 5 | | 14 | 988 | 4 | | 979 | 12.7 |
| | 6 | | 10 | 1004 | 1 | | 995 | 11.2 |
| | 7 | | 4 | 1013 | 3 | | 1004 | 10.4 |
| 5 | 5 | 0.5 | 11 | 1054 | 8 | 0.98 | 1036 | 7.5 |
| | | 3 | 9 | 1013 | 4 | | 996 | 11.1 |
| 6 | | 10 | 4 | 1140 | 2 | 0.97 | 1106 | 1.3 |
| 6 | 3 | 7 | 4 | 1076 | 10 | 0.97 | 1049 | 6.3 |
| 7 | 3 | | 12 | 1064 | 5 | 1.00 | 1064 | 5.0 |
| 6 | 5 | | 3 | 1026 | 6 | 1.00 | 1026 | 8.4 |
| 6 | 7 | | 6 | 1050 | 4 | 0.97 | 1023 | 8.7 |
| 7 | 7 | | 12 | 1021 | 5 | 1.00 | 1021 | 8.8 |
| 7 | 9 | | 6 | 1032 | 13 | | 1032 | 7.9 |
| 8 | 5 | 5 | 5 | 976 | 2 | 1.00 | 976 | 12.9 |

[1] "ON" cycle time

[2] "OFF" cycle time

[3] Number of measurements

[4] Ave measured electrical work to produce 50 standard cc $H_2$

[5] Estimate of maximum error in measurement to 95 percent confidence, assuming data follow t-distribution

[6] Hydrogen collection system efficiency

[7] Average electrical work corrected for $H_2$ collection efficiency

[8] Percent improvement in power consumption efficiency, related to steady state power consumption of 1120 watt-sec for production of 50 standard $cm^3 H_2$ at 2.60 V.

been lower than for the 5.0 second one, another iso-OFF at 0.5 second could have been generated without loss of accuracy of control by the "OFF" cycle timer. As it was, the minima for both data sets occurred at about 5.0 minute "ON" cycle time, and specific integral power consumption was lower for the 5.0 second iso-OFF. In the search for the optimum specific integral power consumption, then, the region of interest lay on the 5.0 minute iso-ON with optimum "OFF" cycle time probably greater than 1.5 second. Cell No. 5 yielded only two valid power measurements before failure at cycles 5.0/0.5 and 5.0/3.0, showing the optimum to be greater than 3.0 second "OFF" time.

The first datum from Cell No. 6 was at cycle 5.0/10.0, and it showed that the minimum specific integral cell power consumption for the 5.0 minute iso-ON lay between 3.0 and 10.0 second "OFF" cycle time. A 7.0 second constant "OFF" cycle time data set was decided upon as a suitable intermediate. Both Cells No. 6 and 7 were used in the acquisition of the 7.0 second iso-OFF. Midway along the operation time of Cell No. 6, the hydrogen collection system developed a leak, going from 0.97 collection efficiency to about 0.7. After repair of the leak, collection efficiency was 1.00, but only one more valid datum was measured before cell failure. Cell No. 7 served to complete the 7.0 second constant "OFF" time measurements and to confirm the validity of the Cell. No. 6 data.

The measured optimum cyclic specific integral power consumption was 976 watt-sec for the production of 50 standard cc $H_2$, at 5.0 minute "ON" and 5.0 second "OFF" cycle times, in the Cell No. 4 data set. The only Cell No. 8 datum with operating conditions common with Cells No. 3 through 7 was in confirmation of that measured optimum. The two measured values were in good agrement, differing by 3 watt-sec and representing a 12.8 percent improvement in power consumption efficiency relative to steady

state operation. The functional relationship between specific integral cell power consumption and cycle parameters for the BRITE anode cell studies is shown in "contour map" form in Figure 20. The full three dimensional "surface" could not, of course, be portrayed with the limited data of the present work. It is apparent, however, that the optimum is in the immediate area of 5.0 minute "ON" and 5.0 second "OFF" cycle parameters.

Cell No. 8 was further used to gather specific integral cell power consumption data in the region of the measured 5.0/5.0 optimum. Change of integral power consumption was to be observed with change of three major independent variables: Cell Voltage, Air Inlet Temperature, and Air Flow Rate. The cycle parameters were held constant at 5.0 min "ON" and 5.0 sec "OFF", and all other independent variables were unchanged. The results are summarized in Table VII below.

TABLE VII

Cyclic Power Consumption Variation With Cell Voltage, Air Temperature, and Air Flow Rate, Cell No. 8, 5.0/5.0 Cycle

| $E_T$ (volt) | Air Flow (scc/sec) | Air Temp (°F) | N[1] | Work[2] (watt-sec) | Error[3] (watt-sec) | %[4] IMP |
|---|---|---|---|---|---|---|
| 2.60 | 24.0 | 84 | 5 | 976 | 2 | 12.7 |
| 2.60 | 51.0 | 84 | 6 | 923 | 3 | 17.6 |
| 2.40 | 24.0 | 84 | 6 | 893 | 1 | 13.6 |
| 2.60 | 24.0 | 74 | 5 | 989 | 4 | 11.7 |

[1] Number of measurements.
[2] Average electrical work required for production of 50 scc $H_2$.
[3] Maximum error to 0.95 confidence, assuming t-distribution.
[4] Percent improvement relative to steady state specific power consumption: 1120 watt-sec at 2.60 V, 1034 watt-sec at 2.40 V.

FIGURE 20

BRITE Anode Cell Power Consumption

as a Function of Cycle Parameters

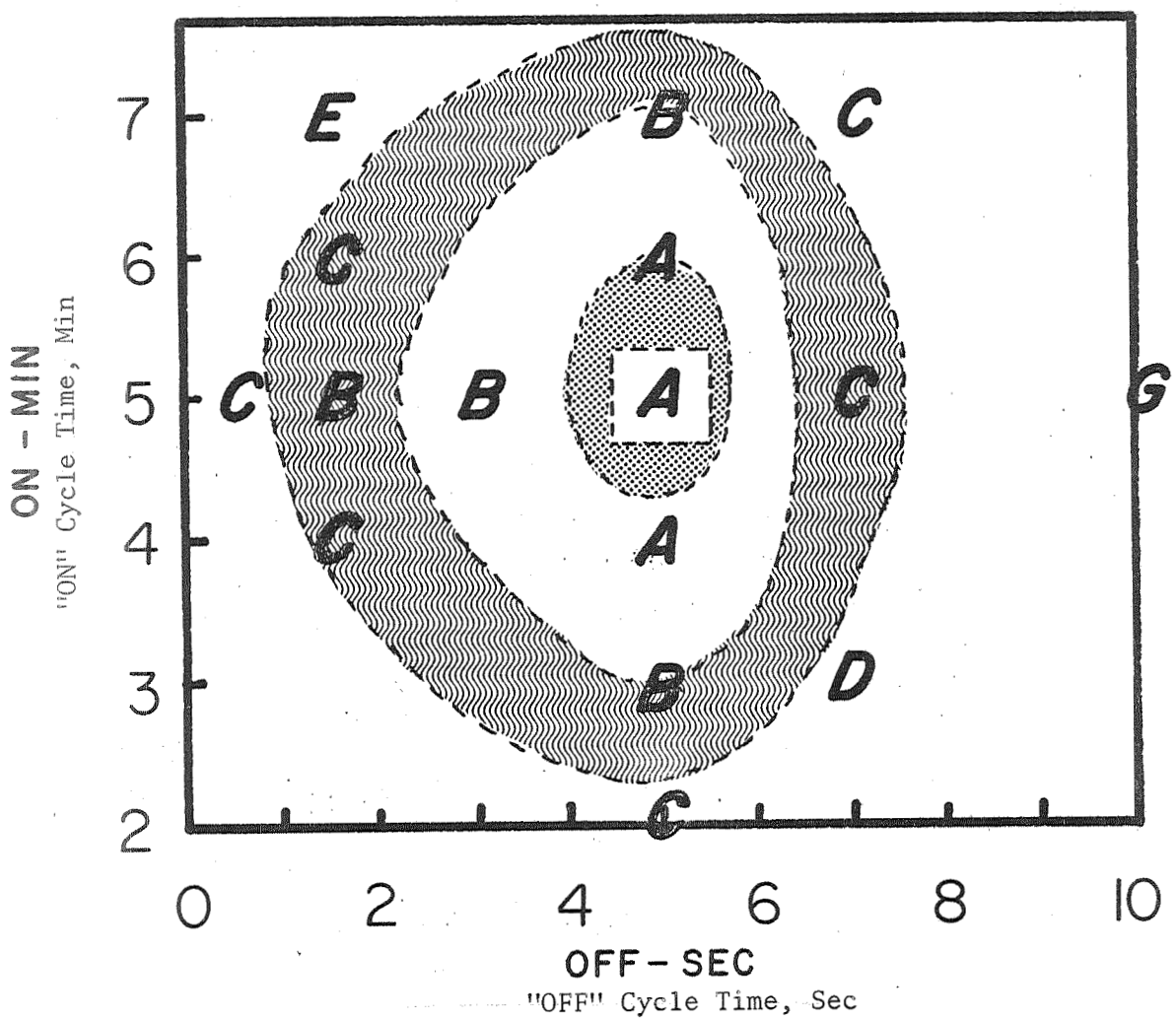


Measured Data Points

| Code | | Work | | 50 scc $H_2$ |
|---|---|---|---|---|
| A | = | 980 | - | 1000 watt-sec |
| B | = | 1000 | - | 1020 " |
| C | = | 1020 | - | 1040 " |
| D | = | 1040 | - | 1060 " |
| E | = | 1060 | - | 1080 " |
| F | = | 1080 | - | 1100 " |
| G | = | 1100 | - | 1120 " |

2B. Discussion of Results

The major results of the cyclic operation power consumption investigation of Cells No. 3 through 8, with BRITE anode, were the following:

1. Specific power consumtpion (integral power required for the electrolysis of a given mass of water) varies with both "ON" and "OFF" cycle times, and minima exist with respect to both variables.

2. At the operating conditions studied, measured specific power consumption was minimized at the 5.0 minute "ON" and 5.0 second "OFF" cycle. The efficiency improvement relative to steady state operation was 12.8 percent.

3. Cyclic power consumption efficiency increase is not a strong function of applied cell voltage or inlet air temperature, but is strongly dependent on inlet air flow rate.

4. The BRITE type electrode is suited for extended and severe operation of the WVE cell.

With respect to the first two results, the variation in specific integral power consumption with "ON" cycle time was sufficiently explained in the discussion of the PT-TA electrode cell data. The primary different between the BRITE and PT-TA data sets was with respect to variation of specific integral cell power consumption with "OFF" cycle time. In the immediate region of zero "OFF" time, BRITE anode cell specific power consumption increased with decreasing "OFF" time, the reverse of the PT-TA electrode cell case.

Part of the explanation lies in the different amounts of atomic oxygen capable of being contained on the surfaces of the two types of electrode. The solid BRITE electrode has a much smaller specific surface area, and contains much less adsorbed atomic oxygen at the end of the "ON"

part of the cycle. With more sparse surface coverage, the fuel cell reaction cannot be as effective as in the case of the PT-TA electrode upon initiation of the "OFF" part of the cycle. This was confirmed by experimental observation of the BRITE anode cell under constant current charge/discharge, shown in Figure 21. No "plateau" cell voltage was observed upon discharge. Cell voltage dropped to less than 0.05 volt much as the initial voltage drop to 0.25 volt upon discharge of the PT-TA cell. Rather than maintain a plateau, the voltage continued to drop very slowly toward zero. That indicated that the fuel cell reaction was not generating sufficient current to maintain electrode coverage relative to the desorption rate caused by the grounding of the electrode.

Consumption of product hydrogen and oxygen in the "OFF" cycle was, therefore, not the strong factor that it was in the PT-TA cell. The discussion of the PT-TA cell power consumption results, with respect to length of "OFF" cycle time, could only be expected to apply to the BRITE anode cell at large "OFF" times. The eventual specific power consumption increase with increasing "OFF" time measured in the BRITE anode cell data set confirmed that. Even with the low rate of product consumption in the "OFF" cycle, a sufficiently large period of "OFF" cycle time would cause the amount of hydrogen and oxygen consumed to be significant.

The absence of significant fuel cell reaction during the "OFF" cycle, with the BRITE anode cells, is probably the reason that the increase in specific integral power consumption with decreased "OFF" cycle time was observed in the region of zero "OFF" time. Since the two electrode types are essentially the same, except for specific surface area, it is assumed that significant fuel cell reaction in the PT-TA cell simply masked the

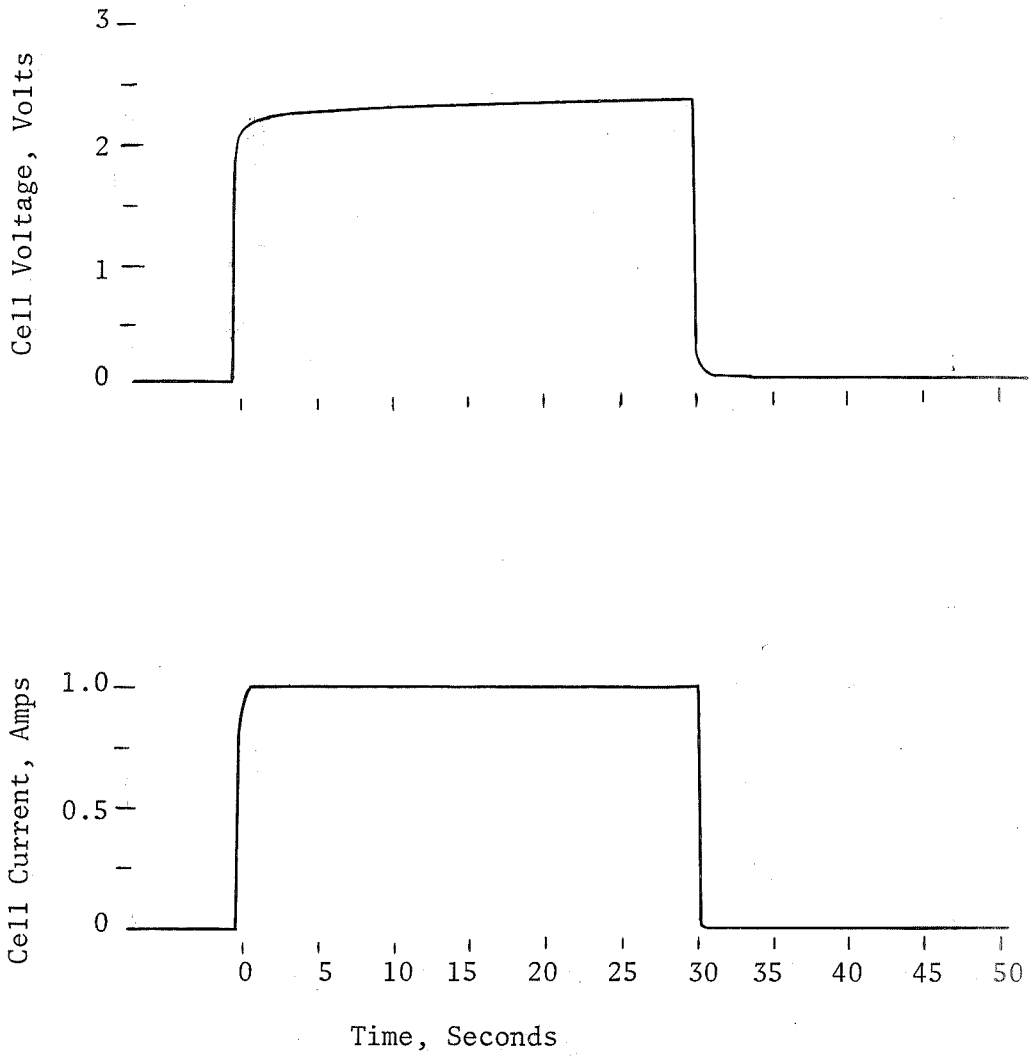


FIGURE 21

Constant Current Charge/Discharge Curve for a Cell with a BRITE Anode

effect in the earlier investigation. No explanation is presently available for the effect.

The third result, relating power consumption efficiency to three other variables at constant cycle, showed one or more transport phenomena affecting cell efficiency. Most striking was the increase from 13 to 18 percent in improvement in power consumption efficiency by doubling the feed air flow rate. How supplying more feed water to the cell and increasing convective cell cooling caused the efficiency increase is not understood. Decreasing air temperature, and increasing cell cooling by providing a larger driving force for heat transfer, had no significant effect on performance. The increased supply of feed water, causing electrolyte dilution, was apparently the reason for the performance increase with increased feed air flow rate. Future work may resolve the question. Finally, there was no significant difference in relative cell power consumption efficiency measured between two different cell voltages. Since steady state cell current at 2.40 volt was twenty percent lower than at 2.60 volt, the result would tend to indicate that power consumption efficiency under cyclic operation was an electrode phenomenon, directly related to characteristic potential.

The final conclusion, that BRITE anode WVE cells are suitable for extended and severe operation, reflects the observation that in no case was cell failure observed to result from the type anode used. The anode used did have serious drawbacks. The first was the high overvoltage, resulting in an optimum measured cyclic specific power consumption higher than that in the PT-TA cell under steady state operation. The second was the relatively coarse mesh size of 45, which allowed cell flooding far more readily than the fine-mesh PT-TA electrodes. It did not fall

apart, however, which makes it superior for the extended missions for which water vapor electrolysis is intended.

3. Conclusions and Recommendations

Cyclic operation of the water vapor electrolysis cell has been shown to increase power consumption efficiency. For cells with PT-TA electrodes, incomplete data showed measured efficiency increases of up to ten percent, relative to steady state operation. Under the same conditions, efficiency in cells with BRITE anodes was shown to increase up to thirteen percent, at the measured optimum as a function of "ON"/"OFF" cyclic operation parameters. It is believed that cyclic operation efficiency improvement will be observed with any electrode displaying oxygen overvoltage.

Each electrode type investigated had serious disadvantages. The PT-TA electrode tended to decompose as an anode, causing cell failure. The BRITE type electrode had an unacceptably high oxygen overvoltage. Neither should be used in an operating water vapor electrolysis life support subsystem. Both were, however, valuable tools in the present research.

Since cyclic operation has been shown to be a significant benefit, future work should concern itself with in-depth studies of cyclic operation performance as a function of more than simply cycle parameters. Until the processes involved are quantitatively understood, there will be no substitute for masses of experimental data. Given enough such data, it is possible that an analytic transfer function could be developed, relating cell performance to the significant independent variables of operation. The empirical approach to mathematical modelling has drawbacks, but it is all that is available in light of the present small understanding of transient processes in electrochemical kinetics.

Since differences in power consumption efficiency in cyclic operation did occur between electrode types studied, it is recommended that extensive further investigations await an electrode type with low overvoltage, long life, and low porosity. The large amount of time that would be involved in future extensive study should not be spent on cells with electrodes unsuitable for efficient, extended operation in spacecraft.

## LIST OF REFERENCES


1. Bockris, J. O., NBS Circular 524, 243 (1953).

2. Byrd, R. B., W. E. Stewart, and E. N. Lightfoot, "Transport Phenomena", Wiley, N.Y. (1965).

3. Clifford, J. E., "Water Vapor Electrolysis Cell With Phosphoric Acid Electrolyte," paper presented at SAE Aeronautic and Space Engineering and Manufacturing Meeting, Los Angeles (1967).

4. Clifford, J. E., J. G. Beach, J. A. Gurklis, E. S. Kolic, J. T. Gates and C. L. Faust, Battelle Memorial Institute, NASA CR-60851 (1964).

5. Clifford, J. E., J. A. Gurklis, J. G. Beach, E. S. Kolic, E. W. Winter, A. C. Secrest, J. T. Gates and C. L. Faust, Battelle Memorial Institute, NASA CR-771 (1967).

6. Clifford, J.E., B. C. Kim and E. S. Kolic, Battelle Memorial Institute, NASA Contract NAS 2-2156, Final Report (1969).

7. Clifford, J. E., A. C. Secrest, J. T. Gates, and C. L. Faust, Battelle Memorial Institute, NASA Contract NAS 2-2156, Annual Report (1966).

8. Connor, W. J., B. M. Greenough, and G. M. Cook, Lockheed Missiles and Space Co., NASA Contract NAS 2-2630, Final Report (1966).

9. Delahay, P., "Double Layer and Electrode Kinetics", Interscience, N.Y. (1965).

10. Engel, A. J., ASEE-NASA Summer Institute, Final Report (1967).

11. Engel, A. J., ASEE-NASA Summer Institute, Final Report (1968).

12. Engel, A. J. and A. M. Bloom, The Pennsylvania State University, NASA Grant No. NGR-39-009-123, Annual Report (1970).

13. Ferguson, A. L., NBS Circular 524, 227 (1953).

14. Foerster, Von F., and A. Piguet, Zeitschrift fur Elektrochemie, 37, 714 (1904).

15. Giauque, W. F., E. W. Hornung, J. E. Kunzler, and T. R. Rubin, J. Am. Chem. Soc., 82, 62 (1960).

16. Hickling, A., and S. Hill, Trans Faraday Soc, 46, 550 (1950).

17. King, C. V., J. Electrochem.Soc., 102(4), 193 (1955).

18. Lange, N. A. "Handbook of Chemistry", 6th ed., Handbook Publishers, Sandusky, Ohio (1946).

19. Lee, W., J. H. Christensen and D. F. Rudd, AIChEJ, 6, 12 (1966).

20. Lewis, G. N., M. Randall, K. S. Pitzer, and L. Brewer, "Thermodynamics", McGraw-Hill, N.Y. (1961).

21. Milner, P. C., J. Electrochem Soc, 107(4), 343 (1960).

22. National Research Council

23. Newman, J., D. Bennion, and C. W. Tobias, Berichte der Bunsengesellschaft, 69, 608 (1965).

24. Robinson, R. A., and R. H. Stokes, "Electrolyte Solutions" Academic Press, N.Y. (1959).

25. Roughton, J. E., J. Appl. Chem., 1(S2), s143 (1951).

26. Schlichting, H., "Boundary Layer Theory", McGraw-Hill N.Y. (1960).

27. Stokes, R. H., and R. A. Robinson, Industrial and Engineering Chemistry, 9, 2013 (1949).

28. Tobias, C. W., M. Eisenberg, and C. R. Wilke, J.Electrochem.Soc., 99(12), 359c (1952).

29. Tovbin, M. V., and A. V. Tovbin, Ukrain Khim Zhur, 22, 146 (1956).

30. Woodman, J. F., "Modern Plastics Encyclopedia", p125, McGraw-Hill N.Y. (1965).

31. Wydeven, T. and E. Smith, Aerospace Medicine, 1045 (1967).

# APPENDIX A

## PROGRAM LISTING, COMPUTER SIMULATION

On the following pages is listed the FORTRAN IV coding for the computer simulation of the water vapor electrolysis cell developed in the present work. The listing is annotated to allow those familiar with the simulation to rapidly locate specific operations. In the listing, the order of appearance is the same as it would be for submitting the simulation for execution: main program, simulation subroutine AMBWVE, and input data.

The main program is short, doing nothing but reading data and calling the subroutine. Utilization of the routine is described briefly in Appendix II. As listed, the package is set for an ARC Lucite WVE cell, operating with bright platinum electrodes at 2.60 volt under conditions such that Figure 7 in the text would be output.

Hard copy, card deck or listing, may be obtained upon request from the authors. Questions, comments or criticisms should be directed to Mr. Bloom, who will reply as speedily as possible.

```
      INTEGER*4 N/ 7/ , IWRITE/ 0/
      REAL*8 CONST(18)
      READ(5,100) (CONST(J),J=1,18)
      CALL AMBWVE(N,CONST,IWRITE)
      STOP
  100 FORMAT(F25.0)
      END
      SUBROUTINE AMBWVE(N,CONST,IWRITE)
C
C
C     SUBROUTINE AMBWVE                                    ALLAN M BLOOM
C     SIMULATION OF NASA WATER VAPOR ELECTROLYSIS CELL UNDER DIRECT
C     CURRENT OPERATION, WITH BRIGHT PLATINUM ELECTRODES
C
      INTEGER*4 N,ITER,I,II,J,JJ,NN,NNN,IWRITE
      REAL*8 DIST,DX,L,DY,W,D,PO,DP,VO,TO,MU,K,CV,MW,HO,CO,M,RO,P(2),RE,
     1EU,FA,FFA,Q,U(2,50),V(50),T(2,50),RHO(2,50),ORF,SQSUM,CONST(18),
     2X(50),Y(50),Z(50),R,A(50),B(50),C(50),BB(50),BBB(50),H(2,50),PE,E,
     3IDEN,FB,GZ,REALN,DEGF(20),HUMID(20),XVELOC(20),DENS(20),YVELOC(20)
     4,RH, ET, EO, EIR, WTFRA, WTFRC, LMC, WMC, HMC, DACID, VOLE, DGLOP,
     5 MGLOP, MCAB, MACID, MH2SO4, JW, ZX, ZTEMP, ZPS, AW, MA, KAPPA,
     6RES, DELTAR, ETA, IDENP,ZZ(50),DLOG, DABS,F/2.306D4/,DCAB/2.2D0/,
     7R1/1.987D0/   , ZIFL, IDEN1
     1 , WW(3), XX(3), RJ, AA, LL, AO(15), LO(20), CP1O(19), CC, DLOG1O,
     1 AWW(3) , CP1
     1,K25(10),K60(10),K95(10),KK25,KK60,KK95,T21
     1,ETA25,LETA(5,3),LOGI(5),L1OI(3),L1OE
     1, CD(21),WF(21),TM(21),PDOUT,PDINC,DXWMC,AMPS,LOX(21),TT,HH,PH,FDH
     1,FDT
      DATA AO / .98,.95,.92,.88,.82,.75,.67,.57,.46,.36,.26,.16,.09,.04,
     1.02/ , LO / -43.7,-293.3,-580.,-1000.,-1450.,-1910.,-2470.,-3060.,
     1 -3880.,-4850.,-5730.,-6300.,-6690.,-7010.,-7280.,-7490.,-7700.,
     1 -7870.,-8050.,-8220. / , CP1O / 17.77,18.61,17.93,16.66,15.33,13.
     139,11.63,10.20,11.48,15.06,20.39,22.54,21.77,20.61,19.00,17.22,15.
     121,13.20,10.49 /
     1,K25/.823,.810,.763,.695,.615,.524,.428,.336,.253,.182/
     1,K60/1.211,1.224,1.186,1.105,1.000,.873,.732,.600,.479,.378/
     1,K95/1.513,1.562,1.551,1.486,1.366,1.221,1.059,.901,.752,.627/
     1,LETA/-.1135,-.0237,.0154,.0374,.0795,-.1013,-.0146,.0314,.0554,
     1 .1035,-.0711,.0149,.0674,.1021,.1691/
     1,LOGI/-3.,-2.,-1.5229,-1.3010,-1./
 1000 FORMAT('0DIST',D20.5,'    ITER NO',I3)
 1001 FORMAT(' VX  FT/SEC      '  , 10D12.4)
 1003 FORMAT(' T  DEGREE F     '  , 10D12.4)
 1004 FORMAT(' WTFRA = ',F5.2, ' IDEN = ',F10.5)
 1005 FORMAT('  SUM OF SQUARES OF RESIDUALS IS ',D12.3)
 1006 FORMAT(' P(DIST) = ',D15.5)
 1007 FORMAT(' HUMIDITY LB/LB '  , 10D12.4)
 1008 FORMAT('1',56X,'CONSOLIDATED DATA '//
     1' ',42X,'X/L',13X,'LOCAL',10X,'LOCAL',10X,'LOCAL'/
     1' ',35X,'FRACTION OF CELL  CURRENT DENSITY  MATRIX TEMP     MATRIX
     1CONC'/' ',33X,'LENGTH FROM ENTRANCE   AMP/CM**2       DEGREE F
     1 WT FR H2SO4'/' ',34X,'_____________________  _____________  ________
     1_____  _____________')
 1009 FORMAT(' ',42X,F4.2,12X,F6.4,9X,F5.1,10X,F5.3)
 1013 FORMAT(' FRACTION OF     '/' CHANNEL HEIGHT',F10.2,9F12.2)
 1011 FORMAT(' ABOVE ELECTRODE' )
 1014 FORMAT('1',50X,'COMPREHENSIVE DATA'/'0',30X,'LISTED EVERY ',I3,' I
     1NCREMENTS ALONG THE LENGTH OF THE CELL ARE THE FOLLOWING:'//
     1' ',31X,'1. DISTANCE FROM ENTRANCE, CM'/
```

```
     1' ',31X,'2. AIR VELOCITY AT ',I2,' POINTS ACROSS THE FLOW CHANNEL
     1HEIGHT, FT/SEC'/
     1' ',31X,'3. AIR HUMIDITY AT ',I2,' POINTS ACROSS THE FLOW CHANNEL
     1HEIGHT, LB H2O/LB AIR'/
     1' ',31X,'4. AIR TEMPERATURE ',I2,' POINTS ACROSS THE FLOW CHANNEL
     1HEIGHT, DEGREE F'/
     1' ',31X,'5. AIR PRESSURE, DYNE/CM**2'/
     1' ',31X,'6. CONCENTRATION OF SULFURIC ACID IN ELECTROLYTE, WEIGHT
     1FRACTION'/
     1' ',31X,'7. LOCAL CURRENT DENSITY, AMP/CM**2'/
     1' ',31X,'8. ALGORITHM INFORMATION-NUMBER OF ITERATIONS AND SIZE OF
     1 RESIDUALS')
 1012 FORMAT('0',50X,'CELL CURRENT',F8.2,' AMP'  //
     1       '0',50X,'AIR DELTA-T ',F8.2,' DEG F'//
     1       '0',50X,'AIR DELTA-H ',F8.4,' LB/LB'//
     1       '0',50X,'HUM CHANGE  ',F8.2,' PCT')
      R=82.06D00
C
C     INITIALIZE ARRAYS AND COUNTERS
C
      ITER=0
      SOSUM = 0
      NN = N - 1
      NNN = N-2
      DO 9000 I=1,2
      DO 9000 J=1,50
      U(I,J) = 1.0D00
      T(I,J) = 1.0D00
      RHO(I,J) = 1.0D00
      H(I,J) = 1.0D00
 9000 V(J) = 0.0D00
C
C     TRANSLATE ELEMENTS OF INPUT ARRAY INTO MNEMONIC VARIABLES
C
      L    = CONST( 1)
      W    = CONST( 2)
      M    = CONST( 3)
      PO   = CONST( 4)
      TO   = CONST( 5)
      VO   = CONST( 6)
      RH   = CONST( 7)
      IDEN= CONST( 8)
      ET   = CONST( 9)
      MU   = CONST(10)
      K    = CONST(11)
      D    = CONST(12)
      CV   = CONST(13)
      WTFRA=CONST(14)
      WTFRC=CONST(15)
      LMC  = CONST(16)
      WMC  = CONST(17)
      HMC  = CONST(18)
      WRITE(6,1324) L, W, LMC, WMC, HMC, ET, WTFRA, WTFRC, TO, PO, RH,
     1 VO
 1324 FORMAT('1',T50, 'CELL DIMENSIONS'                                  //
     1' ', T40,  ' LENGTH OF AIR CHANNEL          ',F10.2,' CM          '//
     1' ', T40,  ' HEIGHT OF AIR CHANNEL         'F10.3, ' CM          '//
     1' ', T40,  ' LENGTH OF 1 MATRIX COMPARTMENT',F10.3,' CM          '//
     1' ', T40,  ' WIDTH  OF 1 MATRIX COMPARTMENT',F10.3,' CM          '//
     1' ', T40,  ' DEPTH  OF 1 MATRIX COMPARTMENT',F10.3,' CM          '//
```

```
     1' ', T40,  ' CELL VOLTAGE                    ',F10.3,' VOLT      '//
     1' ', T50,  ' CELL OPERATING PARAMETERS'                           //
     1' ', T40,  ' INITIAL ACID CONCENTRATION      ',F10.3,' WTFR H2SO4'//
     1' ', T40,  ' INITIAL CAB-O-SIL CONTENT       ',F10.3,' WTF SILICA'//
     1' ', T40,  ' INLET AIR TEMPERATURE           ',F10.3,' DEGREE K  '//
     1' ', T40,  '           PRESSURE              ',F10.3,' ATM       '//
     1' ', T40,  '           HUMIDITY              ',F10.3,' PERCENT RH'//
     1' ', T40,  '           FLOW RATE             ',F10.3,' CM/SEC    ')
C
C    CALCULATE VALUES DERIVED FROM INPUT DATA
C
      ZX = 647.27D0 - TO
      ZTEMP = ZX/TO          * ( 3.2437814D0 + 5.86826D-3 * ZX
     1 + 1.1702379D-8 * ZX*ZX*ZX ) / (1.0D0 + 2.1878462D-3*ZX)
      ZPS = 218.167D0 / 10.0D0**ZTEMP
      MW = 18
      MA = 29
      HO = (MW/MA) * (RH/1.0D02) * ZPS/PO
      DACID = 1.08D00*WTFRA + 0.86D00
      VOLE = 2.0D00 * LMC * WMC * HMC
      DGLOP = WTFRC * DCAB + (1.0D00-WTFRC) * DACID
      MGLOP = DGLOP * VOLE
      MCAB = WTFRC * MGLOP
      MACID = MGLOP - MCAB
      MH2SO4 = WTFRA * MACID
      REALN = N - 1
      IBLDBL = 0
      LOX(1) = 0
      ZIFFL = 1.0D0/REALN
      DO 9001 I=2,N
 9001 LOX(I) = LOX(I-1) + ZIFFL
      DY = W/REALN
      DX = DY/M
      DIST = -DX
      IPD = 0
      PDOUT = 0
      PDINC = 0.05D0 * L
      DXWMC = DX * WMC
      AMPS = 0
      INCR = IWRITE - 2
      RO = MA*PO/(R*TO)
      P(1) = 1.0D06*PO
      P(2) = P(1)
C
C    DIMENSIONLESS GROUPS FOR TRANSPORT EQUATIONS
C
      RE = W*VO*RO/MU
      FA = K/(DY*RO*CV*VO)
      GZ = 1.0D00/FA
      FFA = 4.13D07*RO*CV*TO
      FB = D/(DY*VO)
      PE = 1.0D00/FB
C
C
C    BEGIN SOLUTION OF TRANSPORT EQNS FOR AIR IN CHANNEL
C
C
C    BOUNDARY CONDITIONS
C
      V(1) = 0.0D00
```

```
      V(N) = 0.0D00
      U(2,1) = 0.0D00
      U(2,N) = 0.0D00
      Q =  0.239D00*IDEN*(ET- 1.48D00)*DX
      T(2,1) = T(2,2) + Q*DY / (DX*K*TO)
    1 IF(IWRITE .EQ. 0) GO TO 7028
      IF(IBLDBL.EQ.1) GO TO 9002
      WRITE(6,1014) IWRITE,N,N,N
      IBLDBL = 1
 9002 INCR = INCR + 1
      IF(INCR.LT.IWRITE) GO TO 7028
      INCR = 0
      WRITE(6,1000) DIST, ITER
C
C     CONVERT TO ENGINEERING UNITS FOR OUTPUT
C
      DO 5000 J=1,N
      XVELOC(J) = U(2,J)*VO/30.48D00
      DEGF(J) = T(2,J)*TO*1.8D00 - 460.0D00
 5000 HUMID(J) = H(2,J) * HO
      WRITE(6,1013)(LOX(I),I=1,N)
      WRITE(6,1011)
      WRITE(6,1001)(XVELOC(J),J=1,N)
      WRITE(6,1003)(DEGF(J),J=1,N)
      WRITE(6,1007)(HUMID(J),J=1,N)
      WRITE(6,1004) WTFRA, IDEN
      WRITE(6,1006) P(2)
      IF(ITER.GT.0) WRITE(6,1005) SQSUM
 7028 ITER = 0
      IF(DIST.LT.L) GO TO 7029
C
C     AT END OF PROBLEM, PRINT OUT CONSOLIDATED OPERATING DATA
C
      DO 7032 I=1,20
 7032 AMPS = AMPS + ( CD(I) + CD(I+1) )/40.0D0
      AMPS = L*WMC*AMPS
      LOX(1) = 0
      DO 7030 I=2,21
 7030 LOX(I) = LOX(I-1) + 0.05D00
      WRITE(6,1008)
      DO 9003 I=1,21
 9003 WRITE(6,1009) LOX(I), CD(I), TM(I), WF(I)
      TT=0
      HH=0
      DO 7031 I=1,NN
      TT = TT + ( T(2,I+1) + T(2,I)) * DY/2.0D0
 7031 HH = HH + (H(2,I+1) + H(2,I)) * DY/2.0D0
      TT = TT/W
      HH = HH/W
      PH =(HH - 1.0D0)*1.0D2
      FDH = HH*HO - HO
      FDT = 1.8D0 * (TT*TO-TO)
      WRITE(6,1012) AMPS, FDT, FDH, PH
      RETURN
 7029 DIST = DIST + DX
    2 ITER = ITER + 1
C
C     STORE GUESSES OF U,V,T IN X,Y,Z TO CHECK CONVERGENCE AFTER ITER
C
      DO 100 J=1,N
```

```
      X(J) = U(2,J)
      Y(J) = V(J)
  100 Z(J) = T(2,J)
C
C     CALCULATE PRESSURE DROP FROM MOM BAL AT WALL
C
      DP = (MU*VO*DX/DY**2)*(2.0D00*U(2,2) - U(2,3))
      P(2) = P(1) - DP
      EU = W/(RE*DY)*(2.0D00*U(2,2) - U(2,3))
C
C     CALCULATE DENSITY AS FUNCTION OF P,T
C
      DO 110 J=1,N
  110 RHO(2,J) = MA*P(2) / (1.0D06*R*T(2,J)*RO*TO)
C
C     CALCULATE V AS FUNCTION OF U,V
C
      DO 120 J=2,NN
  120 V(J) = ( M*RHO(1,J)*U(1,J) - M*RHO(2,J)*U(2,J) + RHO(2,J-1)*V(J-
     1)/RHO(2,J)
C
C     CALCULATE U AS A FUNCTION OF U,V,RHO
C     MATRIX AA OF AA*U = BB IS TRIDI OF VECTORS A,B,C
C
C     CALCULATE CONSTANT VECTOR BB
C
      DO 130 J=2,NN
  130 BB(J-1) = - M*RHO(1,J)*U(1,J)**2 - EU -M*RHO(2,J)*U(1,J)**2
      DO 140 J=2,NN
      A(J-1) = W/(DY*RE) + RHO(2,J-1)*V(J-1)
      B(J-1) = - 2.0D00*W/(DY*RE) - RHO(2,J) * V(J) - 2.0D00*M*RHO(2,J)*
     1U(1,J)
  140 C(J-1) = W/(DY*RE)
      A(1) = 0.0D00
      C(NN-1) = 0.0D00
C
C     SOLVE U=AAINV*BB
C
      C(1) = C(1)/B(1)
      BB (1) = BB(1)/B(1)
      DO 150 I=2,NNN
      ORF = B(I) - A(I)*C(I-1)
      C(I) = C(I)/ORF
  150 BB (I) = ( BB(I) - A(I)*BB (I-1))/ORF
      I=NNN
    4 I=I-1
      BB (I) = BB(I) - C(I)* BB (I+1)
      IF(I.GT.1) GO TO 4
      DO 160 I=1,NNN
  160 U(2,I+1) =  BB(I)
C
C     CALCULATE T AS A FUNCTION OF U,V,RHO
C
      DO 170 J=2,NN
  170 BBB(J-1) = - M*RHO(1,J)*U(1,J)*T(1,J) +P(2)*( M*U(2,J) - M*U(1,J)
     1 + V(J) - V(J-1))/FFA
      BBB(1) = BBB(1) - FA*( T(2,2) + Q*DY/(DX*K*TO) )
      BBB(NNN) = BBB(NNN) - FA*T(2,NN)
      DO 180 J=2,NN
      A(J-1) = FA + RHO(2,J-1)*V(J-1)
```

```
      B(J-1) = - 2.0D00*FA - M*RHO(2,J)*U(2,J) - RHO(2,J)*V(J)
  180 C(J-1) = FA
      A(1) = 0.0D00
      C(NN-1) = 0.0D00
      C(1) = C(1)/B(1)
      BBB(1) =BBB(1)/B(1)
      DO 190 I=2,NNN
      ORF = B(I) - A(I)*C(I-1)
      C(I) = C(I)/ORF
  190 BBB(I) = (BBB(I) - A(I)*BBB(I-1))/ORF
      I=NNN
   40 I=I-1
      BBB(I) =BBB(I) - C(I)* BBB(I+1)
      IF(I.GT.1) GO TO 40
      DO 200 I=1,NNN
  200 T(2,I+1) = BBB(I)
      T(2,1) = T(2,2) + Q*DY / (DX*K*TO)
      T(2,N) = T(2,N-1)
C
C     TEST CONVERGENCE FOR ALGORITHM CALCULATING U,V,T
C
      SQSUM = 0.0D00
      DO 210 I=1,N
  210 SQSUM = SQSUM + (X(I) - U(2,I))**2 + (Y(I) - V(I))**2 + (Z(I) - T(
     12,I))**2
      IF(SQSUM.GT.1.0D-10) GO TO 5
C
C     GIVEN SOLUTION FOR U,V,T, CALCULATE HUMIDITY PROFILE OF AIR
C
      DO 230 J=2,NN
  230 BBB(J-1) = -H(1,J)*RHO(1,J)*U(1,J)*M
      BBB(1) = BBB(1) - FB*RHO(2,1)*(H(2,2)*RHO(2,2) - 9.334D-5*IDEN*DY/
     1(RO*HO*D))/RHO(2,1)
      BBB(NNN) = BBB(NNN) - FB*RHO(2,N)*H(2,NN)
      DO 240 J=2,NN
      A(J-1) = RHO(2,J-1)*V(J-1) + FB*RHO(2,J-1)
      B(J-1) = -RHO(2,J)*U(2,J)*M - 2.0D00*FB*RHO(2,J) - RHO(2,J)*V(J)
  240 C(J-1) = FB*RHO(2,J+1)
      A(1) = 0.0D00
      C(NN-1) = 0.0D00
      C(1) = C(1)/B(1)
      BBB(1) =BBB(1)/B(1)
      DO 250 I=2,NNN
      ORF = B(I) - A(I)*C(I-1)
      C(I) = C(I)/ORF
  250 BBB(I) = (BBB(I) - A(I)*BBB(I-1))/ORF
      I=NNN
  400 I=I-1
      BBB(I) =BBB(I) - C(I)* BBB(I+1)
      IF(I.GT.1) GO TO 400
      DO 260 I=1,NNN
  260 H(2,I+1) = BBB(I)
      H(2,1) = (H(2,2)*RHO(2,2) - 9.334D-5*IDEN*DY/(RO*HO*D))/RHO(2,1)
      H(2,N) = H(2,NN)
C
C
C     EQUATIONS AND DATA DESCRIBING ELECTROCHEMICAL KINETICS OF WVE CELL
C
C
C     STORE PREVIOUS GUESS OF CURRENT DENSITY
```

```
C
      IDEN1 = IDEN
      IFLAG = 0
C
C     MATRIX EQILIBRIUM RH AS FUNCTION OF H(2,1),T,P
C
      ZX = 647.27D0 - T(2,1) * TO
      ZTEMP = ZX/(T(2,1)*TO) * ( 3.2437814D0 + 5.86826D-3 * ZX
     1 + 1.1702379D-8 * ZX*ZX*ZX ) / (1.0D0 + 2.1878462D-3*ZX)
      ZPS = 218.167D0 / 10.0D0**ZTEMP
      AW = HO * H(2,1) * MA / (MW * ZPS )*(P(2)/1.0D6)
C
C     'REVERSIBLE' EMF OF CELL REACTION FOR ELECTROLYSIS
C
      ZTEMP = (P(2)/1.0D6)**1.5
      EO = 1.226D0 - R1* TO * T(2,1) * DLOG(AW/ZTEMP) / (2.0D0 * F )
C
C     ACID CONCENTRATION AS A FUNCTION OF EQUILIBRIUM RH AND T
C     AW DATA FROM ROBINSON AND STOKES,CP FROM GIAQUE ET AL, L FROM ICT
C
      IBASE = 1
      INDEX = 3
      WW(2) = WTFRA
      WW(1) = WTFRA - 0.05D0
      WW(3) = WTFRA + 0.05D0
 2571 DO 2572 I=IBASE,INDEX
      XX(I) = 1.0D0/(1.0D0 + (98.0D0/18.0D0) * (1.0D0/WW(I) - 1.0D0))
C     GET AW AT 25C FROM GUESS OF WTFR ACID
      ZTEMP = 20.0D0 * WW(I)
      J = ZTEMP
      RJ = J
      AA = (ZTEMP-RJ) * (AO(J+1) - AO(J)) + AO(J)
C     GET HEAT CAPACITY AND ENTHALPY AT 25C FROM GUESSED MOLFR ACID
      ZTEMP = 20.0D0 * XX(I)
      J = ZTEMP
      RJ = J
      CP1 = (ZTEMP-RJ) * (CP1O(J+1) - CP1O(J)) + CP1O(J)
      LL = (ZTEMP-RJ) * (LO(J+1) - LO(J)) + LO(J)
      CC = 4.5758D0*DLOG10(AA) - LL/298.0D0 + 2.303D0*(CP1-17.996D0)*
     1 DLOG10(T(2,1)*TO)
      ZTEMP = LL/(T(2,1)*TO) - 2.303D0*(CP1-17.996D0)*DLOG10(T(2,1)*TO)
     1 + CC
 2572 AWW(I) = 1.0D1 ** (ZTEMP/4.5758D0)
C     CHECK TO SEE IF AW FALLS WITHIN RANGEOF CALCULATED AW'S, AND IF
C     NOT, CHANGE THE RANGE ACCORDINGLY
      IF ( AW .GT. AWW(1)) GO TO 2573
      IF ( AW .LT. AWW(3)) GO TO 2574
      GO TO 2575
 2573 WW(2) = WW(1)
      WW(3) = WW(2)
      AWW(2) = AWW(1)
      WW(1) = WW(2) - 0.05D0
      INDEX = 1
      IBASE = 1
      GO TO 2571
 2574 WW(1) = WW(2)
      WW(2) = WW(3)
      AWW(1) = AWW(2)
      AWW(2) = AWW(3)
      WW(3) = WW(2) + 0.05D0
```

```
      INDEX = 3
      IBASE = 3
      GO TO 2571
C     CALCULATE WTFR ACID BY QUADRATIC INTERPOLATION
 2575 WTFRA = (AW-AWW(2))*(AW-AWW(3))/((AWW(1)-AWW(2))*(AWW(1)-AWW(3)))
     1 * WW(1)
     1+       (AW-AWW(1))*(AW-AWW(3))/((AWW(2)-AWW(1))*(AWW(2)-AWW(3)))
     1 * WW(2)
     1+       (AW-AWW(1))*(AW-AWW(2))/((AWW(3)-AWW(1))*(AWW(3)-AWW(2)))
     1 * WW(3)
C
C     DETERMINE CAB-O-SIL CONTENT OF ELECTROLYTE
C
      MACID = MH2SO4 / WTFRA
      WTFRC = MCAB / (MACID + MCAB )
C
C     CONDUCTIVITY OF H2SO4 AS FUNCTION OF WTFRA,T - DATA OF ROUGHTON
C
      T21 = TO*T(2,1)  - 273.0D0
      ZTEMP = 20.0D0*WTFRA - 5.0D0
      J = ZTEMP
      RJ = J
      ZIFL = ZTEMP - RJ
      KK25 = ZIFL*(K25(J+1)-K25(J)) + K25(J)
      KK60 = ZIFL*(K60(J+1)-K60(J)) + K60(J)
      KK95 = ZIFL*(K95(J+1)-K95(J)) + K95(J)
      KAPPA = (T21-60.0D0)*(T21-95.0D0)*KK25/2450.0D0
     1      + (T21-25.0D0)*(T21-95.0D0)*KK60/(-1050.0D0)
     1      + (T21-25.0D0)*(T21-60.0D0)*KK95/2450.0D0
      RES = 1.0D0 / KAPPA
C
C     CORRECT RESISTIVITY OF H2SO4 FOR CAB-O-SIL CONTENT - DATA OF BLOOM
C
      DELTAR = 2.4000D0 * WTFRC * RES
      RES = RES + DELTAR
C
C     OHMIC POTENTIAL DIFFERENCE BETWEEN ELECTRODES
C
    3 EIR = IDEN * RES * HMC * 2.0D00
C
C     OVERVOLTAGE IS TOTAL CELL VOLTAGE MINUS IR VOLTAGE AND REV EMF
C
      ETA = ET - EIR - EO
C
C     CALCULATE CURRENT DENSITY FROM DATA OF CONNORS AS A FUNCTION OF
C     WTFR ACID AND OVERVOLTAGE, BY LIN INT OF LOG(I) VS LOG(ETA) CURVES
C
C     CONVERT ETA TO EQUIVALENT OVERVOLTAGE AT 25 C
      ETA25 = ETA - 0.25D-2 * ( T(2,1)*TO - 298.0D0)
      L10E = DLOG10(ETA25)
C     SEARCH OVERVOLTAGE ARRAY FOR INTERPOLATION POINTS
      DO 471 I=1,3
      J=0
  473 J=J+1
      IF(LETA(J,I) .GT. L10E) GO TO 472
      IF(J .LT. 5) GO TO 473
C     EXTRAPOLATE BEYOND 100 MA/SCM
      JJ=4
      JJJ=5
      GO TO 474
```

```
  472 IF(J .GT. 1) GO TO 475
C     EXTRAPOLATE TO CD LOWER THAN 1 MA/SCM
      JJ=1
      JJJ=2
      GO TO 474
  475 JJ=J-1
      JJJ=J
C     COMPUTE LOG(I) AT  55,60,65 WT PCT AT ETA25
  474 L10I(I) = LOGI(JJ) + (L10E-LETA(JJ,I))*(LOGI(JJJ)-LOGI(JJ))/(LETA(
     1JJJ,I)-LETA(JJ,I))
  471 CONTINUE
C     INTERPOLATE TO GET LOG(I) AT WTFRA
      ZTEMP = (WTFRA-0.60D0)*(WTFRA-0.65D0)*L10I(1)/ 5.0D-3
     1       -(WTFRA-0.55D0)*(WTFRA-0.65D0)*L10I(2)/ 2.5D-3
     1       +(WTFRA-0.55D0)*(WTFRA-0.60D0)*L10I(3)/ 5.0D-3
      IDENP= 10.0D0**ZTEMP
      ZIFL=DABS( (IDENP-IDEN)/IDEN)
      IDEN = IDENP
      IF ( ZIFL .LE. 1.0D-2 ) GO TO 33
C
C     THE LOOP TO 3 BALANCES IR VOLTAGE AND OVERVOLTAGE
C
      IFLAG = IFLAG + 1
      GO TO 3
C
C     AVE OF PRESENT AND PREVIOUS CURRENT DENSITY USED FOR SUCCEEDING
C     ITERATION, NECESSARY TO PREVENT INSTABILITY OF ALGORITHM
C
   33 IDEN = (IDEN + IDEN1) / 2.0D00
      0 =  0.239D00*IDEN*(ET-E0-T0*T(2,1)*19.5D0/2.306D4-EIR)*DX
C
C     IF CURRENT DENSITY USED IN AIR CHANNEL SECTION AND IN ELECTROCHEM
C     SECTION ARE NOT THE SAME, RECYCLE AT SAME INCREMENT IN X
C
      IF(IFLAG .GT. 0 ) GO TO 5
C
C
C     ADVANCE ONE INCREMENT IN THE X-DIRECTION, ROW I BECOMES ROW I-1
C
C
      P(1) = P(2)
      DO 220 I=1,N
      U(1,I) = U(2,I)
      RHO(1,I) = RHO(2,I)
      H(1,I) = H(2,I)
  220 T(1,I) = T(2,I)
      IF(DIST.LT.PDOUT) GO TO 1
      IPD = IPD + 1
      PDOUT = PDOUT + PDINC
      CD(IPD) = IDEN
      WF(IPD) = WTFRA
      TM(IPD) = T(2,1)*T0*1.8D0 - 460.0D0
      GO TO 1
C
C     PREVENT BECOMING HUNG IN AN INFINITE LOOP
C
    5 IF(ITER.LT.99) GO TO 2
      WRITE(6,1000) DIST, ITER
      WRITE(6,1005) SQSUM
      RETURN
```

```
      END
      THE FOLLOWING IS THE DATA SET
4.75                    LENGTH OF AIR CHANNEL
0.159                   FLOW CHANNEL HEIGHT
1.0                     RATIO DY/DX
1.0                     INLET AIR PRESSURE
302.                    INLET AIR TEMPERATURE
35.2                    INLET AIR VELOCITY
50.0                    INLET AIR PERCENT RH
0.10                    GUESS OF CURRENT DENSITY AT INLET OF CELL
2.60                    CELL VOLTAGE
.0002                   VISCOSITY OF AIR
0.000062                THERMAL CONDUCTIVITY OF AIR
0.239                   DIFFUSITY OF AIR - WATER
0.178                   HEAT CAPACITY OF AIR CV
0.55                    WEIGHT FRACTION H2SO4
0.1                     WEIGHT FRACTION CAB-O-SIL IN GLOP
4.75                    LENGTH OF MATRIX COMPARTMENT
4.75                    WIDTH OF MATRIX COMPARTMENT
0.075                   DEPTH OF MATRIX COMPARTMENT
```

# APPENDIX B

## USER'S GUIDE, SUBROUTINE AMBWVE

This is a short instruction manual on the use of the FORTRAN IV subroutine named AMBWVE. The subroutine represents the digital computer simulation of the NASA water vapor electrolysis cell developed by Mr. A. M. Bloom, of the Department of Chemical Engineering of the Pennsylvania State University. Full documentation of the program may be found in the texts of annual reports under NASA Grant No. NGR 39-009-123, dated March 1970 and March 1971. The FORTRAN IV coding of the routine is presented in Appendix I. It is fully annotated, but maximum understanding requires the prior reading of the program documentation. This manual is intended to allow use of the computer simulation with a minimum of knowledge of the mechanics of the routine.

General The computer simulation of the WVE cell is subroutine written in IBM FORTRAN IV. Certain incompatabilities exist between IBM FORTRAN IV and other essentially similar languages. When using other than an IBM machine, have a competent programmer make the necessary small changes. The routine is linked to a calling program by the statement "CALL AMBWVE(N,CONST,IWRITE)". The significance of the routine call parameters will be discussed later. The routine is large, contained on about 560 80-column cards in the source language, with 23072 bytes required by the object code and 9760 bytes required array area. This is not important information unless a computer of significantly smaller size than an IBM OS 360/67 is used. The routine uses double precision for all real numbers. The routine

requires about two minutes of execution time for each call, and prints from fifty to several thousand records. The number of records is dependent on the amount of output information desired, and it is controlled by the IWRITE routine call parameter.

Input/Output Two integers and eighteen "real" numbers are input to the routine via the call statement. The integers are N and IWRITE. The variable N refers to the finite increment analysis of the transport properties of the feed/product air channel, being the number of increments across the air channel in the direction perpendicular to flow. A lot of success has been had with N = 7, and it is recommended. IWRITE is a control parameter, the value of which determines the amount of routine output. The 18 real numbers are in the double precision array CONST, and consist of algorithm information, air physical constants, and WVE cell independent variables. The routine returns nothing to the calling program, with all output going to a line printer. The parameters CONST and IWRITE are discussed more fully below.

Putting all real number input into the array CONST(18) was done arbitrarily, and any competent programmer can alter the form of the input to suit. The elements of the array are the following:

CONST( 1) = Length of air flow channel, cm

CONST( 2) = Height of air flow channel, cm

CONST( 3) = Ratio of height to length of air channel increment (1.0)

CONST( 4) = Pressure of inlet air stream, abs atm

CONST( 5) = Temperature of inlet air stream, °K

CONST( 6) = Ave velocity of inlet air stream, cm/sec

CONST( 7) = Relative humidity of inlet air stream. %RH/100

CONST( 8) = First guess of inlet-side cell current density, amp/$cm^2$

CONST( 9) = Total cell voltage, volt

CONST(10) = Viscosity of air, poise

CONST(11) = Thermal conductivity of air, cal/cm-sec-°K

CONST(12) = Mass diffusivity of air-water binary, $cm^2$/sec

CONST(13) = Constant volume heat capacity of air, cal/g-°K

CONST(14) = Weight fraction sulfuric acid charged to cell

CONST(15) = Weight fraction silica in electrolyte charged to cell

CONST(16) = Length of electrolyte compartment, cm

CONST(17) = Width of electrolyte compartment, cm

CONST(18) = Depth of one of the two electrolyte compartments, cm

As stated in the text, two WVE cell independent variables are built into the routine: inlet air velocity profile and electrode overvoltage-current-composition data. The model presently contains overvoltage data for solid platinum electrodes, and such data for other electrodes of interest must be inserted. The present model calculates current density from overvoltage and composition by linear interpolation of LOG (current density), LOG (overvoltage) data at a given electrolyte acid concentration. A competent programmer, well versed in the model and armed with excellent experimental data, is required to insert overvoltage data. Alterations are extremely messy.

Computer simulation output is controlled by the value of the integer IWRITE. If IWRITE = 0, only independent variables for a given execution and consolidated data will be output, as in Figures 6 through 10 in the text of the present annual report. If IWRITE is greater than zero, controlled amounts of comprehensive data will also be output. These

are cell dependent variables calculated at selected points along the length of the air channel, presently the following:

1. Distance from cell inlet
2. Air velocity profile across flow channel
3. Air temperature profile across flow channel
4. Air humidity profile across flow channel
5. Air pressure
6. Local sulfuric acid concentration
7. Local cell current density
8. Number of iterations required for heat and mass transfer model segment, and size of residual vector at convergence.

For IWRITE = Z, the above information will be output at every Zth increment along the length of the flow channel. A competent programmer with understanding of the model may easily add to or delete from the above list to suit.

Use of Simulation The simulation is a mathematical analog of the NASA water vapor electrolysis cell operating at steady state, As such, it can and should be viewed as a WVE cell that gives a lot of data quickly. Model executions are exactly equivalent to experimental trials, and should be planned accordingly.

completed at least one year in their studies for an associate degree in engineering technology. Also initiated under this program is a Pennsylvania survey of vegetation damage. Agricultural extension personnel and county agents were trained to recognize air pollution damage to crops and are now reporting damage seen in their daily work to the Center for analysis.

A two year course leading to the Associate Degree in Air Pollution Technology is given at the Berks Campus of the Pennsylvania State University. The graduate of this program is trained to be responsible for the calibration, installation, and operation of air sampling and monitoring equipment. He may also be expected to investigate complaints, conduct plant inspections, make source evaluations, and formulate recommendations based on his findings.

Address requests for more information concerning the training programs to the Director, Center for Air Environment Studies, 226 Chemical Engineering II, The Pennsylvania State University, University Park, Pennsylvania 16802.

## Publications Available

AIR POLLUTION TITLES, a current awareness publication service, is available on a January-December subscription basis. This publication is a quick guide to current literature and has some capacity as a retrospective searching tool. APT uses a computer-produced, Keyword-in-Context (KWIC) format to provide a survey of current air pollution and related literature. During the year over 1,000 journals are scanned for pertinent citations.

Subscriptions to APT at $15/year, cover issues per year as follows: No. 1, January-February; No. 2, March-April; No. 3, May-June; No. 4, July-August; No. 5, September-October; No. 6, cumulative issue for the year, including November-December citations. The 1971 subscription of APT is now available. Cumulative issues for 1967, 1968, 1969 and 1970 are available; the cost is $10 each.

INDEX TO AIR POLLUTION RESEARCH was published in July of 1966, 1967, and 1968. Each Index included government sponsored research in the air pollution field and the results of a survey of air pollution research projects conducted by the industrial, sustaining, and corporate members of the Air Pollution Control Association and the American Industrial Hygiene Association, and research supported by other industries and non-profit organizations.

The Index utilizes the Keyword-in-Context (KWIC) format for rapid scanning of project titles. In addition, this publication provides a complete bibliography including mailing addresses where additional information about the project may be obtained. Beginning with the 1967 edition, a section containing citations of papers resulting from the research in progress was included. Copies of the 1966 and 1967 editions are available at $1.25 each. The 1968 edition costs $2.

NOTE: The National Air Pollution Control Administration of the United States Public Health Service selected the Center for Air Environment Studies to prepare A Guide to Air Pollution Research which paralleled and replaced the 1969 Index. By contract agreement, the National Administration is managing the distribution of all copies.

HANDBOOK OF EFFECTS ASSESSMENT VEGETATION DAMAGE was published in 1969 as part of the survey of vegetation damage. It describes in detail the many sources of pollution and the effect of pollutants on vegetation; color pictures showing characteristics of plant damage symptoms are included. The cost is $6.

Requests for additional information and orders should be addressed to: Information Services, Center for Air Environment Studies, 226 Chemical Engineering II, University Park, Pennsylvania 16802.